INFORMATION FUSION IN MULTIBIOMETRIC SYSTEMS

BY

Ahmed A. Bahjat

A Thesis Presented to the
DEANSHIP OF GRADUATE STUDIES

KING FAHD UNIVERSITY OF PETROLEUM & MINERALS

DHAHRAN, SAUDI ARABIA

In Partial Fulfillment of the
Requirements for the Degree of

MASTER OF SCIENCE

In

Computer Science

June 2009

King Fahd University of Petroleum & Minerals

Dhahran 31261, Saudi Arabia

Deanship of Graduate Studies

This thesis, written by **AHMED ABDULLAH MOHAMMED BAHJAT** under the direction of his thesis advisor and approved by his thesis committee, has been presented to and accepted by the Dean of Graduate Studies, in partial fulfillment of his requirements for the degree of **MASTER OF SCIENCE IN COMPUTER SCIENCE**.

THESIS COMMITTEE
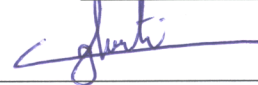
_____
Dr. Lahouari Ghouti (Thesis Advisor)
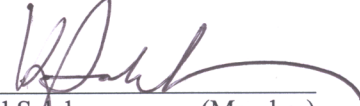
_____
Dr. Khaled Salah   (Member)

_____
Dr. Mohamed Deriche   (Member)

_____
Dr. Kanaan Faisal
Department Chairman

_____
Dr. Salam A. Zummo
Dean of Graduate Studies

_____19/10/29_____
Date

I would like to dedicate my thesis to

My parents

My wife

and my son Abdulrahman

Acknowledgments

TABLE OF CONTENTS

LIST OF TABLES

LIST OF FIGURES

THESIS ABSTRACT

Name: Ahmed Abdullah Mohammed Bahjat

Title: Information Fusion in Multibiometric Systems

Major Field: Computer Science

Date of Degree: June 2009

Information fusion has been recognized as an important component in the design and implementation of multibiometric systems. Recently, improved matching and recognition performance have been reported in the literature for multimbiometric systems. Information fusion plays a major role in such systems. In fact, for multibiometric systems, information fusion can be viewed as a scheme to improve the quality of the biometric trait sample for more accurate matching performance and reduced false accept/reject rates. It is worth noting that the application of information fusion encompasses several stages in multibiometric systems ranging from raw samples acquisition to matching decision of accept or reject. In this thesis, we focus on the inclusion of the information fusion solution at the sample and pre-feature levels. In particular, we propose two efficient fusion schemes. One scheme is to fuse fingerprint images, and the second is to fuse iris images. The scheme of fusing fingerprint

images is based on digital image watermarking, while the scheme of fusing iris images is based on a statistical modeling of the normalized iris images applied at the pre-feature level. For both fusion schemes, we show that the multibiometric systems using information fusion yield more acceptable performance than traditional biometric systems.

ملخص الرسالة

أحمد بن عبد الله بن محمد بهجت	**الاســـــــــــم:**
دمج المعلومات في أنظمة التعرف الحيوية	**عنوان الرسالة:**
علوم الحاسب الآلي	**التخصـــــــص:**
رجب 1430	**تاريخ التخرج :**

أسلوب دمج المعلومـات يعتبر عنصرا هامـا في تصميم وتنفيذ نظم التعرف الحيوية المتعددة. في الآونـة الأخيرة، أظهرت الدراسات تحسنا كبيرا في صحة المطابقة وسرعة الأداء في أنظمـة التعرف الحيوية المتعددة. وأسلوب دمج المعلومات هو من أهم العوامل المؤدية إلى هذا التحسن. في الحقيقة ، يمكن النظر إلى أسلوب دمج المعلومـات في أنظمة التعرف الحيوية المتعددة على أنه أداة لتحسين أداء الأنظمة الحيوية وتقليل معدل الأخطاء في المطابقة أو مـا يعرف بالسماح الخـاطئ أو الرفض الخـاطئ. ومن الجدير بالذكر أن تطبيقـات أسلوب دمج المعلومـات تشمل عدة مراحل في أنظمـة التعرف الحيوية المتعددة، من مرحلـة جمـع الأدلـة الحيويـة إلى اتخـاذ القرار المناسب. في هذه الرسالة، نركز اهتمامنا على استخدام دمج المعلومـات في مراحـل الأدلـة الحيويـة و مـا قبل استخلاص المعلومات الحيوية من هذه الأدلة. تحديدا، نطرح أسلوبين جديدين في الدمج بكفاءة عاليـة. الأول في دمج صور بصمة الأصبع والأخر في دمج صور قزحية العين. أسلوب الدمج المستخدم في صور بصمة الأصبع مبني على تقنية العلامـة المائية ، أما أسلوب الدمج في قزحية العين مبني على جودة المعلومات الإحصائية المستخلصـة من خصـائص صـور القزحية المعدلة. في كلا الأسلوبين، أظهرت الدراسـة تميزا ملحوظا في كفاءة التعرف مقارنـة بالطرق التقليديـة في أسـاليب التعـــرف التقليدي ــة.

Chapter 1

Introduction

1.1 Introduction

Biometric systems refer to recognition systems used for the identification of individuals based on a feature vectors derived from their physiological and/or behavioral characteristic. Biometric systems are gradually introduced to replace the *conventional* means of person identification/authentication. Unlike the conventional means that are based on the person knowledge ("*what the person knows*") and identification physical proofs ("*what the person carries*") like the password or ID cards, biometric systems are based on the personal physiological and/or behavioral traits ("*who the person is*").

Biometric systems are generally based on face, facial features, voice, hand geometry, handwriting, signature, retina, iris and fingerprint [1]. Biometric systems work by first capturing a feature sample such as recording a digital sound signal for voice recognition, or capturing the face details into a digital color image for face recognition. Other biometric traits are used in a similar fashion using different capture devices. Then, the acquired biometric samples are transformed using specific mappings and transformations (to be elaborated later in this Thesis) into a compact biometric template for efficient

time/space considerations in retrieval, matching and recognition processes. Usually, the compact biometric templates provide a normalized, efficient and highly discriminating representation of the feature, which can then be objectively compared with other templates for identification, matching and recognition purposes. Most biometric systems are operated in two different operational modes. The first mode (enrolment) allows the enrolment (addition) new biometric templates to a new database (or an existing one). In the other mode (identification), a template is created for an individual and then possible matching templates are searched for in the populated biometric databases [2].

Over the last years, the need for reliable user authentication techniques has been rapidly increasing. In the United States of America, the demand for such systems has been witnessing an annual growth of 10.4% in 2009. Such substantial growth has been mainly driven by technological innovations, falling prices and relatively high crime rates [3]. Biometrics systems and smart cards are expected to have the main share of the market growth [3, 4]. The air transportation business will attract the largest investments and will be the subject of the highest market growth [4]. Figure 1 gives the details of the total biometric revenues between years 1999 and 2005 [5]. The expected annual revenues of the biometric industries from the year 2009 till 2014 are given in Figure 2. It is quite interesting to note the shift in scale of revenues from the covered time frames in Figure 1 and Figure 2. The expected growth starting from the year 2009 lies in the billion dollars range which clearly indicates the expected penetration of biometric systems in several aspects of day-to-day businesses.
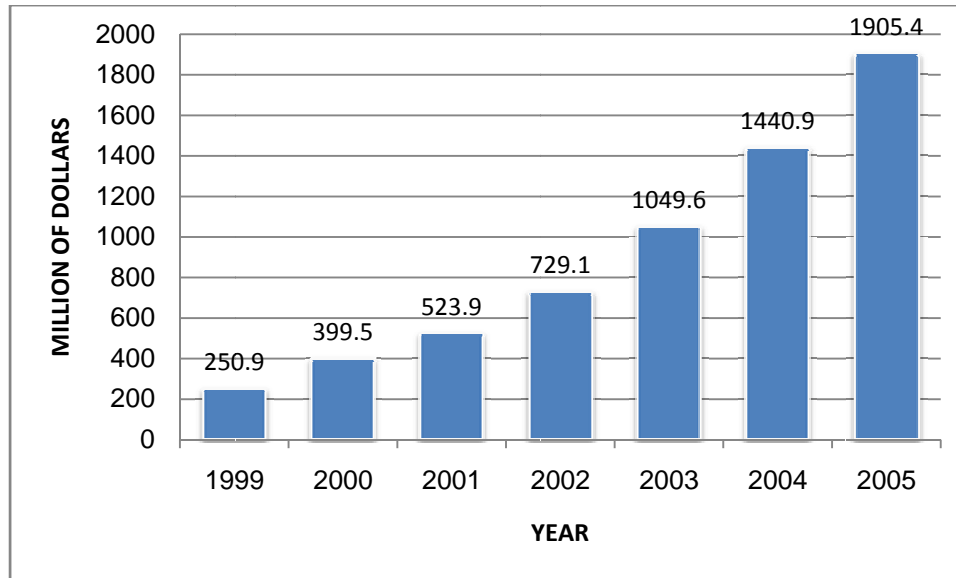
Figure 1: Biometric Market Revenues between 1999 and 2005 [5].
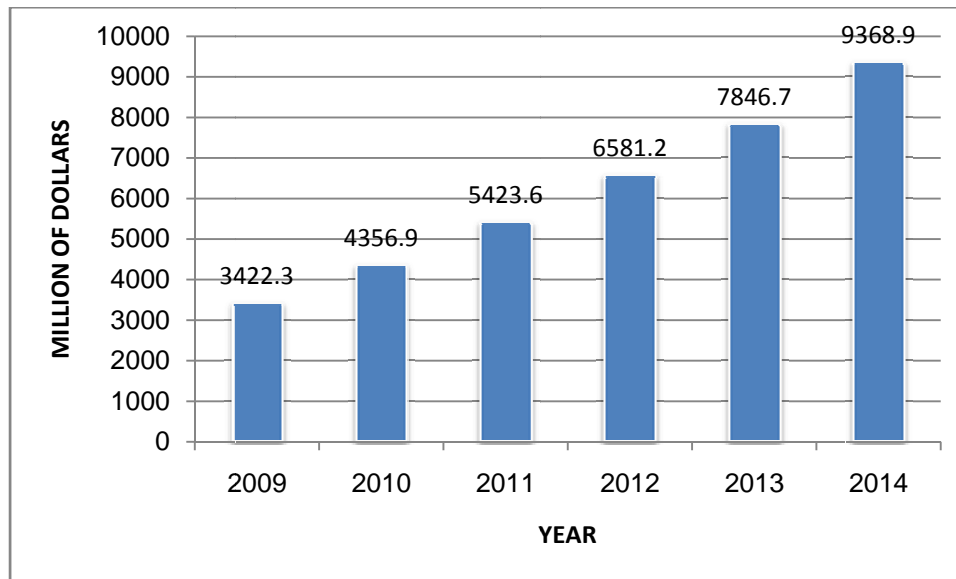
Figure 2: Expected Market Revenues between 2009 and 2014 [5].

The application of biometric systems can be categorized into three main groups [3]:

1- Commercial applications such as computer network login, electronic data security, e-commerce, Internet access, automated teller machines (ATM) or credit

card use, physical access control, mobile phone, personal digital assistant (PDA), medical records management, distance learning, etc.

2- Government applications such as national ID card, managing inmates in a correctional facility, driver's license, social security, welfare-disbursement, border control, passport control and identification, etc.

3- Forensic applications such as corpse identification, criminal investigation parenthood determination, etc.

1.2 **Overview of Biometric Uni and Multi Systems**

As explained earlier, biometric systems are becoming one of the fastest growing personal identification systems thanks to their high precision and accuracy in identifying individuals based on their physiological and/or behavioral characteristics. They overcome the limitations of token-based and knowledge-based identification systems. Biometrics is classified into two main groups: 1) physiological and 2) behavioral. The former group is based on the person's behavioral traits such as the gait, voice, keystrokes and signature. The latter one relies on the person's physiological traits. These traits include face, fingerprint, iris, retina, hand geometry, palm-print and DNA. Figure 3 gives a summary of the various biometric traits currently in use with biometric systems. Moreover, biometric systems are considered as pattern recognition systems that process such traits to identify the person based on a prior knowledge of his specific biometric data.
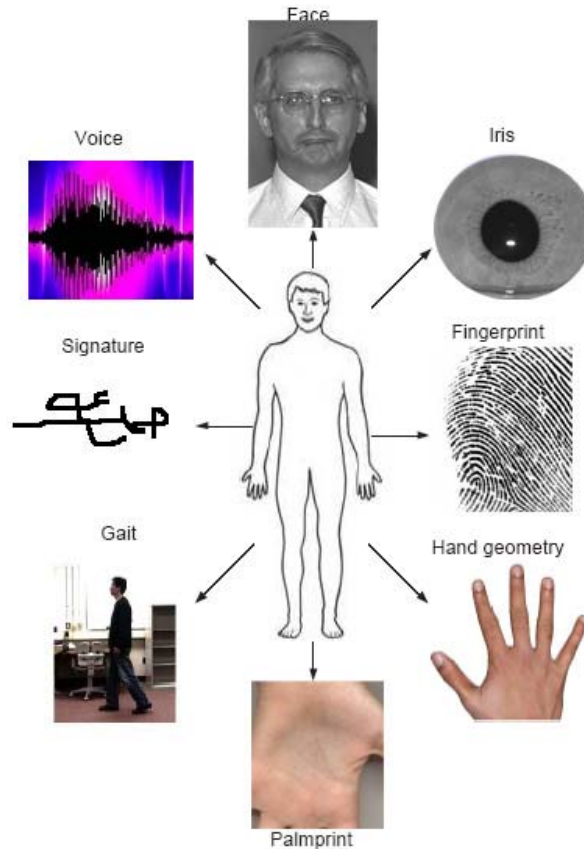
Figure 3: Different biometric traits for person identification systems [3].

In this Thesis, we will restrict our research efforts to physiological biometric systems for the following reasons:

- They enjoy fewer limitations than their counterparts.

- They ensure uniqueness of individuals.

- Pattern recognition algorithms provide simple, yet efficient, feature representations.

- Wider application opportunities (Physical access [mainly, border control], logical access [e-banking], social benefits).

Biometric systems are widely implemented worldwide for boarder control, restricted access of privileged information, secured online banking systems, and social insurance programs and so on. Although, uni-biometric systems (biometric systems based on single source of evidence) are widely deployed and used, they have several limitations that hinder their reliability and make them less reliable in identification and authentication applications. Some of these limitations are outlined below [3]:

- **Accuracy:** Noisy sensor data, non-universality, inter-class similarity and lack of invariant representation.

- **Scalability:** If the number of data samples, N, is large, identification becomes an issue.

- **Security and Privacy:** Spoofing can take place in many traits such as fingerprint, signature and voice.

In response to these limitations, multibiometric systems have been recently introduced as an improved means for person's identification and recognition purposes. Such systems rely on multiple evidence rather than single biometric evidence [3]. By integrating multiple biometric samples or multiple traits, more efficient and reliable systems can be devised. Information fusion has been proposed to achieve the integration of the multiple biometric traits at different stages of multibiometric systems [7, 8]. It should be noted that the resulting systems can be either be hybrid or simple systems depending on the type of information fusion strategy being adopted and applied. Figure 4 shows the major differences between uni- and multibiometric systems. The integration of several biometric samples and/or traits is made possible only by the incorporation of the

information fusion module which highlights the importance of the latter module in the successful development of multibiometric systems since uni-modal could be considered in an ensemble but without allowing possibly an improved matching and recognition performance.
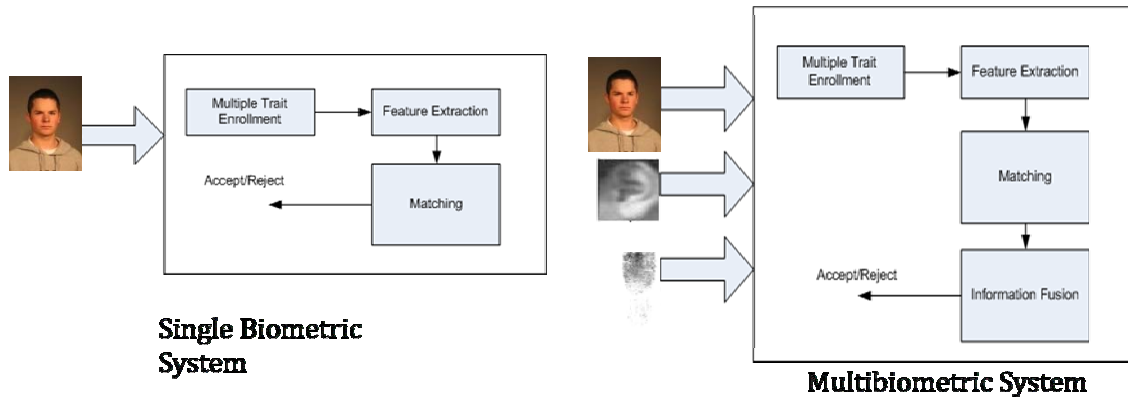
Figure 4 : Single Biometric System vs. Multibiometric Systems[3].

Multimodal biometric systems can be designed to operate in five different modes [3]:

1) Multiple-Sensor Mode: In this mode, the raw biometric data is acquired from multiple sensors, processed and integrated to generate new data from which features can be extracted. Needless to mention the increased hardware, software and computational costs caused by such integration. However, the incorporation of sources from multiple sensors significantly improves the segmentation and registration procedures in addition to improving the matching accuracy [3].

2) Single-Biometric Multiple-Representations Mode: In these systems, the same biometric data is processed using multiple algorithms at the mapping and feature levels. For instance, a multiresolution algorithm based on texture analysis and a minutiae-based

7

algorithm can operate on the same fingerprint image in order to extract diverse feature sets that would greatly improve the performance of the overall system. This mode is characterized by its cost efficiency since it does not require the use of multiple sensors. Furthermore, the user is not required to interact with multiple sensors thereby enhancing user convenience and comfort. However, it does require the introduction of new feature extractor and/or matcher modules which may increase the computational requirements of the system [2].

3) Single-Biometric Multiple-Units Mode: Multiple instances of the same biometric trait are considered in this mode. For example, the left and right irises of the same person are considered for fusion and further processing. Systems pertaining to this mode generally do not necessitate the introduction of new sensors nor do they entail the development of new feature extraction and matching algorithms and are, therefore, more cost efficient than those systems belonging to the previous mode. However, in some cases, a new sensor arrangement might be necessary in order to facilitate the simultaneous capture of the various units [2].

4) Single-Biometric Multiple- snapshots Mode: In this mode, a single sensor is used to capture multiple snapshots of the same biometric trait. A *mosaicing* scheme may then be used to assemble the multiple impressions and create a composite image. One of the main issues in this mode is the determination of the number of samples or snapshots that have to be acquired from an individual. It is important to well capture the variability, as well as the typicality, of the individual's biometric data in the captured samples [3].

5) Multiple-biometrics Mode: Multibiometric systems requiring more than one modal are classified under this mode. For instance, the iris and fingerprint of the same person can be

used for the matching, identification and recognition purposes. Systems belonging to this mode are usually known as *multimodal* biometric systems [2].

Unlike the first four modes where multiple sources of information are derived from the same biometric trait, in the last mode, useful biometric information is derived from different biometric traits.

As stated previously, information fusion can take place at different stages of the system under consideration. However, fusion at the matching score level seems to be the logical choice as it is relatively easy to access and combine scores presented by the different modalities [2]. Furthermore, incorporating the fusion process at earlier stages of the multibiometric system is more effective.

In summary, the main advantages of multibiometric systems are outlined below [3]:

- Improve accuracy.

- Address the issue of non-universality problem.

- Provide flexibility to the user.

- Reduce the effect of noisy data.

- Provide the capability to search a large database in computationally efficient manner.

- Resistant to spoof attacks.

- Fault tolerant systems.

Each of the above-mentioned features mitigates one or some of the limitations found in uni-biometric systems. Table 1, gives a comparative summary of the various biometric

traits with respect to key factors such as universality, performance, acceptability and
distinctiveness.

Table 1: Comparison of various biometric technologies (H=High, M=Medium, L=Low) [3].

Biometric characteristic	Universality	Distinctiveness	Permanence	Collectability	Performance	Acceptability	Circumvention
Face	H	L	M	H	L	H	L
Fingerprint	M	H	H	M	H	M	H
Hand geometry	M	M	M	H	M	M	M
Keystrokes	L	L	L	M	L	M	M
Hand veins	M	M	M	M	M	M	H
Iris	H	H	H	M	H	L	H
Retinal scan	H	H	M	L	H	L	H
Signature	L	L	L	H	L	H	L
Voice	M	L	L	M	L	H	L
Facial thermograph	H	H	L	H	M	H	H
Odor	H	H	H	L	L	M	L
DNA	H	H	H	L	H	L	L

Gait	M	L	L	H	L	H	M
Ear Canal	M	M	H	M	M	H	M
Face	H	L	M	H	L	H	L

1.3 **Problem Statement**

Biometric systems based on a single source of information (unimodal systems) are known to suffer from several limitations like the lack of uniqueness, non-universality and noisy data and hence, may not be able to achieve the desired performance requirements of real-world applications. In contrast, multibiometric systems combine information from multiple evidence in order to arrive to a more reliable decision in terms of matching and rejection rates [3]. In this Thesis, we will propose two multibiometric systems using fingerprint and iris data, respectively. In both systems, information fusion is carried out at the sensor level with minor differences in the second system where more precisely fusion takes place at the pre-feature level as it will be explained in details later in this Thesis. Both systems are based on state-of-the-art pattern matching and recognition algorithms, namely the Gabor filterbank approach [9] and the Daugman algorithm [10] for the fingerprint and iris data, respectively. The improvement in performance, due to the proposed information fusion schemes, will be detailed with in-depth analysis and performance measures. Performance comparison will be carried out against the selected state-of-the-art pattern matching systems.

1.4 **Thesis Objectives**

The Thesis objectives are mainly motivated by the influence that have the increased robustness and improved accuracy on the acceptance of biometric systems as a cost-efficient and reliable means for person identification and verification which would implicitly contribute to better privacy and security.

In summary, the main objectives of this Thesis are:

1- Investigate a novel scheme for information fusion at the sensor level that would enable the development of a new multibiometric system based on multiple instances (samples) of fingerprint images.

2- Study the suitability of iris image modeling for quality-based iris fusion at the pre-feature level that would enable the development of a new multibiometric system based on multiple instances (samples) of normalized iris images.

3- Investigate the use of state-of-the-art statistical image models for the representation of iris textures in the wavelet domain.

4- Study in details the performance improvement of the proposed algorithms through extensive computer simulation using widely accepted large and medium scales biometric databases.

1.5 **Thesis Contributions**

The objectives set henceforth have been fully achieved in this Thesis. The main contributions reported in this Thesis are summarized as follows:

1- Propose a new algorithm for fingerprint fusion at sensor level using a wavelet-based digital image watermarking technique.

2- Apply state-of-the-art statistical image models for the representation of iris textures in the wavelet domain.

3- Propose a new algorithm for iris fusion at the pre-feature level using statistical modeling of iris texture and novel quality measures.

4- Demonstrate the improvement in matching and recognition performance of the latest pattern recognition algorithms being currently in use for fingerprint- and iris-based biometric systems.

As mentioned in the previous Section, a series of computer simulation experiments are conducted to evaluate the performance improvement due to the proposed information fusion algorithms using standard large-scale biometric databases. A freely available fingerprint database is considered for this purpose. For the iris-based experiments, a high quality, high resolution commercial iris database is used. The efficiency of the proposed approaches is demonstrated through extensive quantitative comparisons with latest fingerprint- and iris-based biometric systems that do not include information fusion modules.

1.6 **Thesis Organization**

The Thesis is organized as follows: Chapter 2 gives a detailed account of previous work in physiological uni- and multibiometric systems. Information fusion algorithms proposed for multibiometric systems are given therein. Chapter 3 begins with the mathematical preliminaries and details of the main image transforms used for the fingerprint- and iris-based benchmark biometric systems. Namely, the discrete wavelets transform (DWT) and the Gabor wavelet transform (GWT) are discussed in details relevant to the research reported in this Thesis. Additionally, digital watermarking using discrete wavelet transform is outlined along with the properties of texture modeling. The Chapter concludes with a description of the performance measures used later in this Thesis. In Chapter 4, the two information fusion algorithms, developed in this Thesis, are given in details. We show the building blocks of both algorithms and how they can be integrated to achieve better performance in multibiometric systems. Experimental experiments and computer simulations carried out in this Thesis are reported in Chapter 5. Also, biometric databases, used in this part, are discussed and their properties highlighted. In Chapter 6, the Thesis concludes with the drawn conclusions and suggestions for possible future work.

Chapter 2

Literature Review

The major sources for information are contained in the Reference section of this document. We have identified background material as well as published articles on information fusion strategies in multibiometric systems. The major issues are concerned with the potential impact of information fusion of optimizing the GAR (Genuine Accept Rate) and decreasing the FAR (False Accept Rate) in identification and verification of biometric samples against biometric templates.

Section 2.1 of this chapter reviews the physiological biometric systems namely the iris and the fingerprint based systems. In Section 2.2 details the multibiometric systems and information fusion in literature.

2.1 Physiological Biometric Systems

2.1.1 Fingerprint Recognition

Fingerprint-based person identification system attracts many researchers to investigate and propose novel methods that improve the accuracy and speed of such systems. Consequently, a lot of approaches for fingerprint recognition were proposed in the literature. These include preprocessing fingerprint images, extracting representation

features, constructing and encoding the most convenient representation of the features, and various methods of matching algorithms.

The majority of the available techniques in this field, including ours, concentrate on the process of feature extraction and encoding. A detailed review of the most popular approaches will be summarized. The first proposal of automating fingerprint recognition can be tracked down to late sixteenth century, [12] but in this summery we will focus on the important advances of fingerprint recognition rather than the history of fingerprint recognition system.

Many research done in fingerprint recognition uses the minutiae features as a representation of a fingerprint pattern. The matching is done between minutiae of claimed identity and the stored templates in the database. In the other hand some researchers treat the fingerprint as texture. For instance, Benhammadi et al. [13] proposes a new hybrid fingerprint recognition algorithm that bases the matching on minutiae texture map orientation. The proposed algorithm has the advantage of skipping the fingerprint relative alignment stage result in better accuracy. In the same path Wen et al. [14] introduces an algorithm that is based on a bank of Gabor filter and wavelets to extract the feature of fingerprint in different orientation as FingerCode to be used for matching. Su et al. [15] uses both minutiae and ridges for matching in order to reduce the false matching. The result shows improve in speed as well as accuracy of matching. Nikam and Agarwal [16] present a hybrid scheme where minutiae and wavelet statistical features are used for matching to improve accuracy of recognition.

Another approach in dealing with fingerprint recognition system is to use the image itself as a template and query rather than a minutiae points of fingerprint pattern. The matching is done by different correlation measurements [16].

2.1.2 Iris Recognition

Iris recognition has become a popular research in recent years. Due to its reliability and accuracy of recognition it is used in the highly secured areas like country boarders. The three main stages of an iris recognition system are image preprocessing, feature extraction and template matching.

Wildes [17] gives accounts of the main reasons behind the use of iris images as a trusted and highly reliable human trait for discriminating individuals. Until the past few years, several new algorithms for iris feature extraction have been proposed. However, very little contributions have been made to propose new matching mechanisms in order to improve the accuracy of iris recognition systems at large. For instance, Ives et al. [18] show that histogram analysis can be used instead of Daugman algorithm [10] for feature extraction of human iris. An algorithm of extracting human iris features using the wavelet transform is proposed by Khan et al. [19]. In their work, Khan et al. perform iris matching using the well-known Hamming distance (HD). Ko et al. [20] propose a new method for the extraction of the iris feature using the cumulative sum based grey change analysis. Iris edge maps have been proposed for feature extraction in [21]. It should be noted that some of the proposed approaches consider the use of specific iris minutia

points where these are extracted from the iris image in analogy to what is being done in fingerprint identification/matching systems [22].

On the other hand, studies have been carried out to analyze the effect of improving the classifier instead of improving the feature extraction process on the recognition accuracy. Anna et al. [23] adopt a Canny transform to extract features and probabilistic wavelet neural network as an iris biometric classifier. Miyazawa et al. [24] propose a new algorithm for iris matching based on phase correlation analysis. Experimentally, Miyazawa system achieves lower overhead in processing time and stored information for samples.

2.2 **Multibiometric Systems**

Many research findings have been reported in the area of information fusion to multibiometric. Duca et al. [25] propose an algorithm based on Bayes theory in order to fuse individual experts opinions. The modalities used in their system are face and speech for each person involved. Experimental results show that fusion improves accuracy over the uni-biometric systems by reaching success rates of 99.5%.

Hong and Jain [26] utilize the benefit of fast recognition in Face systems and a drawback of reliability by using fusion to utilize the reliability of fingerprint recognition and performance of face retrieval. The integrated system overcomes the limitation of face recognition and the fingerprint verification process. Their systems works very well in terms of response time and it meets the accuracy requirements.

However, Chatzis et al. [27] used information fusion of personal authentication modality. At the decision level, fusion takes place using fuzzy k-means and fuzzy vector quantization algorithm and median radial basis function. Their simulation results shows that median radial basis function outperform other fuzzy function for biometric recognition especially with two modalities

A multi-view face and gait recognition system was proposed by Shakhnarovich et al. [28] using an image-based visual hull. Image sequences captured from multiple cameras are passed to an unmodified face or gait recognition algorithm. The proposed algorithm shows an integrated face and gait recognition provides improved performance over a single modality of one of them alone.

Feature level fusion has been applied on several samples as presented in [29]. Ross and Govindarajan [30] discuss fusion at the feature level in three different scenarios and the results are encouraging. They use hand and face biometric as a case study. Fusion of gait and face for human identification has been studied by Kale et al. [31]. They implement a decision level fusion in order to combine expert's decisions from multiple modalities. Gait recognition was used as a filter to reduce the sample space for identification for face recognition. They also implement a score level fusion for both modalities as another approach of information fusion.

Face and speech have been studied by [32-34] and the results indicate that performance improvement can be achieved only if the soft biometric traits are complementary to the primary biometric traits. Face, fingerprint and hand geometry also have been experimented by Ross [2].

Multi-sensor fusion has been studied for fingerprint verification by Marcialis and Roli [35]. In their work, they implement a sensor level fusion using optical and capacitive sensors. The result outperforms single sensor fingerprint recognition systems. Chang et al. [36] however uses the 2D and 3D images of face to build their datasets, they involve 198 persons face in their study. They used match score level in order to get a decision of identification and their conclude that 2D and 3D have similar recognition performance when considered individually, however combining 2D and 3D results using a simple weighting scheme outperforms either 2D or 3D alone, combining results from two or more 2D images using a similar weighting scheme also outperforms a single 2D image, and combined 2D+3D outperforms the multi-image 2D result.

 Dass et al. [11] propose an optimal framework for combining the matching scores from multiple modalities using the likelihood ratio statistic computed using the generalized densities estimated from the genuine and impostor matching scores. They claim that some parts of the score distributions can be discrete in nature; thus, estimating the distribution using continuous densities may be inappropriate. They present two approaches for combining evidence based on generalized densities: i) the product rule,

which assumes independence between the individual modalities, and ii) copula models, which consider the dependence between the matching scores of multiple modalities.

Fierrez-Aguilar et al. [37-38] present an on-line signature verification system exploiting both local and global information through decision-level fusion. Global information is extracted with a feature-based representation and recognized by using Parzen Windows Classifiers. Local information is extracted as time functions of various dynamic properties and recognized by using Hidden Markov Models. Experimental results are given on the large MCYT signature database (330 signers, 16500 signatures) for random and skilled forgeries. Feature selection experiments based on feature ranking are carried out. It is shown experimentally that the machine expert based on local information outperforms the system based on global analysis when enough training data is available. Conversely, it is found that global analysis is more appropriate in the case of small training set size. The two proposed systems are also shown to give complementary recognition information which is successfully exploited using decision-level score fusion.

In [39], Campbell presents an approach to combine Support Vector Machine with speaker detection using generative and discriminative approaches by mapping a whole speech utterance onto a fixed length vector. Ho [40] uses a multiple classifier system and rank level fusion in order to solve the difficult pattern recognition problems involving large class sets and noisy input because it allows simultaneous use of arbitrary feature descriptors and classification procedures. Decisions by the classifiers can be represented as rankings of classes so that they are comparable across different types of classifiers and

different instances of a problem. However, in [41], Woods et al. apply the multiple classifiers using local accuracy estimates of each individual classifier's in a small region of feature space surrounding an unknown test sample and they suggest a methodology for determining the best mix of individual classifiers. Lu [42] applies the multiple classifiers for face recognition and it outperforms individual classifiers. This technique however can be applied to protect privacy as it proposed as a framework by Yanikoglu and Kholmatov [43].

Decision-level fusion has also been applied in many different samples for verification. Prabhakar and Jain [44] studied the effect of that scheme in fingerprint verification and they achieve 5% better accuracy. Fierrez-Aguilar [45] applied a novel score-level fusion strategy based on quality measures for multimodal biometric authentication. The proposed fusion function is adapted every time an authentication claim is performed based on the estimated quality of the sensed biometric signals at this time. The proposed scheme is shown to outperform significantly the fusion approach without considering quality signals by about 20%.

A summary of the most important research carried out in the literature for multibiometric systems in different fusion levels are summarized in Table 2.

Table 2: Summary of Multibiometric Systems in Literature.

Authors	Multibiometric System	Fusion Level
Duca et al. [25]	Face and speech	Decision level
Hong and Jain [26]	Face and fingerprint	Decision level
Chatzis et al. [27]	Face and speech	Decision level
Shakhnarovich [28]	Face and Gait	Feature level
Ross [6]	Face, fingerprint and hand geometry	Match score
Kale et al. [31]	Gait and face	Match score
Marcialis and Roli [35]	Multi-fingerprint sensor	Sensor level
Ross and Govindarajan [30]	Hand and face	Feature level
Chang et al. [36]	2D / 3D face	Sensor level
Fierrez-Aguilar et al. [37]	Multiple information from online Signature	Decision level

Chapter 3

Mathematical Background

3.1 Introduction

In the Chapter, we will provide the mathematical and technical preliminaries and background necessary to the development of the proposed information fusion schemes. In the sequel, multiresolution analysis (MRA) techniques will be introduced with emphasis on the definition of discrete wavelet transforms (DWT) and their filter-bank implementation. Then, Gabor wavelets are introduced. Required background for the digital watermarking process is laid out followed by the concept of statistical modeling for wavelet-based texture representations. More, specifically the Generalized Gaussian Distribution (GGD) is given in details along with the required algorithms for the estimation of the mode parameters. Finally, a review of biometric performance measures is given with some standard notations.

3.2 Discrete Wavelet Transforms (DWTs)

A discrete wavelet transform (DWT) consists of a critically-sampled digital filter bank. The input signal (1D, 2D or 3D) is processed through two branches of the filter bank. The

information content of the signal being processed is fully conserved although represented in a different form. Moreover, DWT represents a fast computational implementation of the MRA analysis and, therefore, is a more powerful than other existing transforms and mappings such as the Fast Fourier Transform (FFT) or the Discrete Cosine Transform (DCT) [46]. DWT, through MRA, allows for better signal localization in both time and frequency domains [47]. Additionally, DWT is easily implemented through the "a-trous" algorithm developed by Mallat [47]. Mallat's algorithm significantly reduces processing time and storage resources. In Mallat's algorithm, the DWT is computed by successive lowpass and highpass filtering of the signal being processed. For critically-sampled processing, the output of the lowpass filter branch is, then, decomposed further in a recursive manner [47].
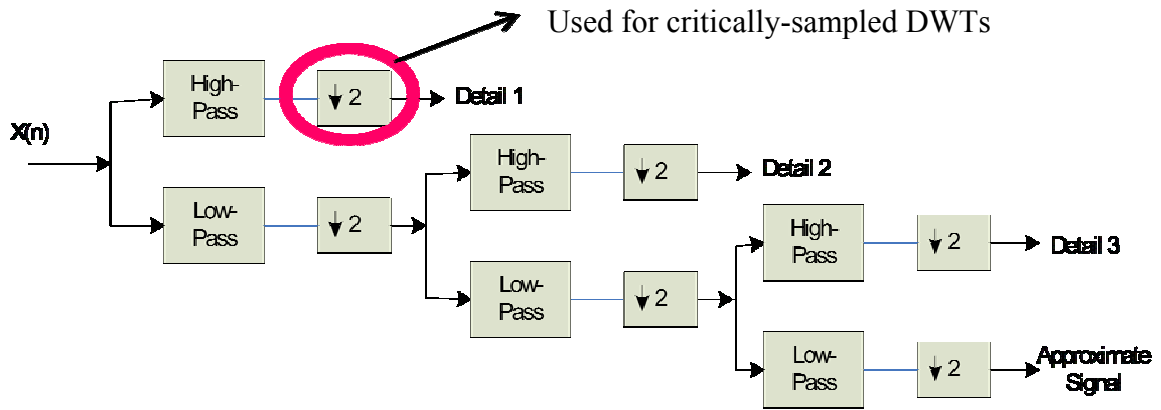
Figure 5: Image Decomposition using Wavelets.

In general any signal, *f(t)*, in L$_2$ norm can be represented by the series:

$$f(t) = \sum_{j,k} a_{j,k} 2^{\frac{j}{2}} \psi(2^j t - k) \tag{3.1}$$

25

where the two-dimensional set of coefficients $a_{j,k}$ represents the set of DWT coefficients of $f(t)$ and $\psi_{j,k}(t)$ represent the scaling functions used for the decomposition of the signal $f(t)$. A more specific form indicating how the $a_{j,k}$'s are calculated and can be written using inner products as [47]

$$f(t) = \sum_{j,k} \langle \psi_{j,k}(t), f(t) \rangle \psi_{j,k}(t) \qquad (3.2)$$

Figure 6 shows a sample fingerprint image (Figure 6-a) along with its 2D DWT representation using two (02) decomposition levels. The approximation image at the second level (Figure 6-c) looks closer to the original fingerprint image with minor differences and a noticeable loss is resolution due to the lowpass filtering being applied. Also, the reconstructed image (Figure 6-d) looks very close to the original image which confirms the information preservation property of the DWT transform.

(a)   (b)   (c)   (d)
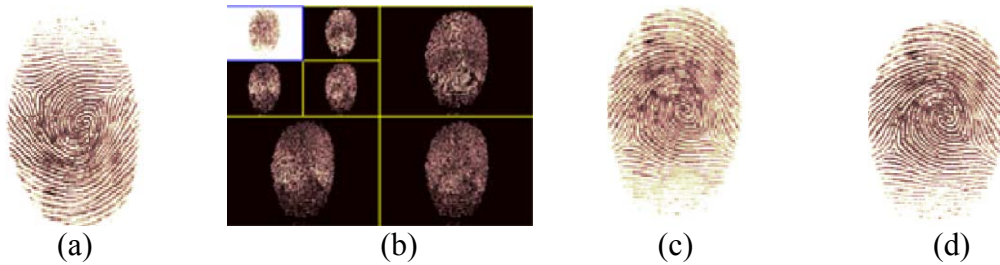
Figure 6: DWT Analysis of Fingerprint Images, (a) Sample Image, (b) 2D DWT using two decomposition levels, (c) Approximation image at second decomposition level, (d) Reconstructed image.
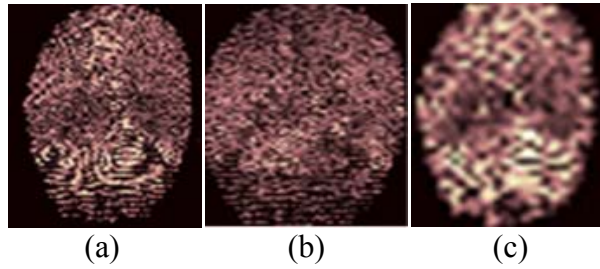
Figure 7: Detail property of DWT Analysis, (a) Horizontal details at level one, (b) Diagonal details at level one, (c) Horizontal details at level two.

The MRA enables DWT to capture the image details at different orientations (horizontal, vertical and diagonal) as indicated in Figure 7. It is worth noting the ability of the DWT to capture the image horizontal details at a varying resolution (Figure 7-a and Figure 7-c). However, the diagonal details are captured with ambiguity due to the lack of the DWT transform to discriminate between diagonal details at 45° and -45° (opposite details) as shown in Figure 7-b.

Finally, it should be noted that for compression purposes, the decomposition mechanism is different as shown in Figure 8. The decomposition structure, shown in Figure 8, has been adopted by the American standard initiated by the US Federal Bureau of Investigation (FBI) for its high compression rate and improved quality of reconstructed images for the storage and transmission of fingerprint images [47]. Unlike the standard DWT decomposition, the wavelet packet tree provides 64 subbands for compression in the wavelet scalar quantization (WSQ) scheme adopted by the FBI.
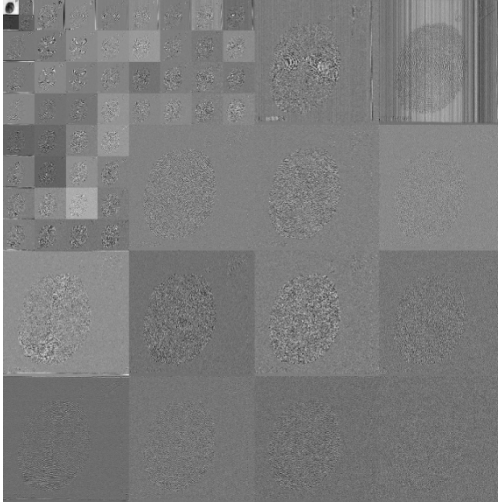
Figure 8: Standard five-level decomposition for WSQ-based compression.

3.3 Gabor Wavelet Transforms

Wavelets are used to decompose the data in the biometric region (iris, fingerprint, face, etc.) into components that appear at different resolutions. A set of wavelet filters is applied to the biometric at each resolution in order to provide a compact and discriminating representation of the pattern. A Gabor filter is constructed by modulating a sine/cosine wave with Gaussian. This allows providing the optimum conjoint localization both in space and frequency, since a sine wave is perfectly localized in frequency, but not localized in space. The decomposition of a signal is accomplished by using a quadrature pair of Gabor filters, with a real part specified by a cosine modulated by a Gaussian, and an imaginary part specified by a sine modulated by Gaussian. The real and imaginary filters are also known as the even symmetric and odd symmetric components respectively. The center frequency is specified by the frequency of the sine/cosine wave, and the bandwidth of the filter is specified by the width of the Gaussian.

As an application of Gabor wavelets, Daugman used a 2D version of Gabor filters in order to encode iris pattern data. A 2D Gabor filter over an image domain (x,y) is represented as [48]:

$$G(x,y) = e^{-\pi[(x-x_0)^2/\alpha^2 + (y-y_0)^2/\beta^2]} e^{-2\pi i[u_o(x-x_0) + v_0(y-y_0)]} \qquad (3.3)$$

where (x_0, y_0) specifies position in the image, (α, β) denotes the effective width and length, and (u_0, v_0) indicates modulation, which has spatial frequency [49]:

$$\omega_0 = (u_0^2 + v_0^2)^{1/2} \qquad (3.4)$$

Daugman used polar coordinates for normalization and in polar form the filters are given as [50]:

$$H(r,\theta) = e^{-i\omega(\theta-\theta_0)} e^{-(r-r_0)^2/\alpha^2} e^{-i(\theta-\theta_0)^2/\beta^2} \qquad (3.5)$$

where (α,β) are the same as in Equation (3.3) and (r_0,θ_0) specify the center frequency of the filter. The demodulation and phase quantization process can be represented as:

$$h_{\{R_e,I_m\}} = sgn_{\{R_eI_m\}} \int_\rho \int_\emptyset I(\rho,\emptyset) \ e^{-i\omega(\theta_0-\emptyset)} e^{-(r_0-\rho)^2/\alpha^2} e^{-i(\theta_0-\emptyset)^2/\beta^2} \qquad (3.6)$$

where $h_{\{R_e,I_m\}}$ can be regarded as a complex-valued bit whose real and imaginary components are dependent on the sign of the 2D integral, and $I(\rho,\emptyset)$ is the raw input image in a dimensionless polar coordinate system.

Another application of Gabor filters in biometric systems is to remove noise and preserve the true ridge and valley structures of a fingerprint in fingerprint recognition systems. It also provides information contained in a particular orientation in the image [51].

Gabor filters are widely used in feature extraction and computer vision, however it suffer from DC component in the even symmetric filter whenever the bandwidth is larger than one octave. This limitation can be overcome by using special type of Gabor filter known as log-Gabor filter, which is Gaussian on a logarithmic scale. This type produces zero DC components for any bandwidth. The log-Gabor function more closely reflects the frequency response for the task of analyzing natural images and is consistent with measurement of the mammalian visual system [47].

Figure 9 shows the decomposition of an iris image using a 2D Gabor wavelet transform at a specific scale and orientation. The normalized iris image shown in Figure 9-b has been decomposed into a real and imaginary Gabor representations illustrated in Figures 9-c and 9-d, respectively.

(a)   (b)   (c)   (d)

Figure 9: Iris sample image (a), Normalized iris image (b), Real part of Gabor-based iris decomposition (c), Imaginary part of Gabor-based iris decomposition (d)

Watermarking is the process of embedding information such as origin, destination, access level, etc. of multimedia data (e.g., image, video, audio, text etc.) in a host data. Watermarking becomes very active research area in recent years. Generally, watermarking is used to protect intellectual property of creator, distributor or simple owner of a multimedia data. Very few researches have been done in using watermarking as a way of fusion. The goal of using watermarking in information fusion is to enhance

the quality of the features being taken from individual when verify it with the database template.

Image watermarking takes place in several domains depending on the application at hand and the application purpose. The main embedding domains are [52, 53]:

1- **Spatial domain:** The first proposed watermarking schemes embed watermarking information payload directly into in the host image in the spatial domain. Using specific image analysis operations (e.g., edge detection), it is possible to get perceptual information about the image. This information is, then, used to guide and/or control the watermark embedding directly in the intensity values of predetermined regions of the host image. Although spatial-domain watermarking techniques were simple and easy to implement, they suffered from poor robustness which hindered their acceptance as standard watermark embedding schemes [52].

2- **Transform domain:** To improve the watermark robustness while preserving its imperceptibility, several transform domains have been considered for injecting the watermark payload into the host image. Such domains include, but not restricted to, Fourier transform, DCT transform, DWT transform. It is interesting to note that several schemes have been proposed using either additive or multiplicative mode [54] where the watermark data is either added directly to the host transform coefficients or modulated in a multiplicative fashion [54]. Moreover, the use of transform domains is favored by well-established models for the characteristics of the human visual system (HVS) which can be astutely taken into account to

achieve higher embedding rates while simultaneously preserving the imperceptibility of the embedding data and the visual quality of the host image [53].

In this Thesis, we will consider the DWT domain for watermark embedding that will be in turned exploited for information fusion of fingerprint image samples pertaining to the same person. More precisely, we will use the Haar DWT transform for its simplicity and integer implementation since it can be implemented using simple arithmetic operations only [55]. Figure 10 outlines the watermarking procedure used for the proposed information fusion technique in this Thesis.
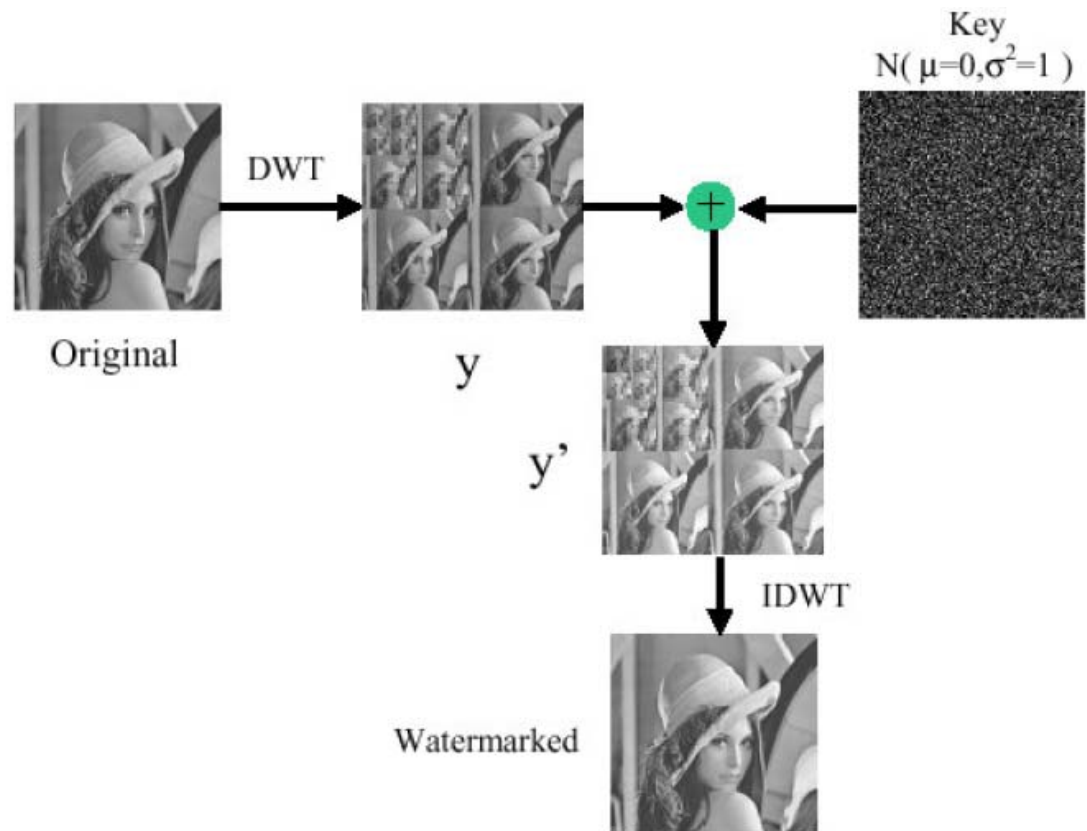
Figure 10: Watermarking embedding procedure using Haar DWT transform.

In order to weight the watermark according to the magnitude of the wavelet coefficients, we used one of the two following relations between the original coefficients y and $\ddot{y}$, the ones containing the watermark:

$$\ddot{y}[m, n] = y[m, n] + \alpha(y[m, n])^2 \, N[m, n] \qquad (3.7)$$

$$\&$$

$$\ddot{y}[m, n] = y[m, n] + \alpha \, |y[m, n]| * N[m, n] \qquad (3.8)$$

It must be pointed out that Equations 3.7 and 3.8, even though they are mathematically different, have the exact same goal which is to put more weight to the watermark added to high value wavelet coefficients. The parameter alpha is to control the level of the watermark; it is in fact a good way to choose between good transparency or good robustness or a tradeoff between the two. Finally, the two dimension inverse wavelet transform of is computed to form $\ddot{y}$ the watermarked image.

3.4 Texture Modeling Using Generalized Gaussian Distributions

Statistical modeling has been widely implemented in content-based information retrieval (CBIR) systems as well as in pattern recognition. Texture modeling becomes easier when the texture is represented in a statistical model using wavelet transformation. For instance, Generalized Gaussian Distributions (GGDs) have been successfully used to model coefficients produced by various types of wavelets transforms. Wouwer et al. [56] proposed a modeling scheme texture images are represented using wavelets. In their work, model parameters were estimated using moment matching techniques. Extracted model parameters were compared used the Euclidian distance as a similarity measure. In [57], Vasconcelos and Lippman proposed a probabilistic formulation of the CBIR problem where several similarity functions were used. It should be noted that classification problems using probabilistic models usually involve two major steps [58]: I) feature extraction and II) similarity Measurement. In the first step, image content is fitted to a specific statistical model whose parameters are estimated using various estimation routines and then in the second step, images based on their model parameters are ranked based on numerical or statistical similarity measures such as the Euclidian distance and Kullback Leibler distance (KLD), respectively.

The PDF of a GGD model is given by the following expression [58]:

$$f_x(x) = \alpha \, e^{-|\beta x|^c} \tag{3.9}$$

Both α and β parameters can be expressed as a function of the so-called shaping factor c and the standard deviation σ [58]:

$$\beta = \frac{1}{\sigma} \left(\frac{\Gamma(3/c)}{\Gamma(1/c)} \right)^{1/2} \tag{3.10}$$

$$\alpha = \frac{\beta c}{2\Gamma(1/c)} \tag{3.11}$$

where $\Gamma(.)$ is the complete gamma function. The shaping factor c is inversely proportional to the sharpness of the PDF. Therefore, the distribution is completely specified by two parameters, c and σ. Note that the Gaussian and Laplacian distributions are special cases of the GGD distribution, given by $c = 2$ and $c = 1$, respectively.

By varying the two parameters of the GGD, α and β, we can achieve a good PDF approximation for the marginal density of coefficients at a particular subband produced by various types of wavelet transforms [58].

Using GGD modeling, the representation of texture images is more accurate than those using the energies of the DWT subband coefficients alone. Therefore, more accurate results are achieved when comparing the GGDs of two images since all the statistical interaction between the image subband coefficients are efficiently captured by the model parameters. Also, more reliable similarity measures are obtained using robust similarity measures such as the KLD measure described later in this Chapter.

In this thesis, normalized iris images will be transformed in the DWT domain and modeled as textures using the GGD models. A robust technique for the estimation of the parameters of the GGD model will be considered [58]. Unlike its counterparts, Maximum-Likelihood (ML) estimator yields more accurate GGD parameters [58].

3.5 **Biometric Performance Measures**

3.5.1 Types of Errors

In order to assess the quality of biometric systems, two types of commonly used measures are considered [3]:

False accept rate (FAR): The probability of accepting an impostor, which basically the threshold depending fraction of the falsely accepted patterns divided by the number of all impostor patterns.

False reject rate (FRR): The probability of rejecting genuine user, which is the fraction of the number of rejected client patterns divided by the total number of client patterns.

Receiver Operating Characteristics (ROC) Curve: Allows defining the operating point for a given FAR/FRR point.

Genuine distribution (GD): The matching score for comparing inter-class samples, i.e., same samples of the same individual are compared against each other.

Impostor distribution (ID): The matching score for comparing intra-class samples, i.e., samples of different individuals are compared against each other.

In theory, client scores (scores of patterns from persons known by the system) should always be higher than the scores of impostors. If this would be true, a single threshold, that separates the two groups of scores, could be used to differ between clients and impostors.

Due to several reasons, this assumption isn't true for real world biometric systems. In some cases, impostor patterns generate scores that are higher than the scores of some

client patterns. For that reason, it is a fact that however the classification threshold is chosen, some classification errors occur.

For example, you can choose the threshold such high, that really no impostor scores will exceed this limit. As a result, no patterns are falsely accepted by the system. On the other hand the client patterns with scores lower than the highest impostor scores are falsely rejected. In opposition to this, you can choose the threshold such low, that no client patterns are falsely rejected. Then, on the other hand, some impostor patterns are falsely accepted. If you choose the threshold somewhere between those two points, both false rejections and false acceptances occur.

In general, a trade-off between these two types of error should be studied and decided depending on the application being designed. For a negative recognition systems where (e.g., preventing users from obtaining welfare benefits under false identities), a false accept results in rejecting a genuine request, whereas a false reject results in a falsely accepting an impostor attempt. On the other hand, in a positive recognition system (e.g., an access control system) a false accept determines the accepting an impostor, whereas a false reject causes the mistakenly rejecting a genuine user [59].
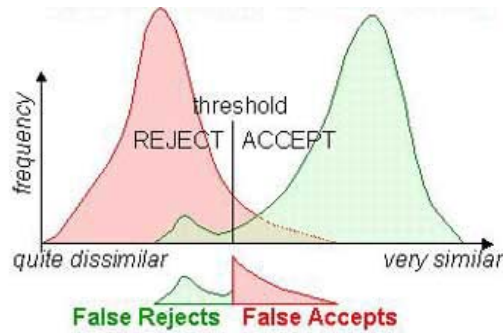
Figure 11: Types of Errors in genuine and impostor distributions.

3.5.2 Similarity Measures

3.5.2.1 Euclidian Distance

The distance between two points is the length of the path connecting them. In the plane, the distance between points (x_1, y_1) and (x_2, y_2) is given by the Pythagorean Theorem:

$$d = \sqrt{(x_2 - x_1)^2 + (y_2 - y_1)^2} \qquad (3.12)$$

For two 3D points, the distance can be computed as follows:

$$d = \sqrt{(x_2 - x_1)^2 + (y_2 - y_1)^2 + (z_2 - z_1)^2} \qquad (3.13)$$

In general for N dimensional distance we can use the following general formula:

$$d = \sqrt{\sum_{i=1}^{n} |x_i - y_i|^2} \qquad (3.14)$$

For curved or more complicated surfaces, the so-called metric can be used to compute the distance between two points by integration. When unqualified, "the" distance generally means the shortest distance between two points. For example, there are an infinite

38

number of paths between two points on a sphere but, in general, only a single shortest path [60].

3.5.2.2 Hamming Distance

Hamming distance is used to measure the similarity between two iris patterns. This measurement is used to recognize whether if two patterns came from the same iris or not. If X and Y are two bitwise templates, and N denotes the total number of bits in the template, then the Hamming distance (HD) is defined as the sum of exclusive-OR between X and Y:

$$HD = \frac{1}{N} \sum_{i=1}^{N} X_i(XOR)Y_i \qquad (3.15)$$

The closest the Hamming distance to 0 the more correlation between two templates is expected. Thus, a zero HD measure means the two templates belong to the same iris and it indicate verification of the identity. The ideal HD measure between two impostor is around *0.5*. In order to get more accurate measurement, we make sure that the IrisCode – template generated from iris – is noise free. So we remove the eyelid and eyelashes from the iris region by using a mask template which is a binary code indicate whether the bit in the template is clear or has a noise. The formula that incorporate noise mask in calculating the HD measure can be drawn as follows:

$$HD = \frac{1}{N - \sum_{j=1}^{N} Xn_j(OR)Yn_j} \sum_{j=1}^{N} X_i \, (XOR)Y_i \, (AND)Xn_i' \, (AND)Yn_i' \qquad (3.16)$$

where X_i and Y_i are the two bit-wise templates to compare, Xn_i and Yn_i denote the corresponding noise masks for X_i and Y_i, and N is the total number of bits represented by each iris pattern [61].

3.5.2.3 Kullback-Leibler Distance (KLD)

In order to compute the similarity between two wavelets subbands we used Kullback-Leibler distance. Two main parameters α and β are used to define the PDF of the Generalized Gaussian Distribution model of a texture which is a subimage of in iris [58]:

$$D\left(p(X; \theta_q)|\ |p(X; \theta_i)\right) = \int p(x; \theta_q) \log \frac{p(x; \theta_q)}{p(x; \theta_i)}\ dx \qquad (3.17)$$

The sum of KLDs between corresponding pairs of subbands is the similarity distance between two textures. Thus the KLD theory provides us with a justified way of combining distances into an overall similarity measurement, and no normalization on the extracted features is needed. if we denote $\alpha_i(j)$ and $\beta_i(j)$ as the extracted texture features from the wavelet subband j of the image I_i then the overall distance between two images I_1 and I_2 (where I_1 is the query image) is the sum of all the distances across all wavelet subbands. It can be formulated as follows [58]:

$$D\left(p(.; \alpha_1, \beta_1)||p(.; \alpha_2, \beta_2)\right) = \log\left(\frac{\beta_1\, \alpha_2\, \Gamma\left(\frac{1}{\beta_2}\right)}{\beta_2 \alpha_1\, \Gamma\left(\frac{1}{\beta_1}\right)}\right) + \left(\frac{\alpha_1}{\alpha_2}\right)^{\beta_2} \frac{\Gamma((\beta_2 + 1)/\beta_1)}{\Gamma(1/\beta_1)} - \frac{1}{\beta_1} \qquad (3.18)$$

Where β is the number of analyzed subbands. Thus the KLD theory provides us with a justified way of combining distances into an overall similarity measurement, and no normalization on the extracted features is needed. The distance function defined in Equation 3.18 is a function of three variables: the ratio of two scales and two shape parameters β_1 and β_2 [58] and it can be formulated as follows:

$$D\left(I_1, I_2\right) = \sum_{j=1}^{B} D(p(.; \alpha_1^{(j)}, \beta_1^{(j)})||p(.; \alpha_2^{(j)}, \beta_2^{(j)})) \qquad (3.19)$$

$$p(x; \alpha; \beta) = \frac{\beta}{2\alpha\Gamma(\frac{1}{\beta})} e^{-(\frac{|x|}{\alpha})\,\beta} \qquad (3.20)$$

Chapter 4

Proposed Multibiometric Fusion

Algorithms

Information fusion becomes vital since no single biometric can provide sufficient solution for high-security applications. Various research studies agreed that it is necessary to use multiple biometrics for verification purposes.

Figure 12: Sample fingerprint from FVC2004 [62].

With the current high demand and awareness of global security, governments as well as business require reliable methods to accurately indentify individual without offence their rights or privacy. Fingerprint and iris recognition systems are proven as reliable techniques, however, the data sensing methods currently in use in both modalities limit their versatility [9].
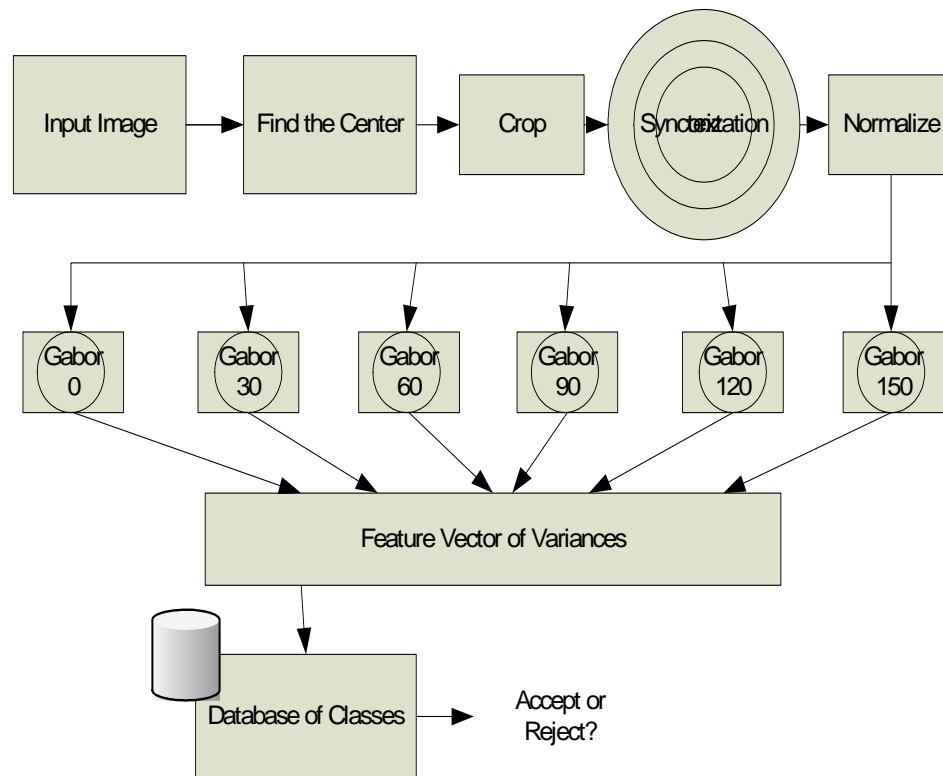
Figure 13: Filter-based fingerprint recognition system.

4.1 **Fusion of Fingerprint Images at the Sensor Level**
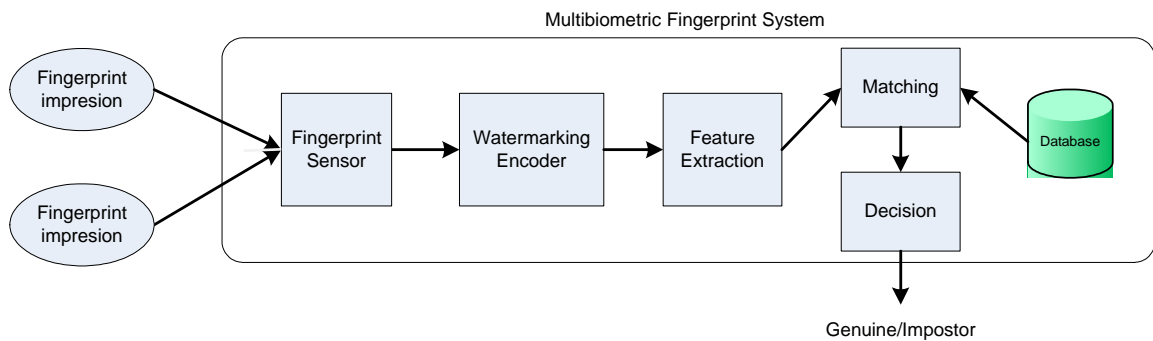
Figure 14: Modified fingerprint recognition system with watermarking.

4.1.1 System Design

The system is decomposed into five modules. The first module is fingerprint sensor module where image acquisitions take place. The second module is the new introduced module where fusion of two images takes place using watermarking technique. The third module is the feature extraction module where the FingerCode produced using filter-based or any other feature extraction algorithm for fingerprints. The forth module is the matching module where two FingerCode being compared using Euclidian distance. The last module is the decision module that either rejects or accepts the individual based on the matching score and system threshold.

4.1.2 The process

The proposed fusion of fingerprint works at the sensor level with the raw fingerprint images. Two fingerprint snapshot is acquired from the individual. We apply a wavelet-based watermarking on one image to embed it in the host image which is the other

snapshot of the same individual. The two samples are from different fingers. The features of the fingerprint are extracted from the new generated image using the following stages:

- Apply the 2D discrete wavelet transform (DWT) for the two impressions of the fingerprint using 3 decomposition levels.

- Compute the approximation and detail coefficients.

- Fuse every detail coefficients into a single coefficient.

- Apply the inverse 2D discrete wavelet transform (DWT) to get the fused fingerprint image.

- Use a bank of Gabor filters to capture the global and local details of fingerprint.

- Produce the FingerCode sequence.

- Matching is based on the Euclidean distance between the two corresponding FingerCodes.

- Filter-based fingerprint: Determine the reference point (core point) and region of interest for the fingerprint image.

- Segment the region of interest around the core point.

- Filter the region of interest in eight different directions using a bank of Gabor filters

- Compute the average absolute deviation from the mean of gray values in individual sectors in filtered images to define the feature vector of the FingerCode.
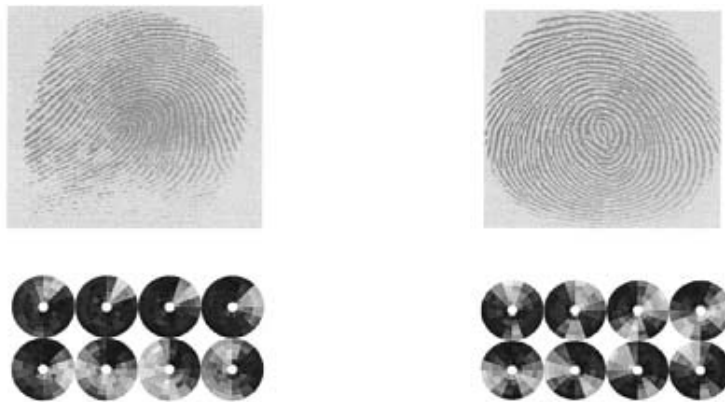
Figure 15: Two different fingerprints and their generated FingerCodes.
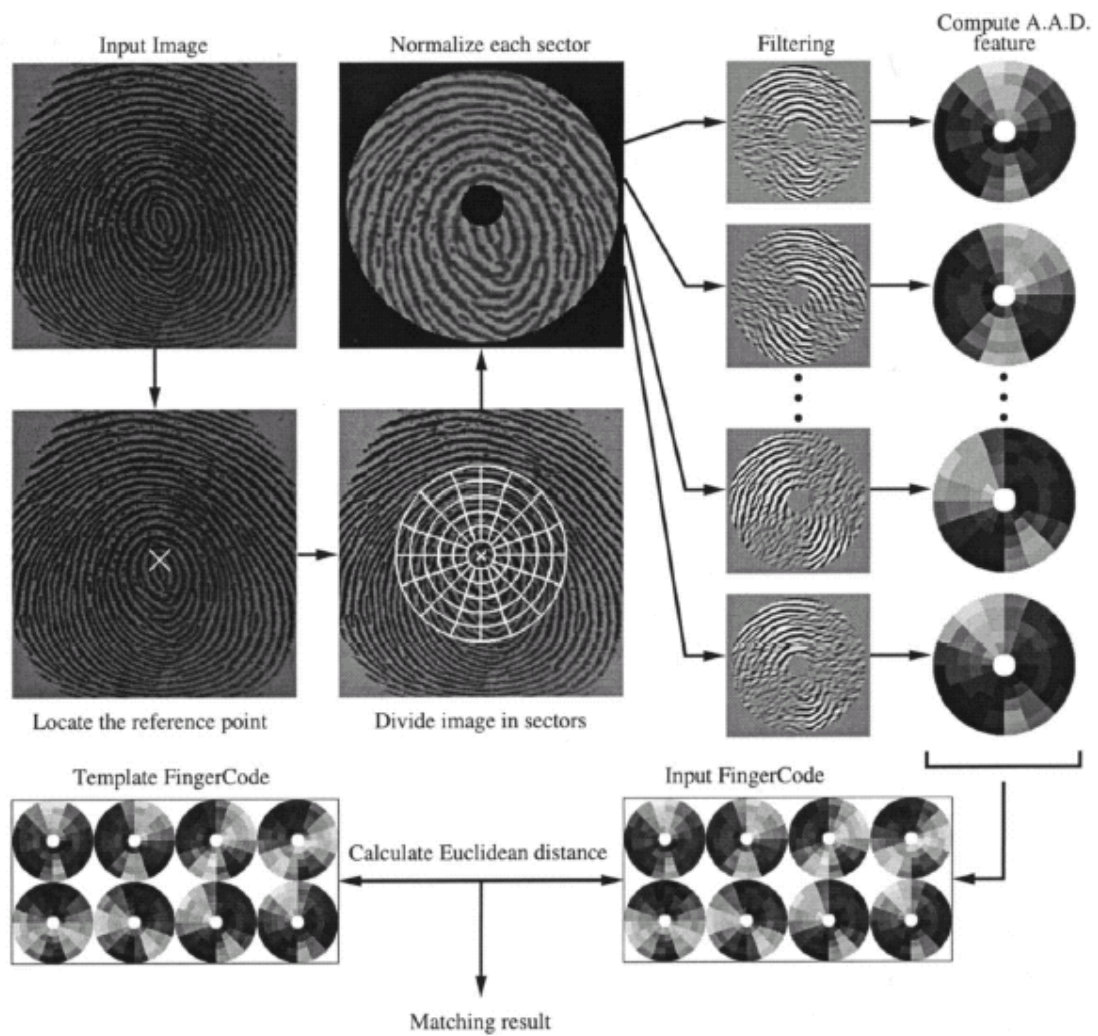
Figure 16: Summary of Filter-based fingerprint matching.

4.1.3 Database used:

FVC2004 DB1 for fingerprint images [62]: The images were collected using optical sensor "V300" by CrossMatch. The images were collected from thirty students (24 years old on the average) enrolled in the Computer Science degree program at the University of Bologna. Each student was invited to present him/herself at the collection place in three distinct sessions, with at least two weeks time separating each session. Forefinger and middle finger of both the hands (four fingers total) of each student were acquired by interleaving the acquisition of the different fingers to maximize differences in finger placement. No efforts were made to control image quality and the sensor platens were not systematically cleaned. At each session, four impressions were acquired of each of the four fingers of each student. During the first sessions, individuals were asked to put the finger at a slightly different vertical position (in impressions 1 and 2) and to alternate low and high pressure against the sensor surface (impressions 3 and 4). During the second session, individuals were requested to exaggerate skin distortion (impressions 1 and 2) and rotation (3 and 4) of the finger. During the third session, fingers were dried (impressions 1 and 2) and moistened (3 and 4). The total number of images is 800 images.

4.2 Fusion of Iris Images at the "Pre-Feature" Level

A novel approach to fuse iris images into a single normalized iris image using a wavelet-based texture retrieval and GGD is presented in this section. Alpha and Beta that describe the GGD becomes the feature for each subband.

4.2.1 The system design

The iris system used on our work can be categorized on the following modules:

1- Iris image pre-processing (Segmentation and Normalization).

2- Iris fusion.

3- Iris feature extraction (generate IrisCode).

4- Iris matching (Calculate the Hamming distance).

In real systems we have to have another module for data acquisition where image being captured and stored in the correct format, but in our system we used a ready iris database MIRLIN so we don't have to worry about iris image acquisition although it is considered as the most important step in iris recognition system.

4.2.1.1 Iris image pre-processing (Segmentation and Normalization)

In the image pre-processing step we take an iris image and extract the iris from the image. This step includes identifying the iris boundary and the noise. In order to do that, first the iris (outer boundary with the sclera) and pupil (inner boundary) are localized. This localization step is done by using a Hough transform and edge detection to calculate the exact parameters of outer and inner circles. Hough transform is being widely used in literature to detect curves in an image. The main strength of Hough transform in detecting shapes in images is that it is not affected by noise or gabs in the shape. Secondly the

noise is identified, namely, eyelid, eyelashes and other irrelevant part of the iris including lightening noise. After the iris boundaries and the noise being determined we use Daugman's Rubber sheet model to normalize the iris by remapping each point within the iris region to a pair of polar coordinates (r, θ) where r is on the interval $[0,1]$ and θ is angle $[0, 2\pi]$.
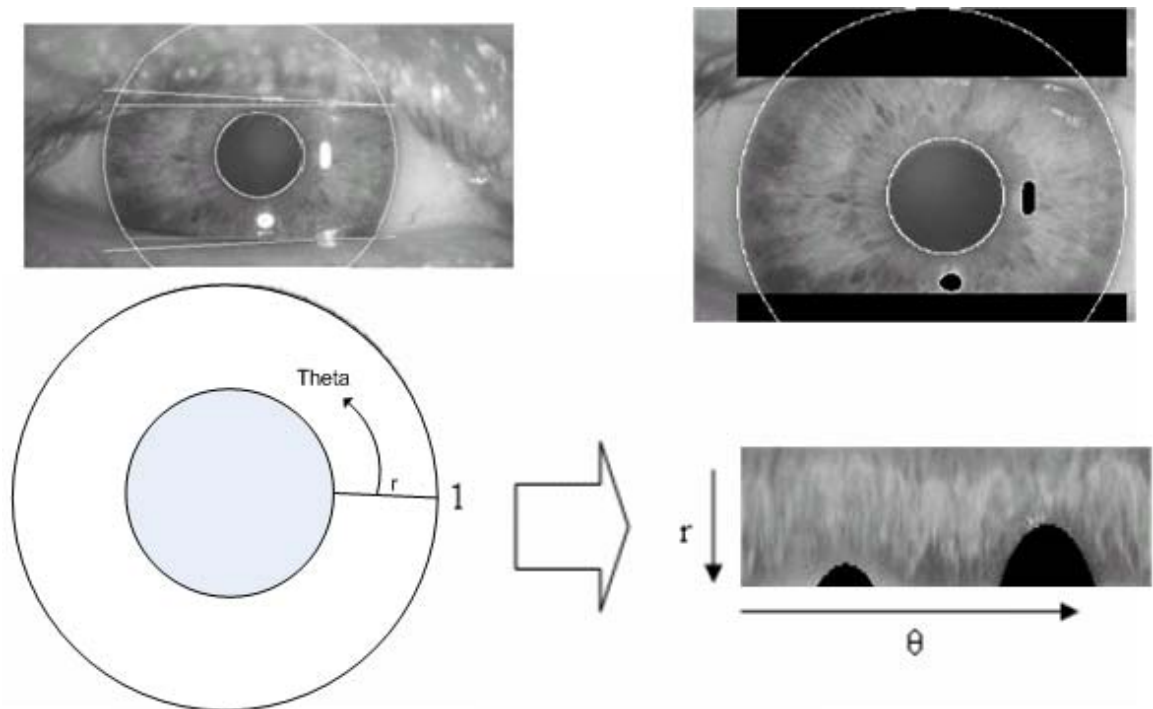
Figure 17: Iris Localization and Normalization process.

4.2.1.2 Iris fusion

In the iris fusion module the normalized iris image is divided into subimages from a set of multiple images from the same iris. Each subimage will be treated as a texture and a perfect match for that texture will be retrieved from the set of iris images. The retrieval

process is described in Section 4.2.2. The normalized image is then reconstructed from the best texture in all subimages.

4.2.1.3 Iris feature extraction (generate IrisCode)

In this module, the IrisCode is generated from the fused normalized iris. The generation of IrisCode which is the feature extracted from the iris is produced by convolving the normalized iris pattern with 1D Log-Gabor wavelets. In order to do this, the 2D normalized iris is isolated into a number of 1D signals, and then these 1D signals are convolved with 1D Gabor wavelet. We consider the rows of the 2D normalized iris as the 1D signals and each row denotes a singular ring of the iris region. We use angular direction which corresponds to the columns of the normalized pattern instead of choosing the radial one since the maximum independence occurs in the angular direction. In order to prevent influence of noise in the output of the filtering we set the intensity values at known noise areas in the normalized pattern to the average intensity of the surrounding pixels. After that Dougman method is applied to the output of filtering to produce four levels by phase quantization. Each filter produces two bits of data for each phasor. This encoding process using Daugman algorithm and Gabor filters produces a bitwise template containing a number of bits of information, and a corresponding nose mask which corresponds to corrupt areas within the iris pattern, and marks bits in the template as corrupt [61].

4.2.1.4 Iris matching

This is the last module in our system since we don't have a decision module. In this module, the produced IrisCode is matched against in a set of stored IrisCode. These

stored iris code are inter-class templates and intra-class templates. The comparisons between two IrisCodes are done using Hamming distance. Only the bits in the IrisCode that correspond to '0' bits in the noise masks of both iris patterns are calculated. Ideally, two IrisCodes from the same iris should give a Hamming distance of '0.0' but in practice this will not occur. This happened because of the different noise in each iris and the normalization process is not perfect. To deal with misalignments in iris between different iris images, Daugman method is also implemented by shifting the IrisCode left and right bit-wise and a number of Hamming distance values are calculated from successive shifts and the lowest is taken.
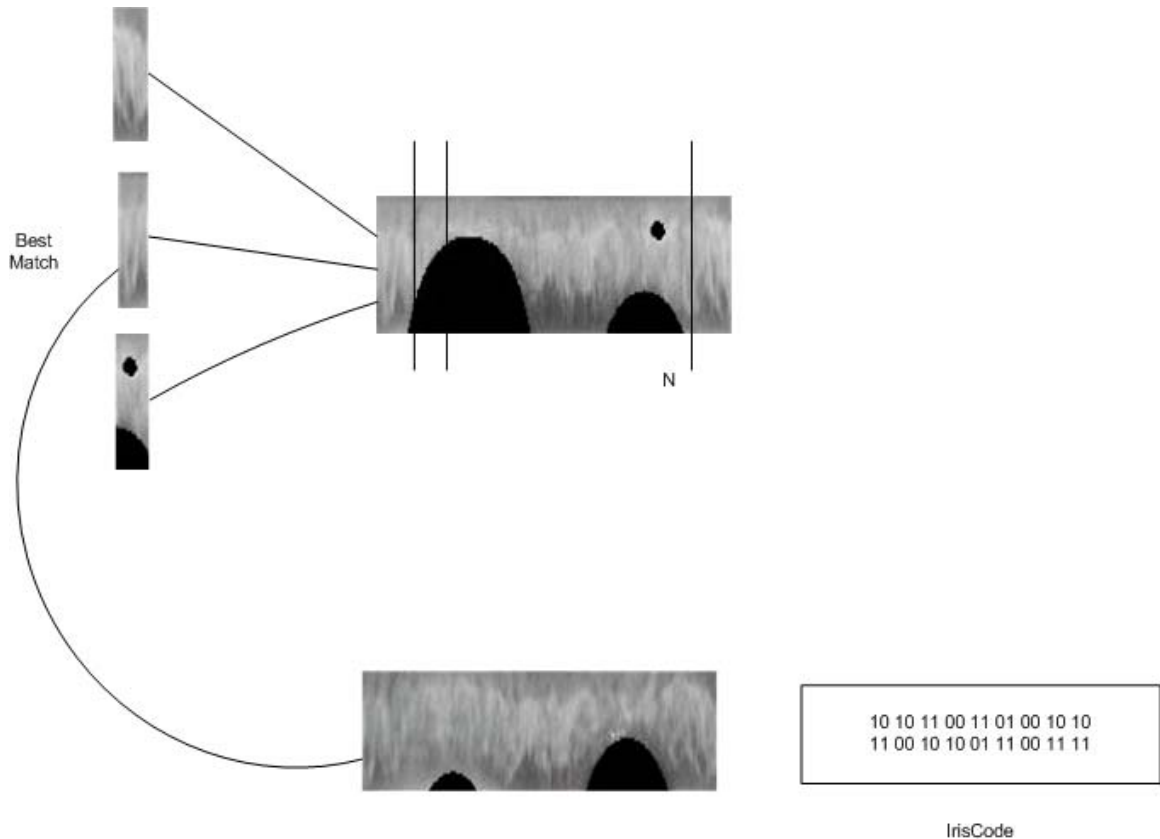
Figure 18: Proposed Fusion Scheme.

50

4.2.2 Database Used:

MIRLIN IRISBASE: The commercial database is provided by Smart Sensors, Inc., UK. The iris images were captured with ISG LightWise LW-1.3-S-1394 camera. It consists of 800 people (1600 images): 20 images for each left and right eyes. In our experiment, we restrict the simulation to the first 400 people only from the database with 10 images per person (5 for right eye and 5 for left eye). The images are high quality images with (1280 * 960) pixel resolution. A typical capture procedure consists of the subject placing his/her head onto the chinrest while the operator adjusts the lens to get the iris texture into focus. A sequence of 200 frames is then acquired from each eye and 20 best ones selected for inclusion into the final database. The entire procedure is carried out in approximately 5 minutes. A daylight cut-off filter was used to remove reflections caused by environmental light sources. The filter passed Infrared light without any attenuation, thereby retaining all image information. Infrared light is used to obtain better iris texture than is possible with the use of visible light. In order to constrict the pupil there is a need for sufficient visible light during the capture. This has the added benefit of protecting the cornea by restricting the amount of light going in. To prevent shadows from appearing over the iris due to eyelashes, the light was shown at an angle from below the camera. The specular reflections were restricted to the pupil region to avoid losing iris texture due to bright spots falling onto it [63].

Chapter 5

Simulation Results

5.1 Introduction

In this Chapter, we will report the performance of the fusion strategies on different biometric databases. Performance evaluation experiments were carried out to find the "best" *separability* index [59], the smallest false match and false accept rates. The reported results clearly indicate the superior performance of multibiometric systems over their uni-biometric counterparts when using the proposed fusion strategies. More specifically, results clearly show that the watermarking process enables efficient fusion of several fingerprint impressions which would allow biometric systems based on multiple fingerprint impressions to have better matching performance than those using single fingerprint impression. Additionally, the proposed iris fusion scheme provides iris-based systems with higher quality iris images that would implicitly yield more accurate recognition rates and less recognition errors.

5.2 Fusion of Fingerprint Images at the Sensor Level

Two different experiments were conducted. In the first one, the performance of a single-fingerprint biometric system was evaluated. Fused fingerprint images resulting from the

watermarking process were used for matching during the second experiment. For equal-foot comparisons, a fixed matching threshold was used in both experiments.

1.2.1 First Experiment:

A filter-based algorithm, based on a bank of Gabor filters, was used [47,9]. The algorithm, described in Chapter 4, captures both local and global details in a fingerprint as a compact fixed length FingerCode [9]. The resulting codes are compared using the Euclidian distance for matching purposes. The matching procedure is carried out among fingerprint samples of the same person (*intra-class* samples) and fingerprints samples of different persons (*inter-class* samples). It should be noted that one person is represented by the impressions of one or more fingers. Intra-class matching results will represent the genuine score and the impostor scores are given by the inter-class matching results. Then, the FRR and FAR results are calculated from the genuine and impostor scores in order to compare the accuracy of the system before and after the watermarking process.

Figure 16 shows the genuine versus impostor distributions. As it can be seen, the two distributions have a wide, though small in area, overlapping. This overlapping indicates that many genuine fingerprint samples would be classified as impostor if the matching threshold is further lowered. In Figure 19, the corresponding genuine and impostor distribution is illustrated. In Figure 20, the FAR and FRR rates are shown. In Figure 21, different false and positive alarm is quantized.
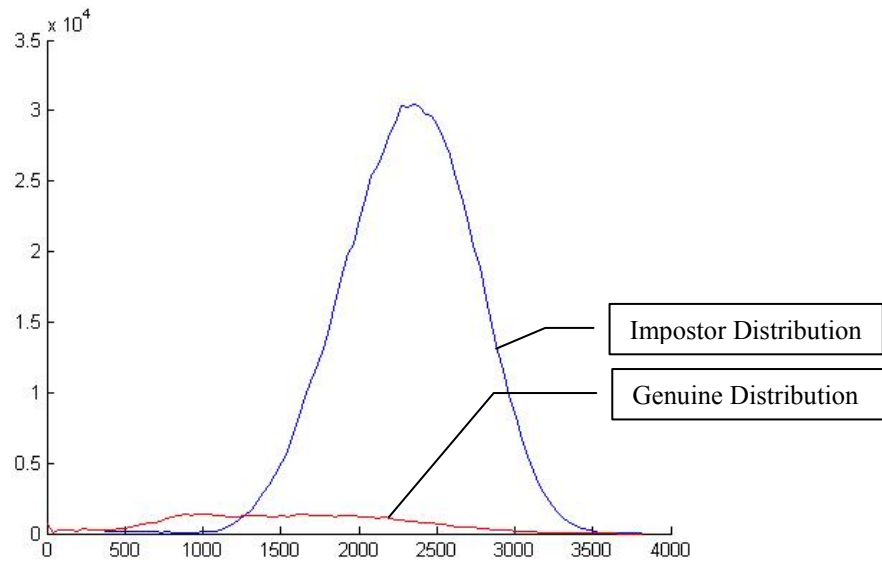
Figure 19: Genuine vs. Impostor density for fingerprint matching without watermarking-based fusion.
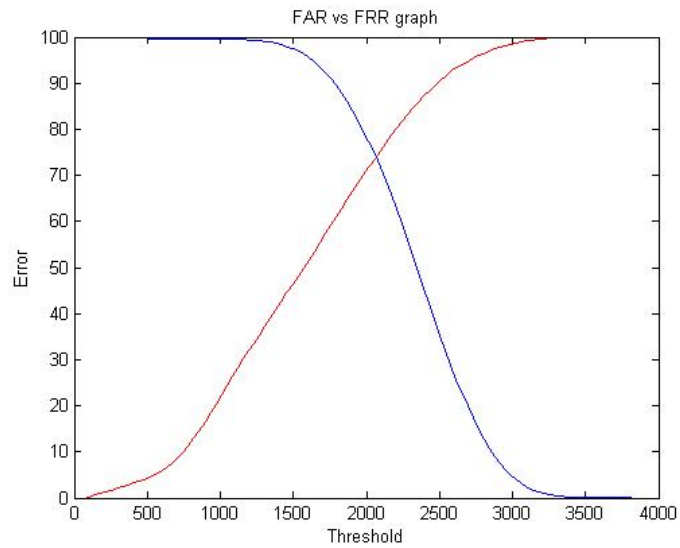
Figure 20: FAR vs. FRR for fingerprint matching without watermarking-based fusion.
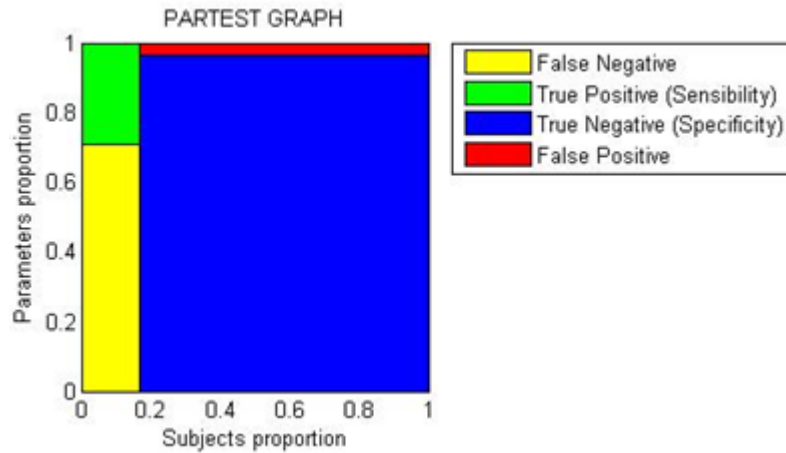
Figure 21: PARTEST Graph for fingerprint matching without watermarking-based fusion.

1.2.2 Second Experiment:

In this experiment, we introduce a pre-processing step before feature extraction. In this step, we do the information fusion after image acquisition using wavelet-based watermarking. First, we applied Haar filter to the host image in order to transform the image into 2D wavelet. We embed the watermark into the high frequency bits of the approximation coefficient of the host image. The watermarked image is built again using inverse wavelet of the coefficients. The rest of the experiment will be as the first experiment where feature extraction and matching is done for genuine and impostor. Figure 22 and Figure 23 shows the performance of the second experiment alone while Figure 24 and Figure 25 presents both experiments genuine and impostor distribution. It shows that the new algorithm reduces the overlapping between the genuine and impostor scores which improves the accuracy of recognition.
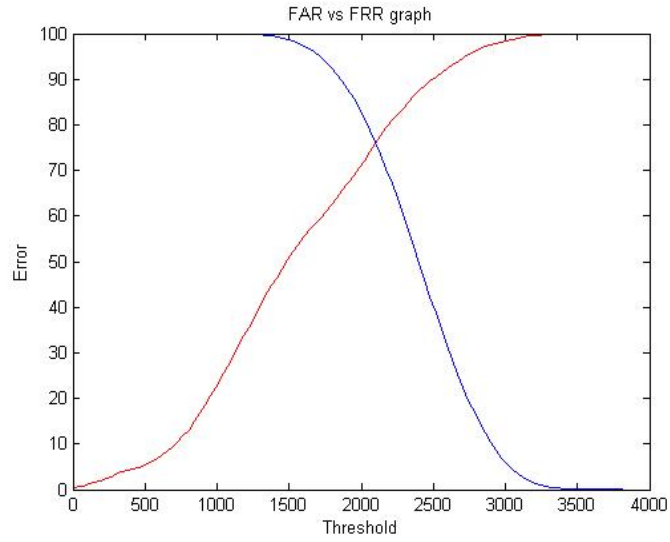
Figure 22: FAR vs. FRR for fingerprint matching with watermarking-based fusion.
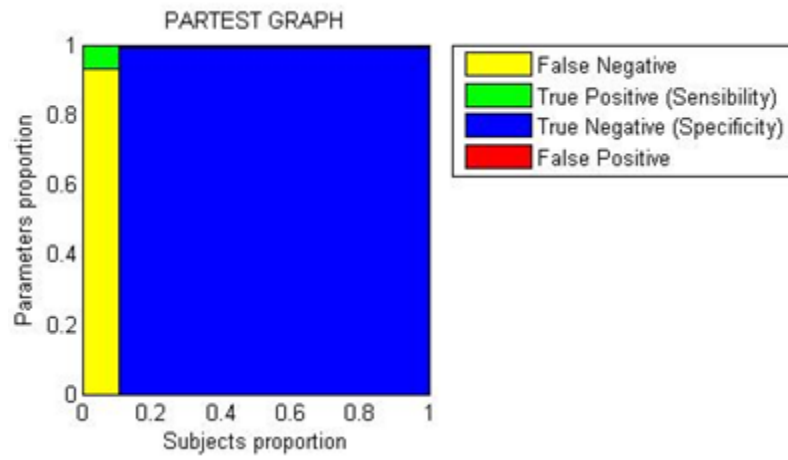
Figure 23: PARTEST Graph for fingerprint matching with watermarking-based fusion.

Table 3: Watermarking embedding code in Matlab.

```
[ca,ch,cv,cd] = dwt2(A,'haar');
c1 = [ch cv cd];

[h, w] = size(ca);

W=dmg(W,A);

[caa chh cvv cdd]=dwt2(W,'haar');
W=caa;

% Adding watermark image.

for i=1:h
    for j=1:w
        if ca(i,j)>Tr
            Ca(i,j)=ca(i,j)+k*W(i,j);
        else
            Ca(i,j)=ca(i,j);
        end
    end
end
```

Table 3, shows a snapshot of the algorithm implemented in Matlab and used for

watermarking.

The experiment results shows that fusion of two fingerprint impressions increases the accuracy of the system identification as shown on the following figures.

Figure 24: Normalized Genuine vs. Impostor for both experiments.
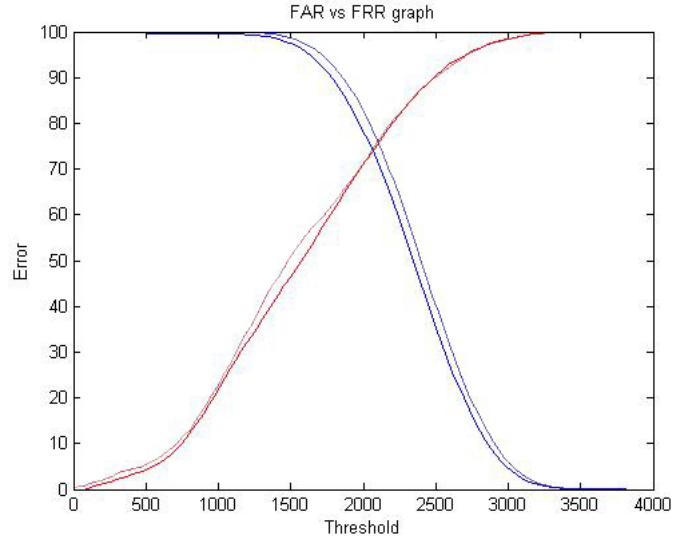
Figure 25: FAR vs. FRR for fingerprint matching with and without watermarking-based fusion.

Test comparisons

	Exp1	Exp 2
Prevalence	16.60%	10.00%
Sensibility	28.60%	6.40%
False positive proportion	71.40%	93.60%
Specificity	96.80%	99.60%
False negative proportion	3.20%	0.40%
Discriminant Power	1.4	1.6
Accuracy or Potency	85.50%	90.30%
Mis-classification Rate	14.50%	9.70%
Predictivity of positive test	64.00%	64.70%
Predictivity of negative test	87.20%	90.50%
Positive Likelihood Ratio	8.9	16.4
Negative Likelihood Ratio	0.7	0.9
Test bias	0.4	0.1

Table 4: Comparison of experiments 1 and 2.

Table 4, presents a comparison between both experiments using different quality measures. It shows clearly that watermark fusion outperform the regular uni-fingerprint matching algorithm specially in terms of False positive and False negative proportions, accuracy, predictivity and mis-classification rate.
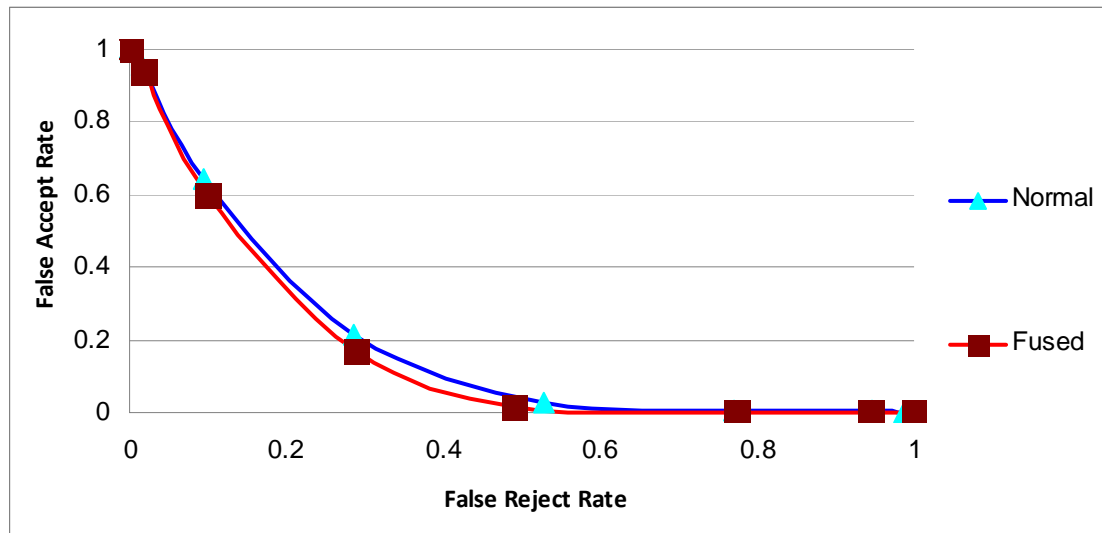
Figure 26: ROC for Fingerprint System.

Figure 26: ROC for Fingerprint System., shows the ROC curve for the experiment before and after fusion and it clearly shows an improvement of accuracy of the proposed fusion scheme.

5.3 Fusion Iris Images at the "Pre-Feature" Level

5.3.1 Experimental Setup

The experiments in this section are performed on the MIRLIN IRISBASE: The commercial database is provided by Smart Sensors, Inc., UK. The iris images were captured with ISG LightWise LW-1.3-S-1394 camera. It consists of 800 people (1600 images): 20 images for each left and right eyes. In our experiment, we restrict the simulation to the first 400 people only from the database with 10 images per person (5 for right eye and 5 for left eye). The images are high quality images with (1280 * 960) pixel resolution. A typical capture procedure consists of the subject placing his/her head onto the chinrest while the operator adjusts the lens to get the iris texture into focus. A sequence of 200 frames is then acquired from each eye and 20 best ones selected for inclusion into the final database. The entire procedure is carried out in approximately 5 minutes. A daylight cut-off filter was used to remove reflections caused by environmental light sources. The filter passed Infrared light without any attenuation, thereby retaining all image information. Infrared light is used to obtain better iris texture than is possible with the use of visible light. In order to constrict the pupil there is a need for sufficient visible light during the capture. This has the added benefit of protecting the cornea by restricting the amount of light going in. To prevent shadows from appearing over the iris due to eyelashes, the light was shown at an angle from below the camera. The specular reflections were restricted to the pupil region to avoid losing iris texture due to bright spots falling onto it [63]. In Figure 42 we present samples of person images left and right eyes from MIRLIN database.
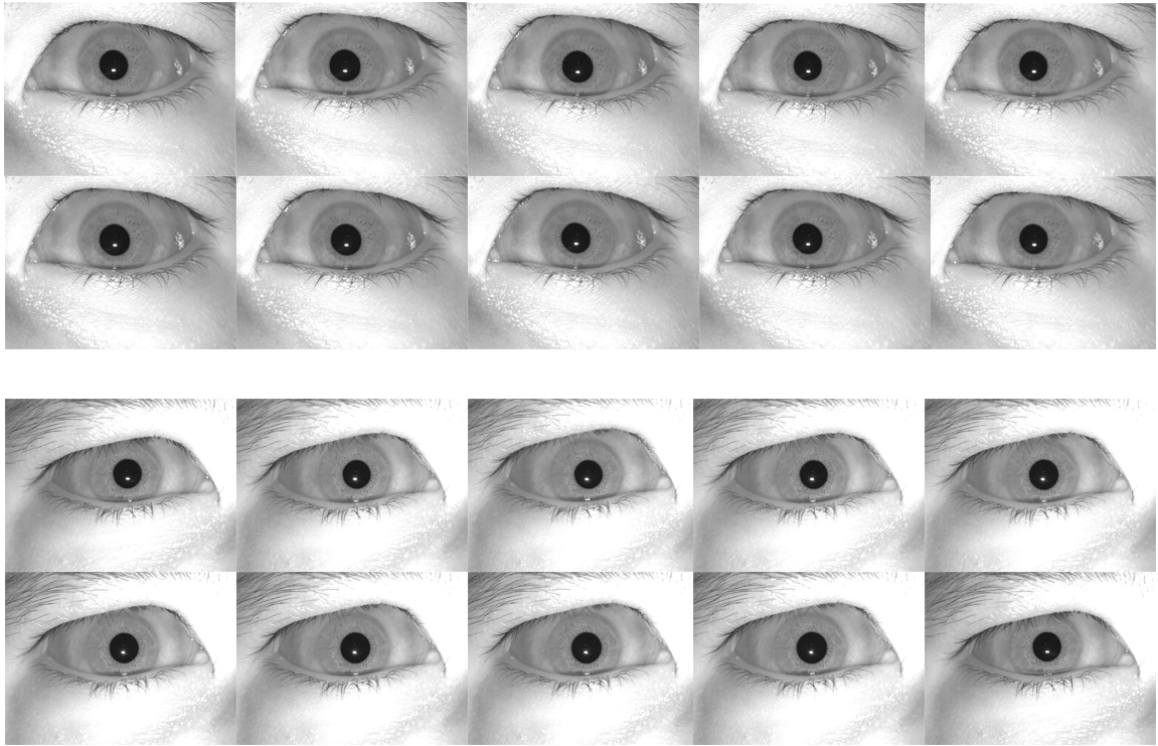
Figure 27: Sample of Person images left and right eyes from MIRLIN database.

The most import variables in the experiments were the information retrieval variables. Namely, the number of wavelet decomposition used in feature extraction of textures, the wavelet filter used (the low-pass and high-pass filters), the edge-handling scheme (periodic or symmetric image extension mode). Each experiment is done in the following steps:

- Find the normalized iris image.

- Divide it into N blocks (12 in our case).

- Each block represents a texture (see Figure 28).
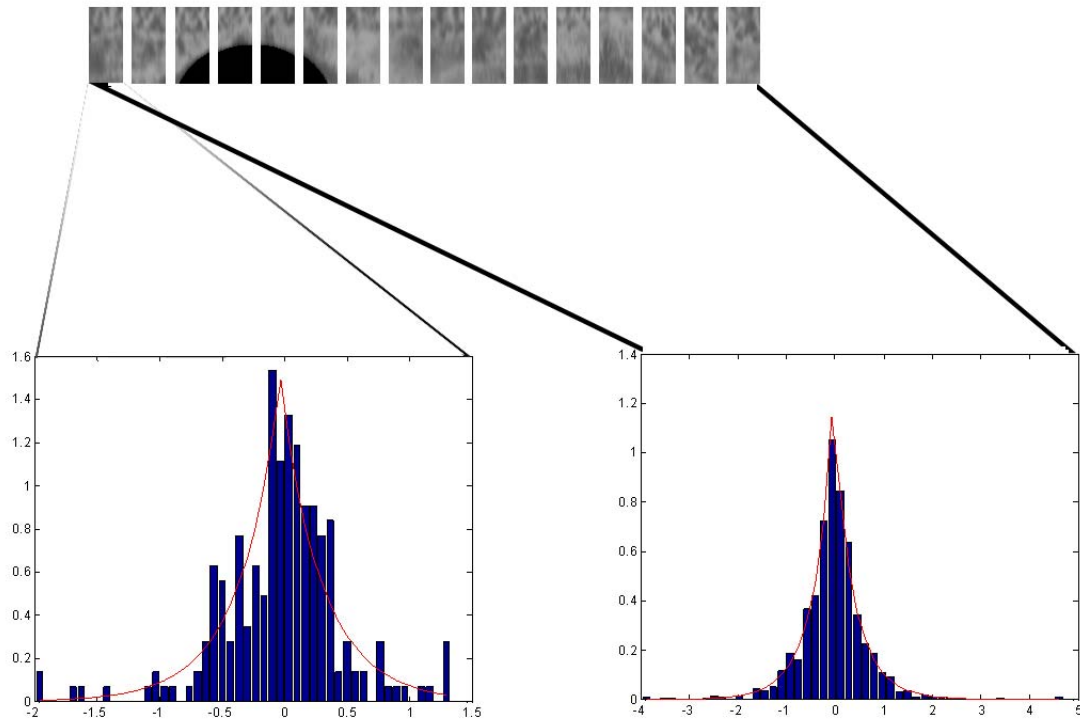
Figure 28: Sample of GGD of the complete eye and a part with fitting approximated using ML.

- A new fused normalized image is constructed by retrieving the best sub-image in each block from the 10 images. The selection procedure is as follows:

  - Apply the DWT filters such as like Daubechies 'db1' or 'db2' .. 'db45'. See Figure 29.
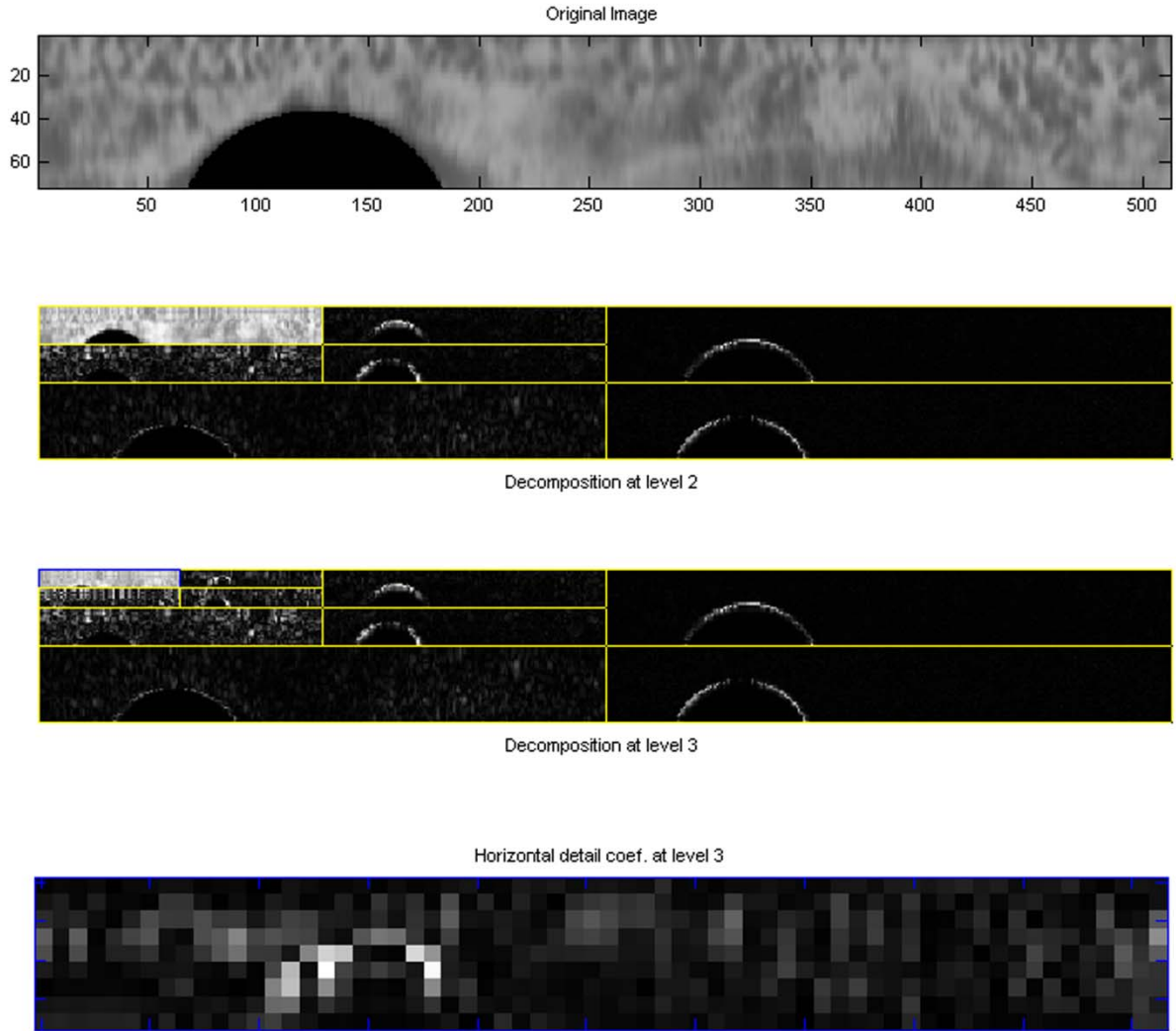
Figure 29: Sample of normalized iris decomposition at level two and level three.

- o Estimate the coefficients, α and β, to construct the feature vectors using the ML estimation algorithm for the GGD coefficients. See Figure 28: Sample of GGD of the complete eye and a part with fitting approximated using ML..

- o Use Kullback-Leibler Distance to select the best match among a set of subimages of the same person (see Figure 30).

- o Reconstruct the normalized iris image from the best match subimages.

- Encode the iris code from the new normalized iris.

- Calculate the HD measures between irises to estimate the Genuine and Impostor distributions.
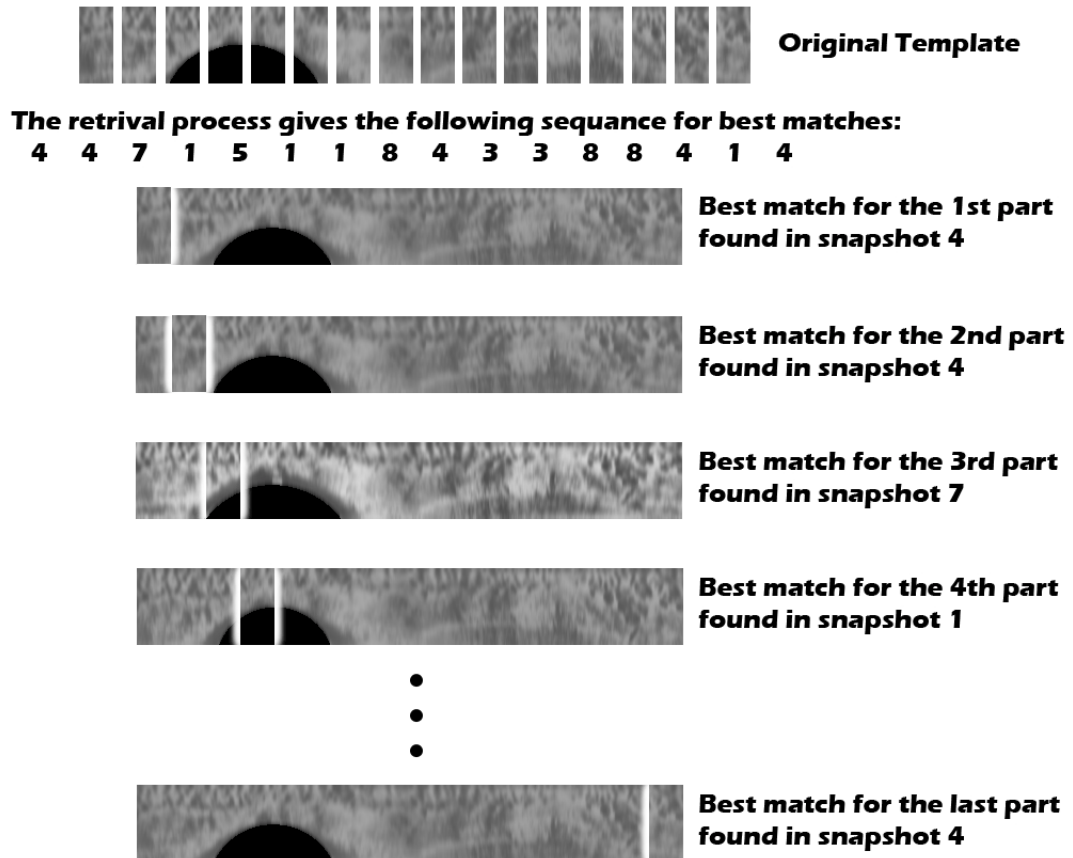
Figure 30: Sample of construction process.

5.3.2 Results

The result of the experiments can be summarized in (Table 5). It shows the decidability indices for our experiment with four different wavelet filters used in wavelet

decomposition namely, Daubechies 1, 6, 8 and 10. It is clear from this Table that the proposed fusion scheme has considerably improved the matching performance.

Table 5: Results of the experiment applying different filters for wavelet decomposition at level two.

Decidability Index	Before	After	Improvement (%)
DWT DB1	0.2848	0.2928	2.80
DWT DB6	0.2843	0.3006	**5.73**
DWT DB8	0.2848	0.3003	5.44
DWT DB10	0.2845	0.3007	5.69

We further investigate the effect of changing the edge-handling scheme of wavelet decomposition (DWT extension modes). The extension modes represent different ways of handling the problem of border distortion in the analysis. 'sym' value means boundary value symmetric replication. 'per' means periodization, This mode produces the smallest length wavelet decomposition. We investigate the effect of changing the mode in the second level and third level of decomposition using "Daubechies 6" the filter that gives us the best results in the previous experiment. We summarize the result of this experiment in (Table 6).

Table 6: The effect of using periodical and symmetric edge-handling at 2nd and 3rd level of decomposition.

Decidability Index	2 Level of Decomposition			3 Level of Decomposition		
	Before Fusion	After Fusion	Percent Improved	Before Fusion	After Fusion	Percent Improved
Periodical edge-handling	0.2848	0.3018	**5.97%**	0.2848	0.3008	5.62%
Symmetric edge-handling	0.2843	0.3006	5.73%	0.2848	0.3018	5.96%

Reported values for the Equal Error Rate for complete set of experiments summarized in (Table 7: EER for the 7 experiments before and after fusion).

Table 7: EER for the 7 experiments before and after fusion.

	Before Fusion	After Fusion
DB06_sym_2	0.7221	0.3799
DB06_per_2	0.7196	0.3481
DB06_sym_3	0.7196	0.3908
DB06_per_3	0.7196	0.3485
DB08_sym_2	0.7196	0.3765
DB01_sym_2	0.7196	0.2879
DB10_sym_2	0.7185	0.3724

5.3.3 Performance Results:

The results of our set of experiments are presented in four graphs for each experiment. The first graph is the genuine versus impostor score distributions that emphasize on the overlapping between the genuine and the impostor curves before and after experiment. The reported matching scores after fusion indicate the improvement in the overall system performance after the incorporation of several iris samples through the proposed fusion scheme. It should be noted that in this graph the impostor distribution is almost the same before and after distribution. The second graph shows the Detection Error Trade-off (DET) curve. This graph clearly present the improvement in the proposed algorithm compared to the regular Daugman's algorithm. The third graph shows the ROC (Receiver Operating Characteristic) curve. The ROC curve illustrates at different thresholds on the matching score the relationship between false accept rate and the genuine accept rate which is almost perfect. The last graph shows the relationship between the FAR and FRR.

5.3.3.1 Experiment 1: using db1, two levels and symmetric edge-handling

This experiment setup shows the least increase in performance in terms of the separation between the genuine and impostor scores distributions as shown in Figures Figure 31-Figure 34. However, this experiment still gives some improvement (around 2.8%) which decreases the FAR as shown in Figures Figure 32 and Figure 34.
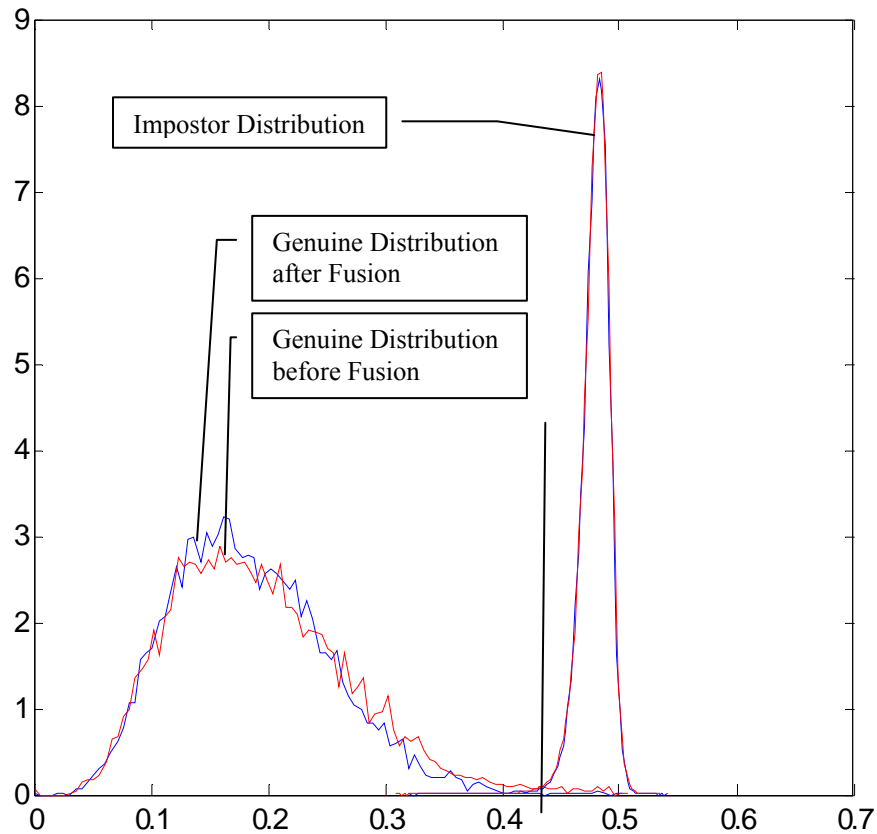
Figure 31: Genuine and Impostor Distribution using db1, two levels and symmetric edge-handling.
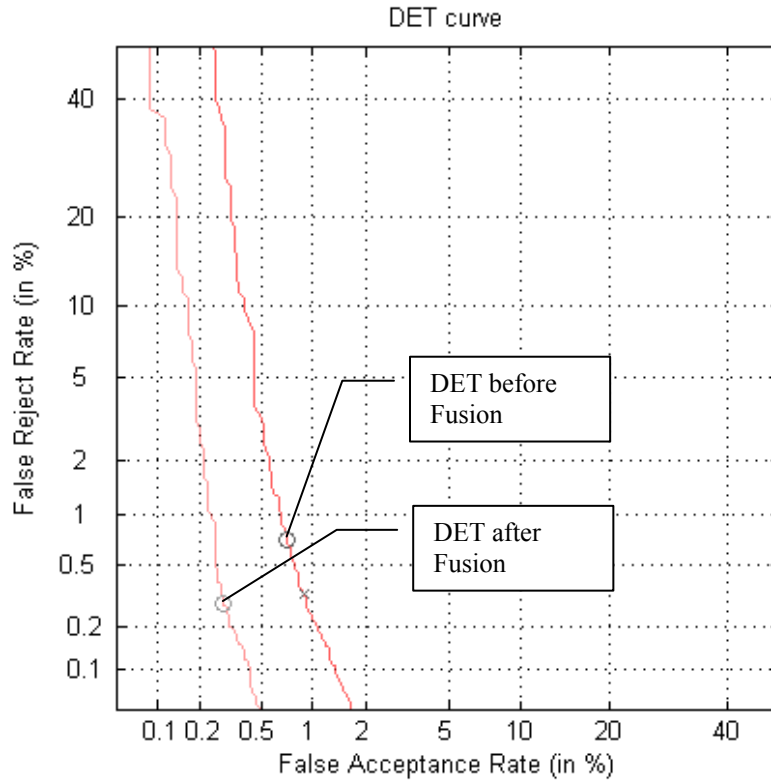
Figure 32: DET Curve using db1, two levels and symmetric edge-handling.
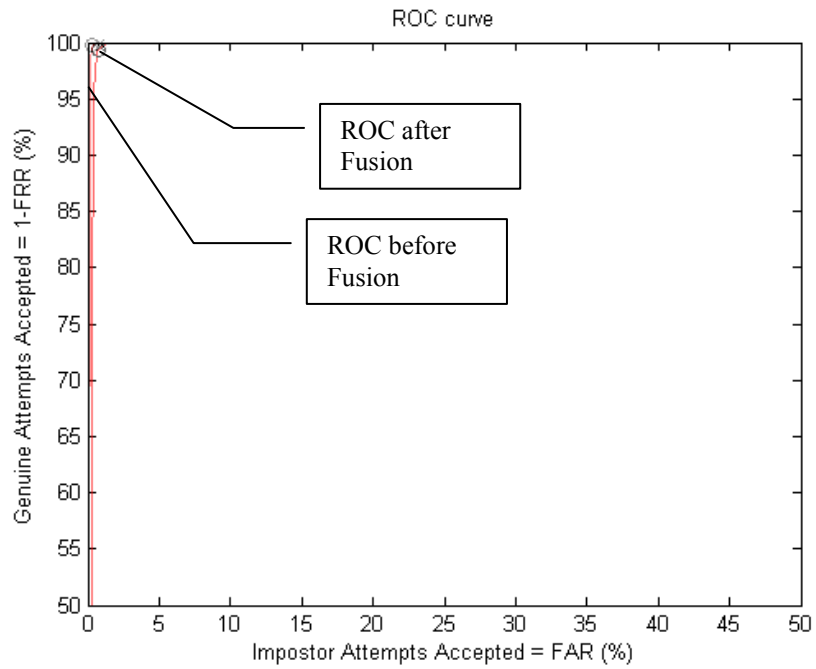
Figure 33: ROC Curve using db1, two levels and symmetric edge-handling.

69
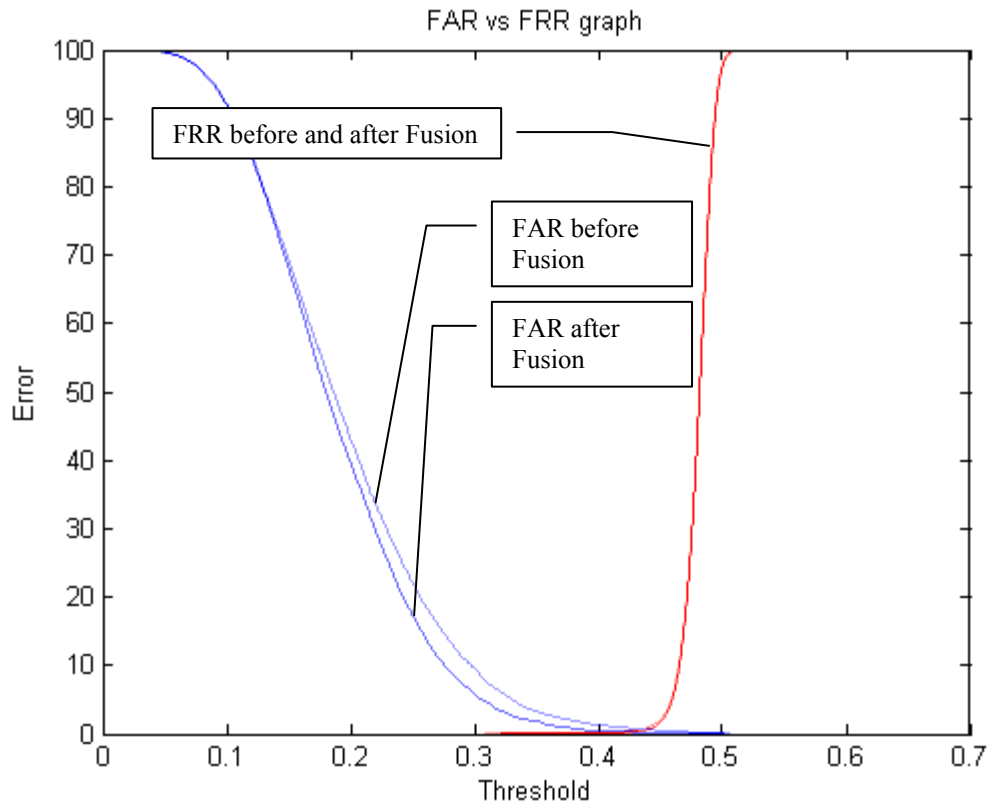
Figure 34: FAR vs. FRR using db1, two levels and symmetric edge-handling.

5.3.3.2 Experiment 2: using db6, two levels and symmetric edge-handling

This experiment configuration perform the second best increase in performance among our set of experiments configurations in terms of the separation between the genuine and impostor scores distributions as shown in Figures Figure 35-Figure 38. Once again, this experiment gives the second most improvement (around 5.73%) which decreases the FAR as shown in Figures Figure 36 and Figure 38.
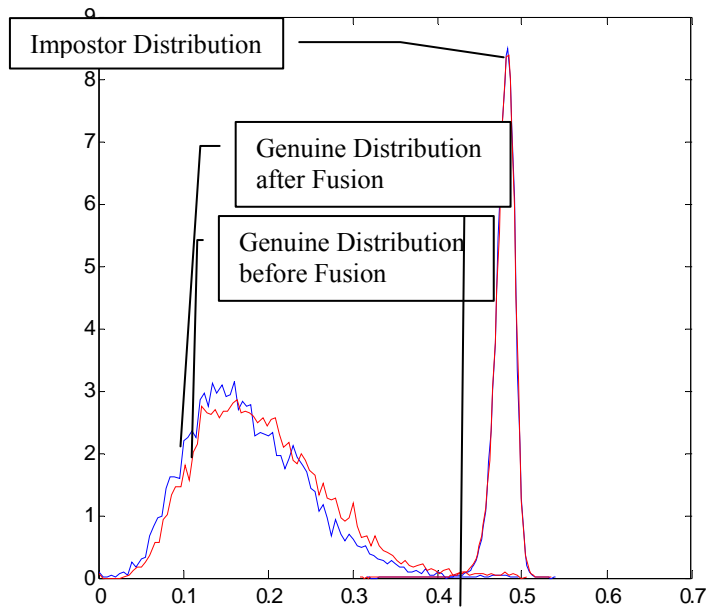
Figure 35: Genuine and Impostor Distributions using db6, two levels and symmetric edge-handling.
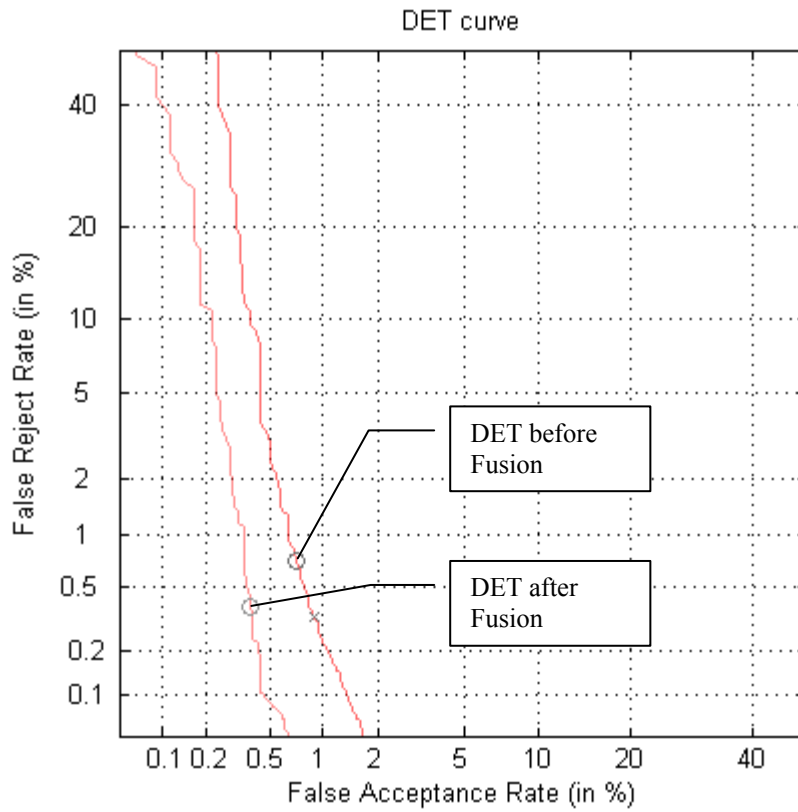
Figure 36: DET Curve using db6, two levels and symmetric edge-handling.

71
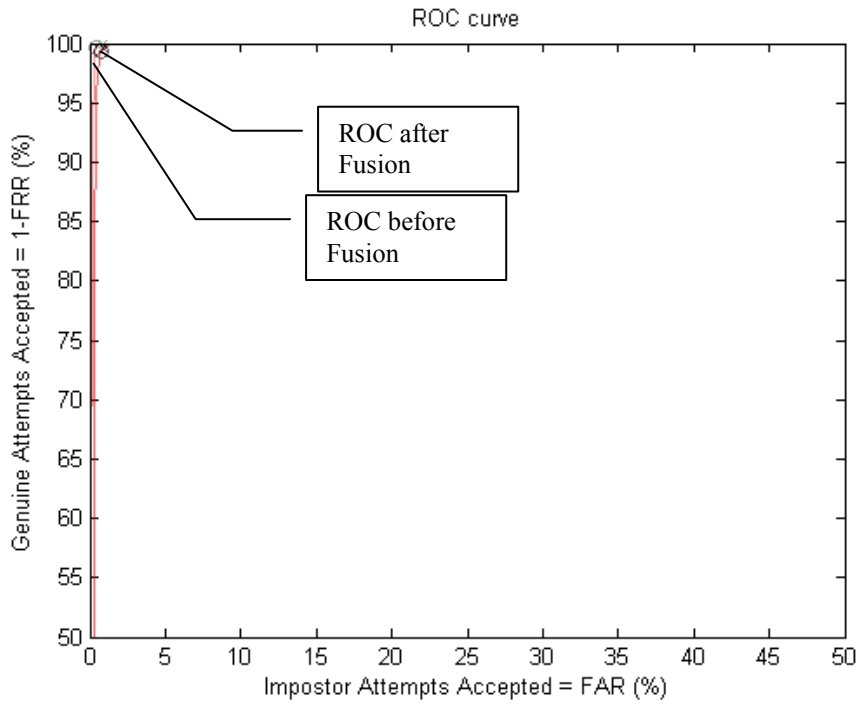
Figure 37: ROC Curve using db6, two levels and symmetric edge-handling.
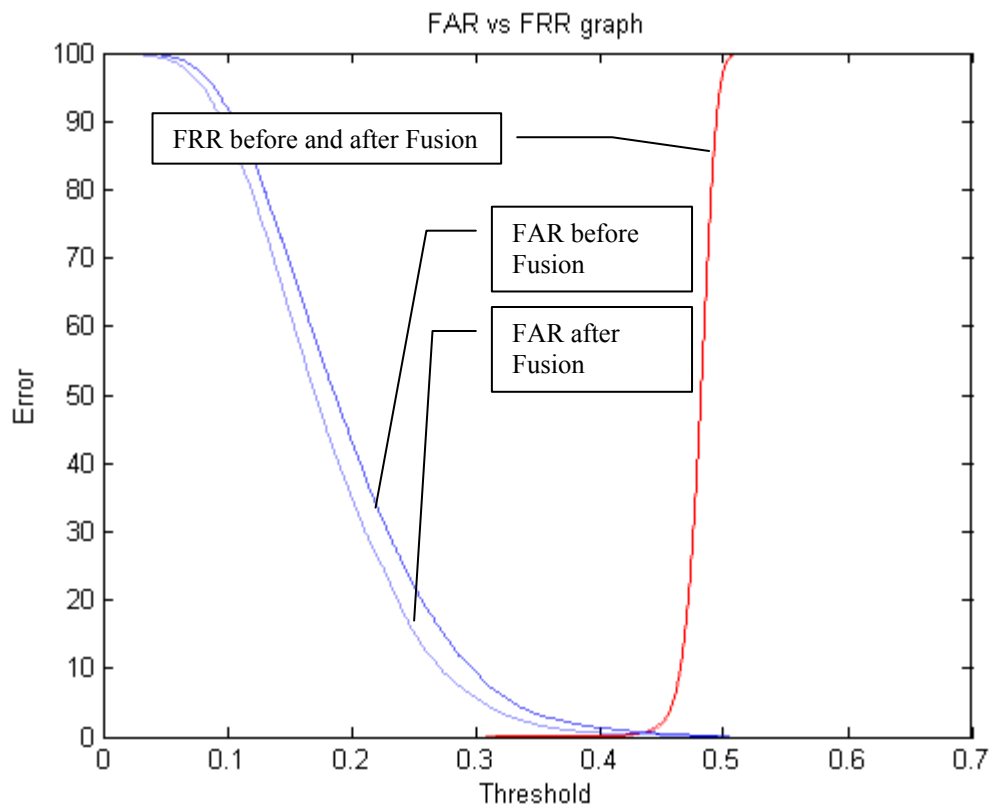
Figure 38: FAR vs. FRR using db6, two levels and symmetric edge-handling.

5.3.3.3 Experiment 3: using db8, two levels and symmetric edge-handling

In this configuration using db8 filter in wavelet decomposition we also achieve quite competitive results with other filters like db6 and db10. The performance is around (5.44%) in the decidability index which indicate a good separation between the genuine scores and impostor scores as shown in Figures Figure 39-Figure 42. This leads to better FAR as clearly shown in Figure Figure 42.
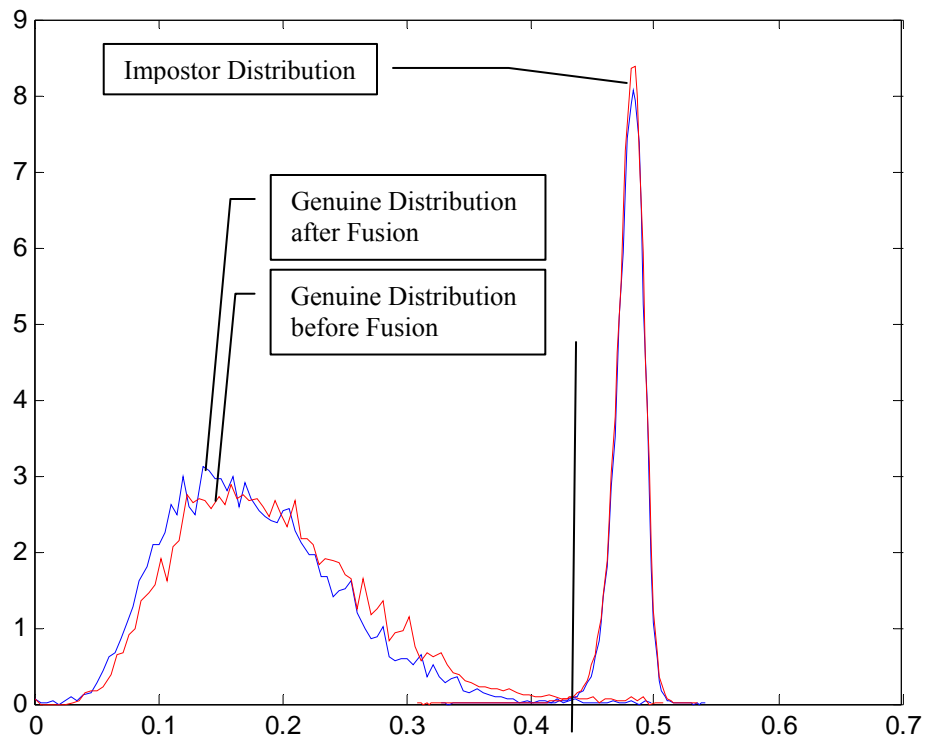
Figure 39: Genuine and Impostor Distributions using db8, two levels and symmetric edge-handling.
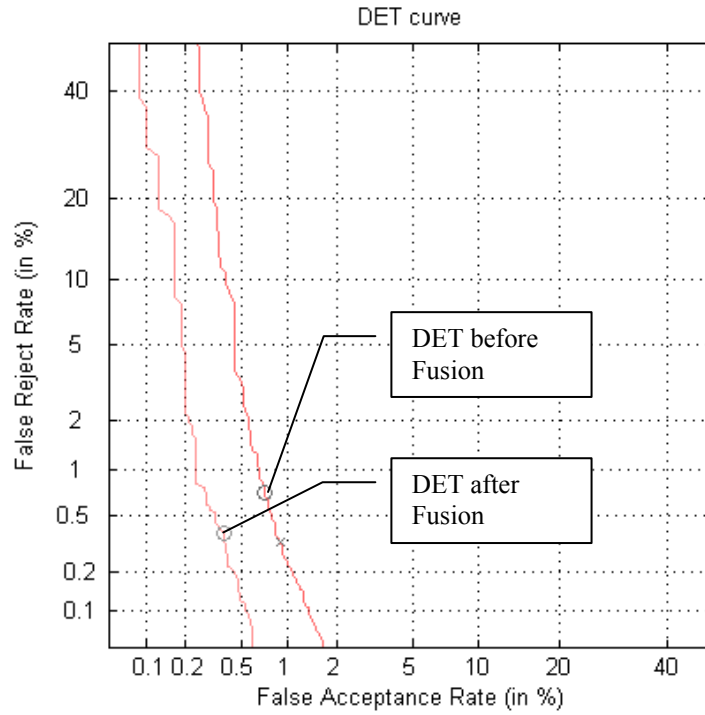
Figure 40: DET Curve using db8, two levels and symmetric edge-handling.
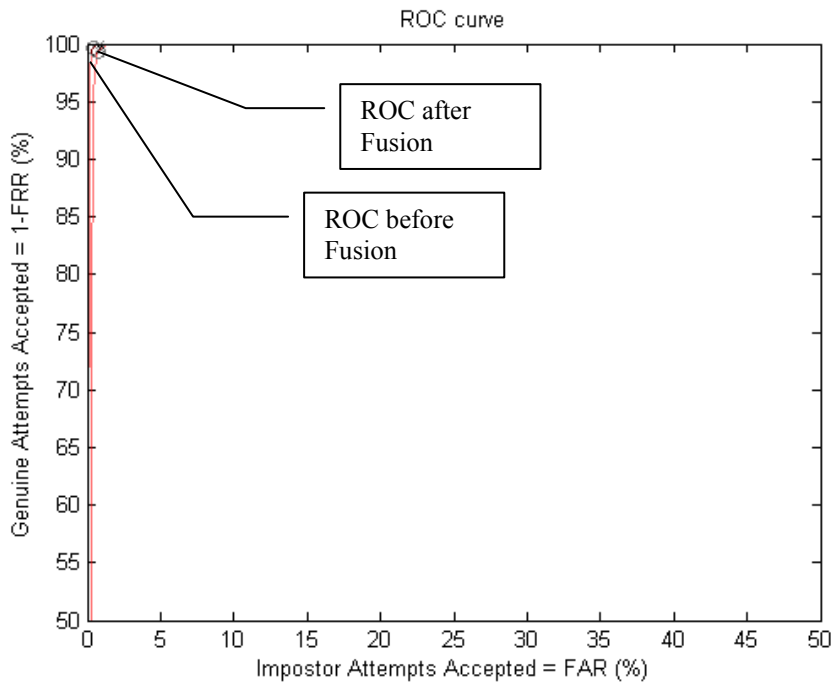
Figure 41: ROC Curve using db8, two levels and symmetric edge-handling.

74
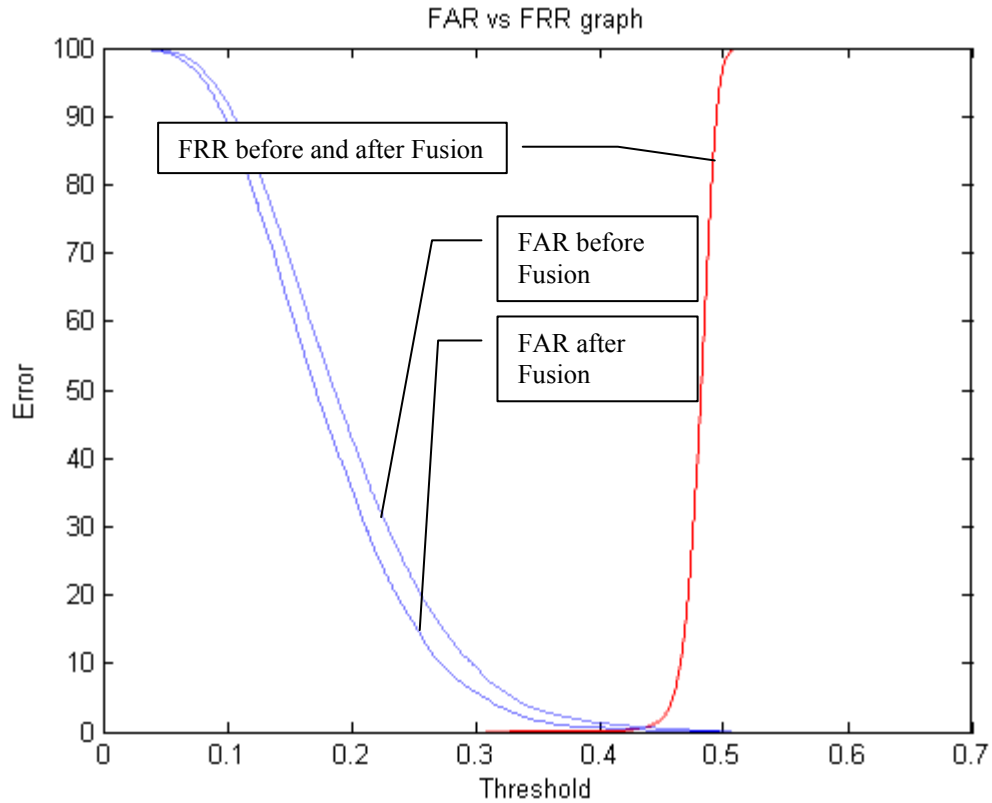
Figure 42: FAR vs. FRR using db8, two levels and symmetric edge-handling.

5.3.3.4 Experiment 4: using db10, two levels and symmetric edge-handling

DB10 is the third filter that shows close results to the optimum with around 5.69% improvement in decidability index as shown in Figure 43. This improvement results in better detection rates and reduces the false alarms as illustrated in Figures Figure 44-Figure 46.
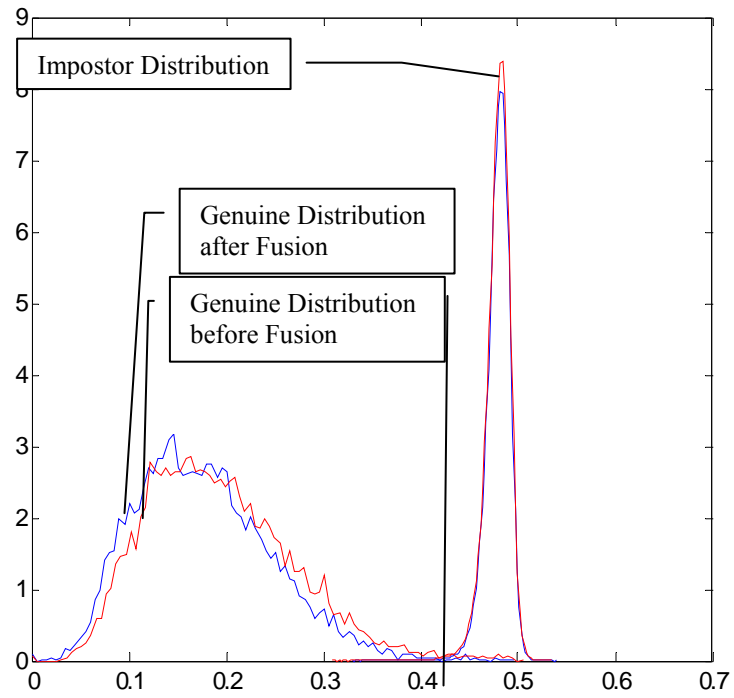
Figure 43: Genuine and Impostor Distributions using db10, two levels and symmetric edge-handling.
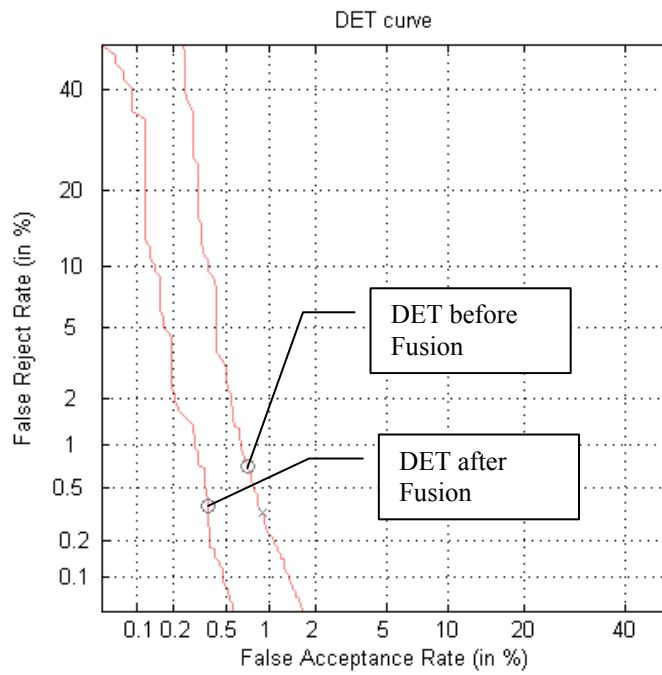
Figure 44: DET Curve using db10, two levels and symmetric edge-handling.
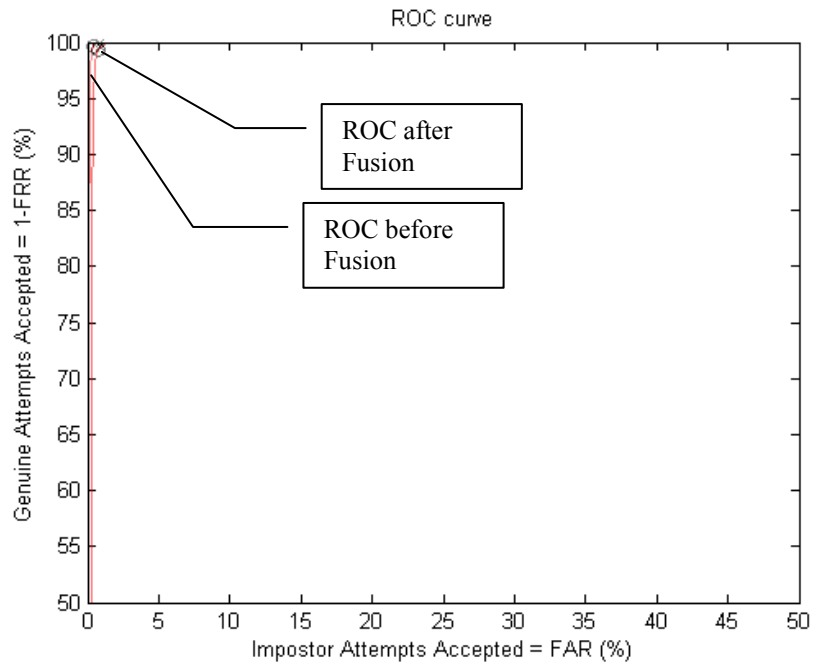
Figure 45: ROC Curve using db10, two levels and symmetric edge-handling.
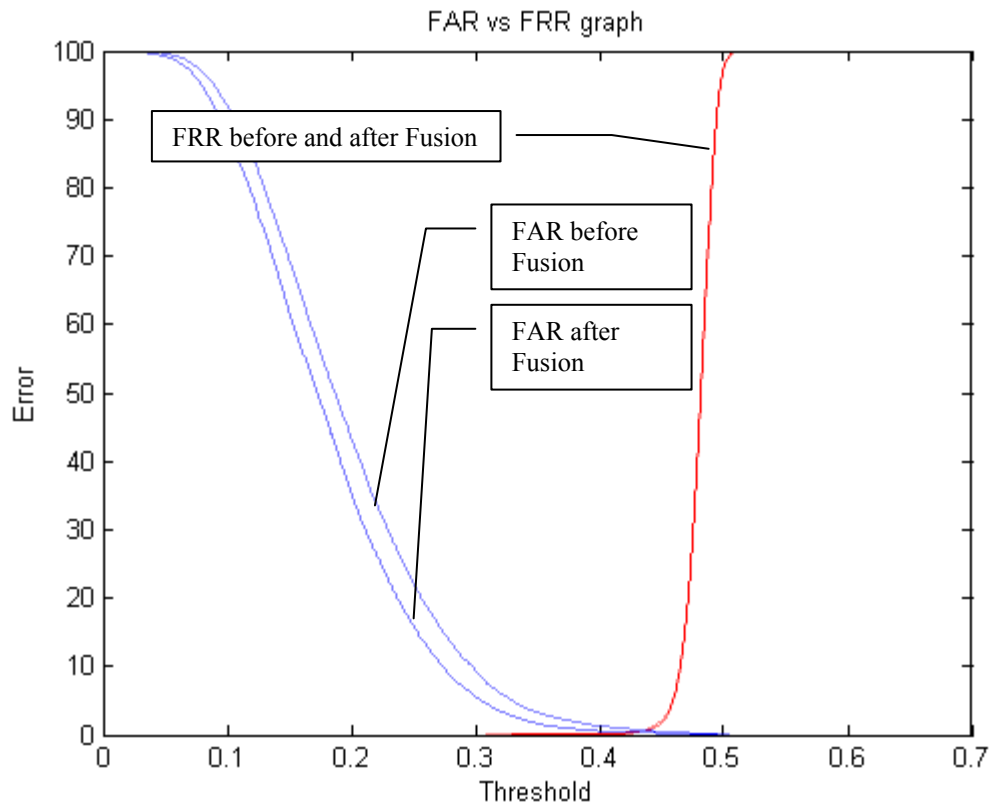
Figure 46: FAR vs. FRR using db10, two levels and symmetric edge-handling.

5.3.3.5 Experiment 5: using db6, two levels and periodical edge-handling

This experiment configuration is similar to experiment 2 except that we changed the DWT mode in edge-handling to use periodization rather than symmetric padding. With around 5.97% of improvement in decidability index as shown in Figure 47 we are able to achieve the optimum results with this configuration. We achieved the least false alarms ratios as shown in Figures Figure 48-Figure 50.
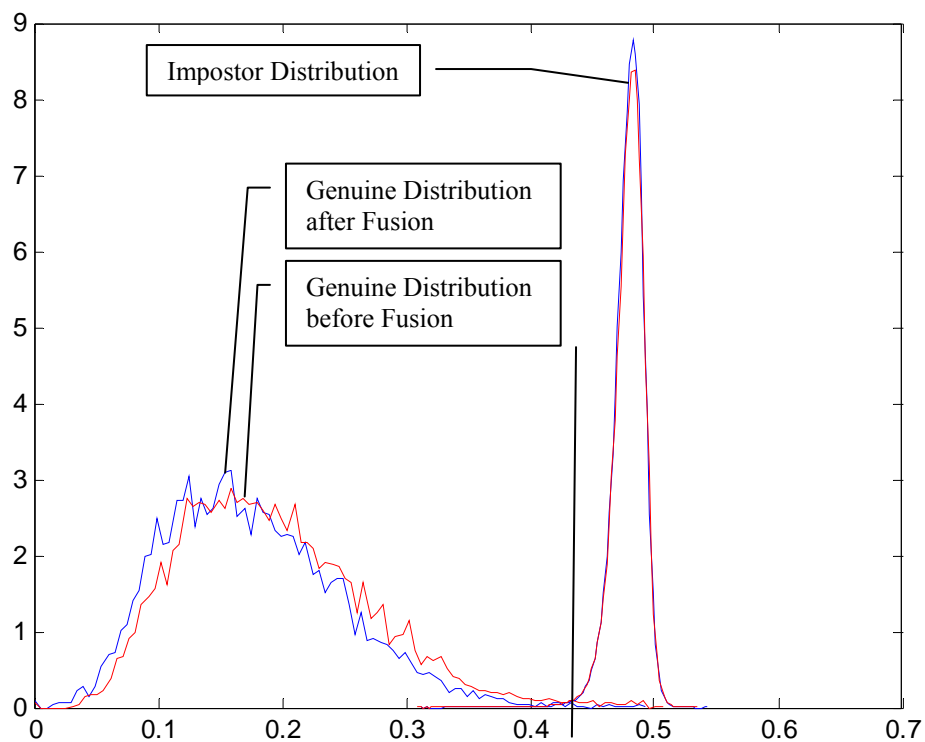
Figure 47: Genuine and Impostor using db6, two levels and periodical edge-handling.
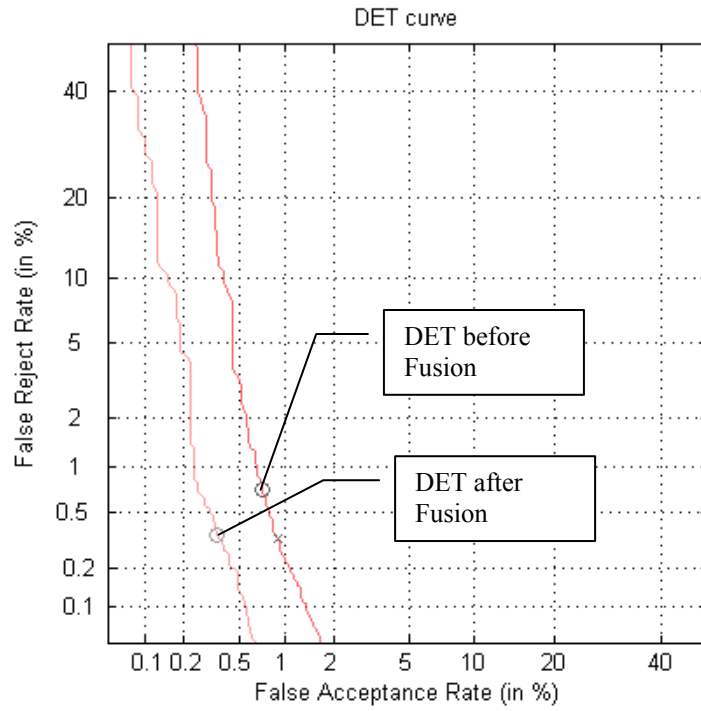
Figure 48: DET Curve using db6, two levels and periodical edge-handling.
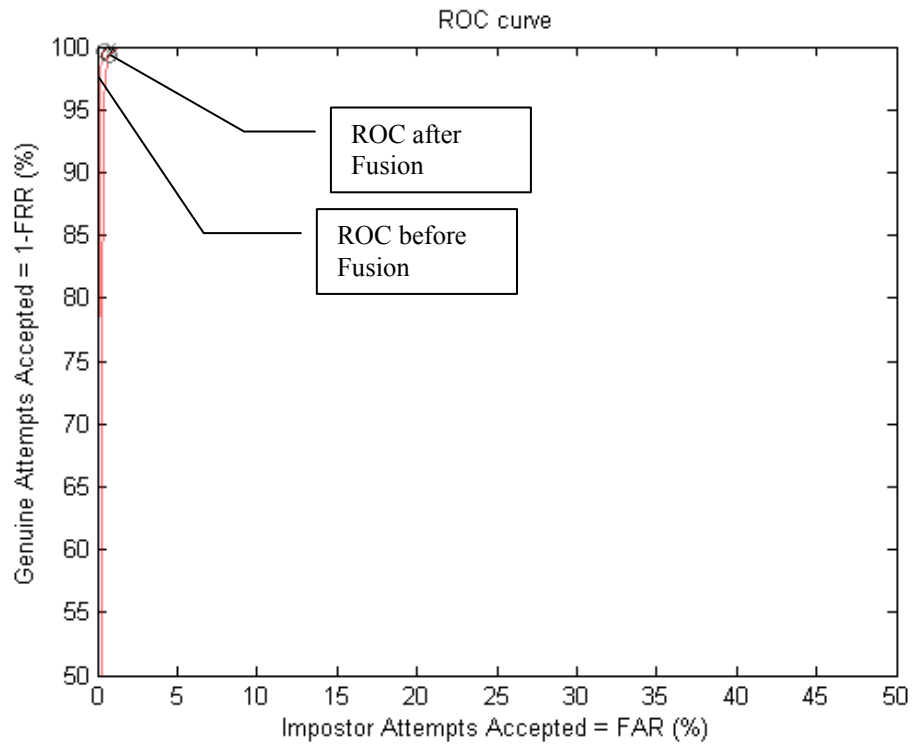
Figure 49: ROC Curve using db6, two levels and periodical edge-handling.

79
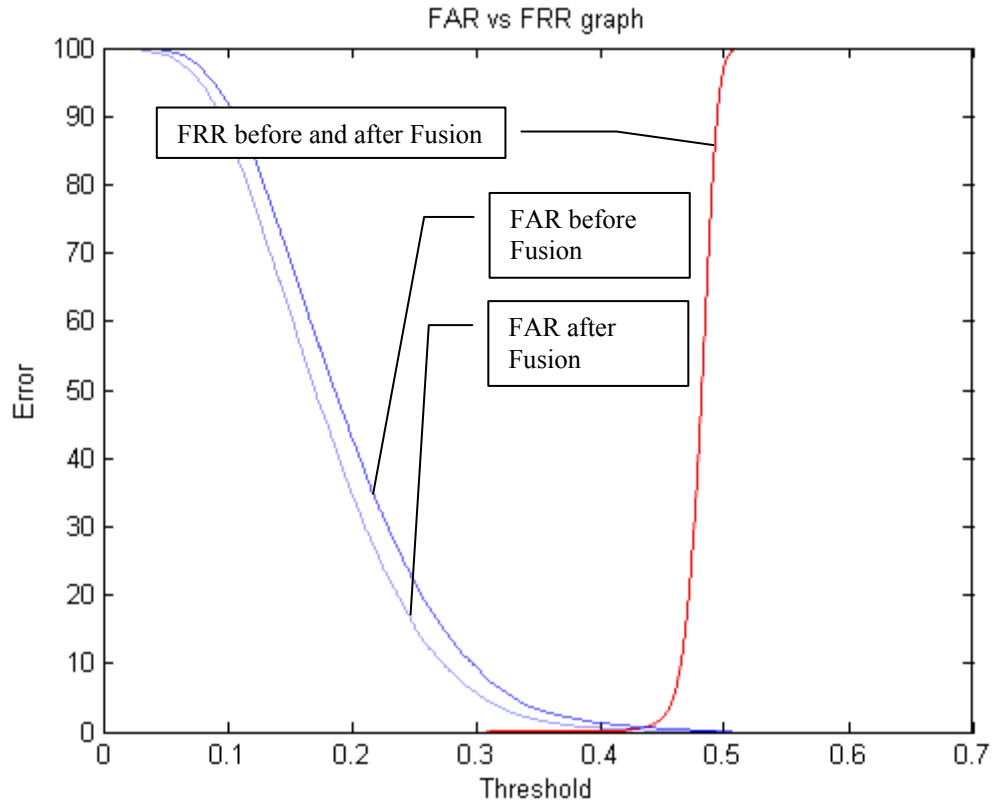
Figure 50: FAR vs. FRR using db6, two levels and periodical edge-handling.

5.3.3.6 Experiment 6: using db6, three levels and symmetric edge-handling

In this experiment setup we also achieved almost the optimum results with around 5.69% of improvement as shown in Figures Figure 51-Figure 54. Although we are using symmetric padding for edge-handling, we outperform similar experiment configuration using periodization but at the third level of wavelet decomposition.
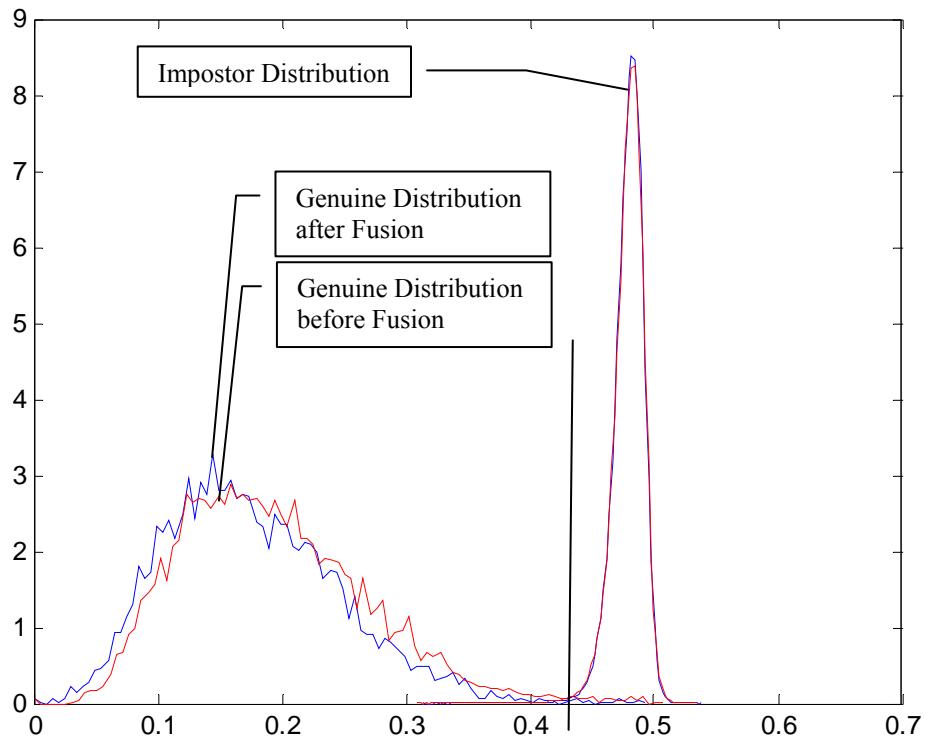
Figure 51: Genuine and Impostor using db6, three levels and symmetric edge-handling.
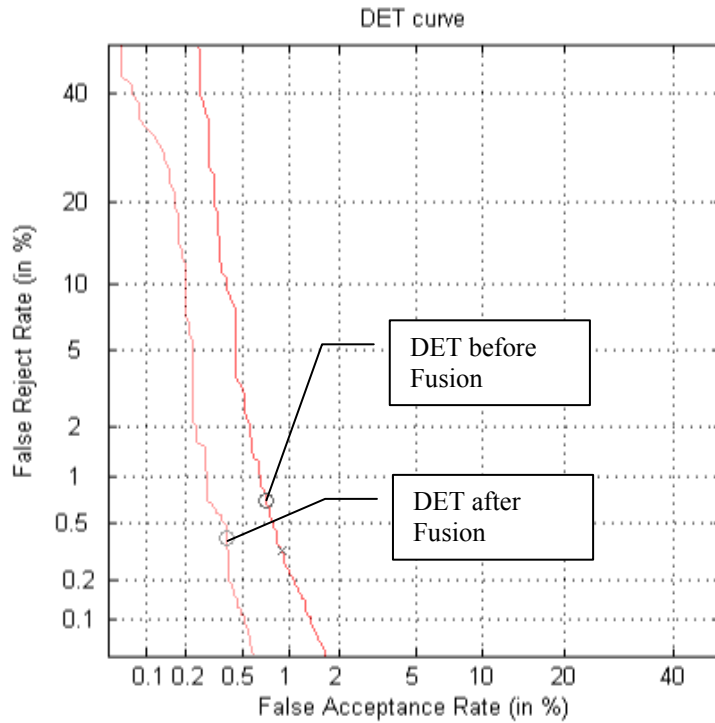
Figure 52: DET Curve using db6, three levels and symmetric edge-handling.
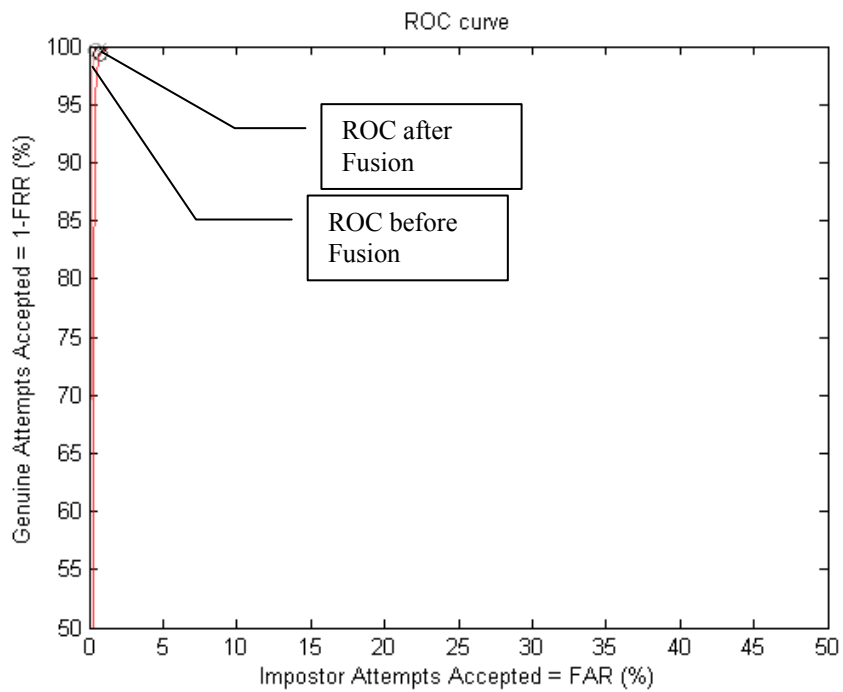
Figure 53: ROC Curve using db6, three levels and symmetric edge-handling.
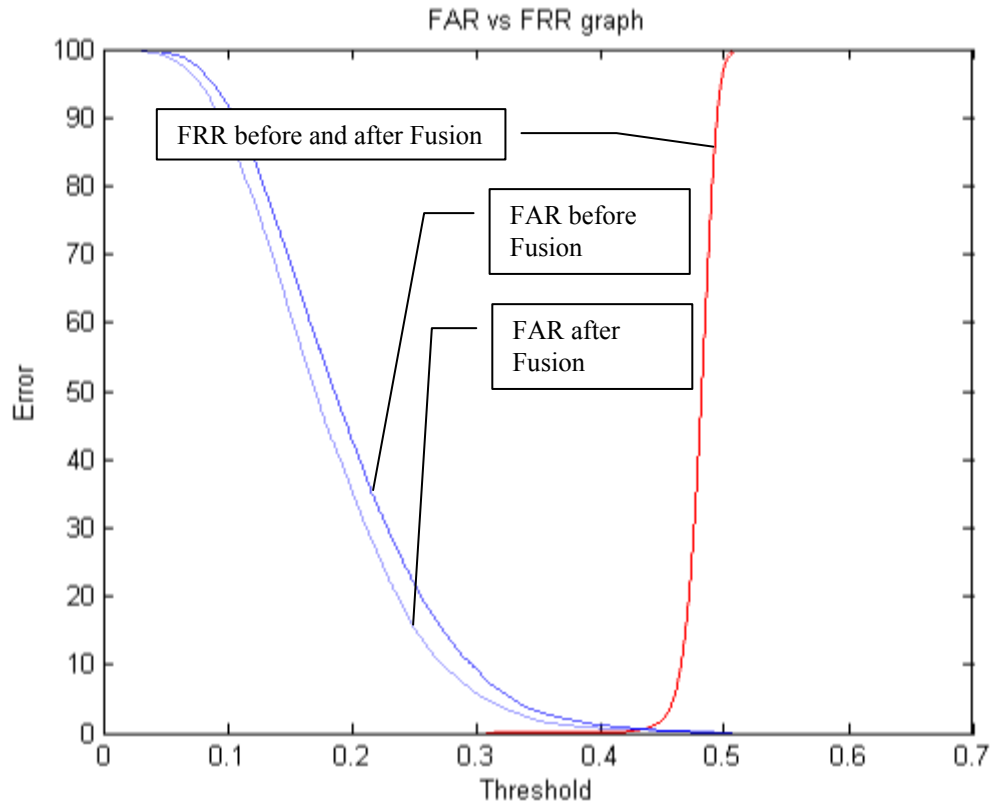
Figure 54: FAR vs. FRR using db6, three levels and symmetric edge-handling.

5.3.3.7 Experiment 7: using db6, three levels and periodical edge-handling

In this setup the results was a little bit an expected. The performance was high but not higher than similar setup with symmetric padding for edge-handling which was not the case in the second level of decomposition. In this setup we were able to achieve around 5.62% of improvement of separation between genuine and impostors scores as shown in Figure 55 and better false alarm rates as shown in Figures Figure 56-Figure 58.
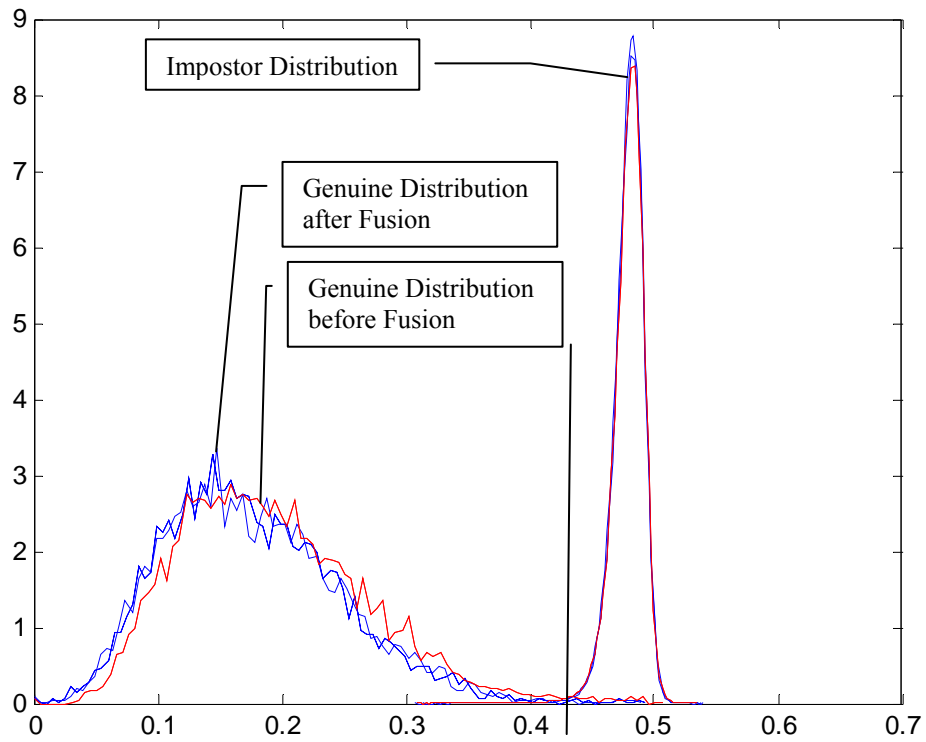
Figure 55: Genuine and Impostor Distribution using db6, three levels, and periodical edge-handling.
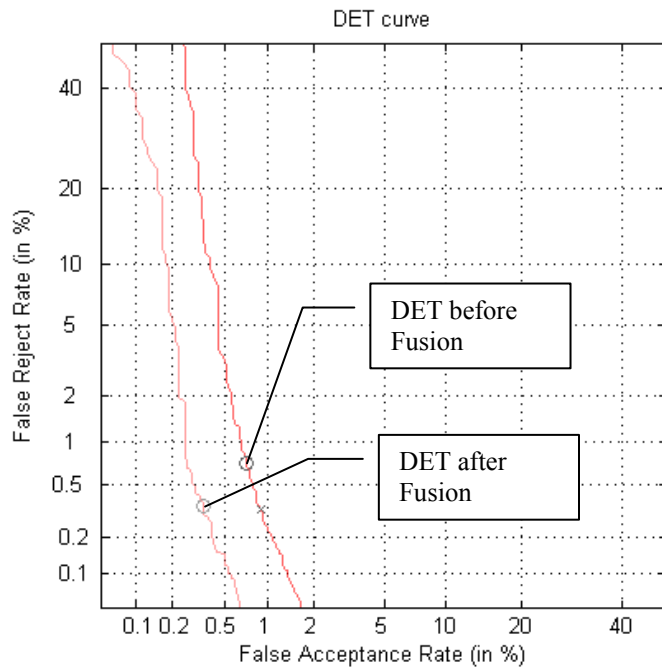
Figure 56: DET Curve using db6, three levels, and periodical edge-handling.
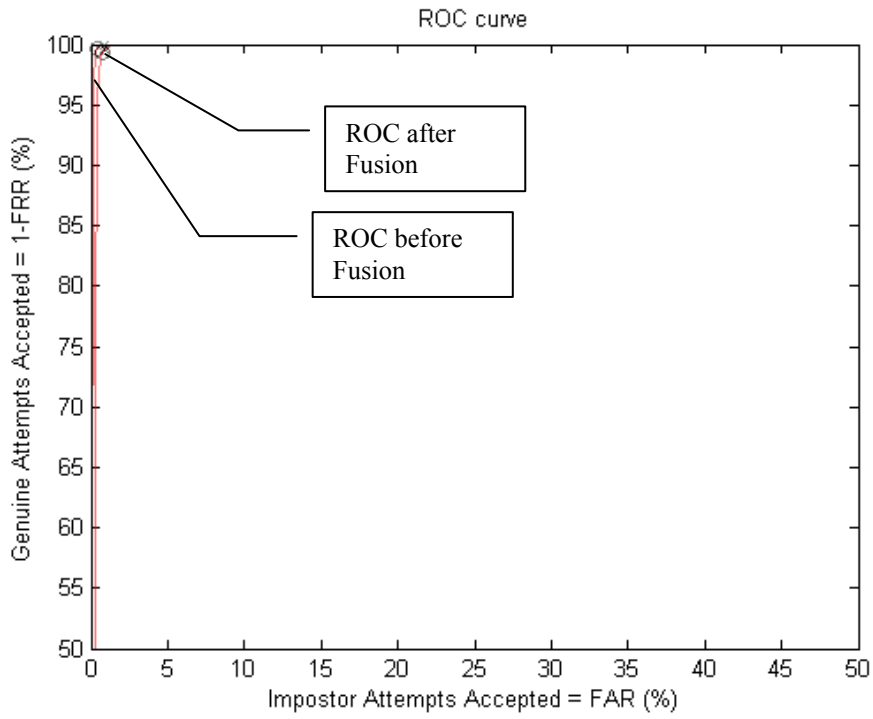
Figure 57: ROC Curve using db6, three levels, and periodical edge-handling.
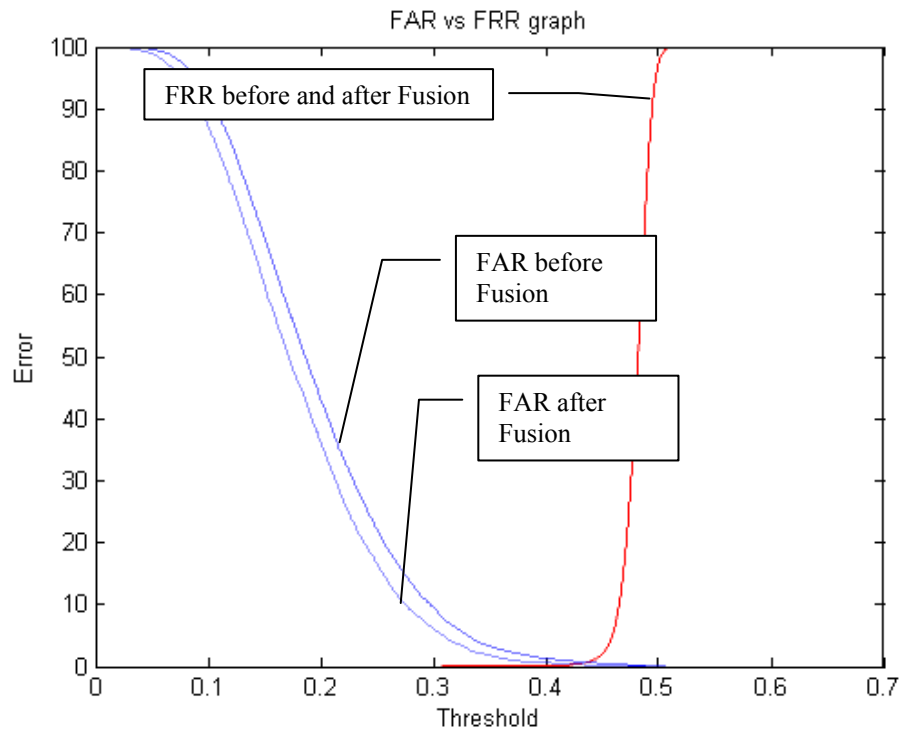
Figure 58: FAR vs. FRR using db6, three levels, and periodical edge-handling.

Chapter 6

Conclusions and Future Work

6.1 Summary of Work

This thesis has presented two novel schemes for information fusion in multibiometric systems. The first scheme, based on digital image watermarking techniques, enables the incorporation of several fingerprint samples for the improvement of the matching performance of fingerprint-based biometric systems. Performance improvements have been evaluated against the FVC2004 fingerprint database. The proposed fusion scheme combines multiple fingerprint impressions into a single one such that the important features of each sample is preserved while the least important one are discarded. High perceptual quality of the fused image is achieved by taking into account the image activity levels measured through wavelet coefficients strengths. Wavelet-based domain is selected for the fusion process due to its ability to "perfectly" capture the HVS modalities. Afterwards, features of the fused image are extracted and compared against stored templates of genuine and impostor samples. It is worth noting that the proposed fusion algorithm does not affect the locations of the minutia points in fingerprints which makes it suitable also for minutia-based systems.

The second fusion scheme merges several iris samples at the "pre-feature" level using a new iris quality measure. Normalized iris images are divided into blocks where each block represents a texture that is modeled using a GGD-based statistical model. The "best" iris block from each iris sample to selected for inclusion in the resulting improved normalized iris image. Then, the resulting iris features are encoded by convolving the normalized iris region with 1D Log-Gabor filters and then the phase components are quantized in order to produce a bit-wise biometric template. The Hamming distance is used as a matching metric. A failure of statistical independence between two templates would result in a match, that is, the two templates are deemed to have been generated from the same iris.

6.2 **Summary of Findings**

Multibiometric systems using multiple impressions of the biometric trait (fingerprint and iris in our case) have been shown to outperform their counterparts that use a single modality. We have clearly shown that digital watermarking can be used as a successful fusion scheme for multiple instances of the same modality (fingerprint images). The accuracy of the multibiometric systems has been shown to improve using such fusion schemes. Also, we have proposed an enhancement of the Daugman algorithm (IrisCode-based) for iris recognition through a new fusion scheme which is based on a novel iris quality measure.

6.3 **Recommendation for Future Work**

The solutions proposed in this Thesis enable multibiometric systems to perform more accurately. However, several research issues need to be further investigated. In what follows, we outline the most important issues:

1- **Embedding capacity:** It would be useful to investigate the embedding capacity of the watermarking scheme to get an accurate estimate of the number of fingerprint samples that can be accommodated for fusion. A more theoretical study of the hiding capacity limits of typical fingerprint images is required for this purpose.

2- **Fusion level:** For filterbank-based fingerprint systems, the incorporation of the proposed fusion scheme at later stages such as the feature level would require the investigation of the suitability of the filterbank representations for watermarking-based fusion. Due to its redundant expansion, caution should be exercised when fusing fingerprint templates in such domains. Very few studies have been proposed regarding watermarking in redundant domains.

3- **Multiple-modalities:** Using more than two biometric traits such as the face, iris and fingerprint would pose several challenges for their fusion. First of all, it will be hard to find a common transform domain which is "optimal" in terms of performance for three modalities.

References

[1] R. Brunelli and D. Falavigna. Person Identification Using Multiple Cues. IEEE Transactions on Pattern Analysis and Machine Intelligence, 17(10):955-966, October 1995.

[2] Ross and A. K. Jain. Information Fusion in Biometrics. Pattern Recognition Letters, 24(13):2115-2125, September 2003.

[3] Ross, K. Nandakumar, and A. K. Jain. Handbook of Multibiometrics. Springer, 2006.

[4] The Freedonia Group, Inc. Biometric & Other Electronic Access Control Systems to 2009 - Demand and Sales Forecasts, Market Share, Market Size, Market Leaders. Available at: http://www.freedoniagroup.com/Biometric-And-Other-Electronic-Access-Control-Systems.html

[5] International Biometric Group, New York, NY; 1.212.809.9491.

[6] Jain, A. K.; Ross, Arun & Prabhakar, Salil, "An introduction to biometric recognition", IEEE Transactions on Circuits and Systems for Video Technology 14th (1): 4-20.Jan,2004.

[7] R. Snelick, U. Uludag, A. Mink, M. Indovina, and A. K. Jain. Large Scale Evaluation of Multimodal Biometric Authentication Using State-of-the-Art Systems. IEEE Transactions on Pattern Analysis and Machine Intelligence, 27(3):450-455, March 2005.

[8] B. Ulery, A. R. Hicklin, C. Watson, W. Fellner, and P. Hallinan. Studies of Biometric Fusion. Technical Report IR 7346, NIST, September 2006.

[9] Jain, A.K, Prabhakar, S., Hong, L., Pankanti, S., Filterbank-Based Fingerprint Matching, IP(9), No. 5, May 2000, pp. 846-859.

[10] J. Daugman, "Biometric personal identification system based on iris analysis," U.S. Patent No. 5,291,560, March 1994.

[11] S. C. Dass, K. Nandakumar, and A. K. Jain. A Principled Approach to Score Level Fusion in Multimodal Biometric Systems. In Proceedings of Fifth International Conference on Audio- and Video-based Biometric Person Authentication (AVBPA), pp. 1049-1058, Rye Brook, USA, July 2005

[12] Maltoni, D., Maio, D., Jain, A.K., Prabhakar, S. "Handbook of Fingerprint Recognition". Originally published in the series: Springer Professional Computing 2nd ed. 2009, XVI, 496 p. 205 illus. With DVD. Hardcover

[13] F. Benhammadi , M. N. Amirouche , H. Hentous , K. Bey Beghdad , M. Aissani, Fingerprint matching from minutiae texture maps, Pattern Recognition, vol.40 n.1, pp.189-197, January, 2007

[14] Miao-li Wen, Yan Liang, Quan Pan, Hong-cai Zhang, A Gabor filter based fingerprint enhancement algorithm in wavelet domain. Communications and Information Technology, 2005. ISCIT 2005. IEEE International Symposium on Publication Date: 12-14 Oct. 2005, vol.2, pp. 1468- 1471.

[15] Fei Su , Xiaohui Xie , Anni Cai, A hierachical fingerprint matching method based on the minutiae and ridge image, Proceedings of the 6th WSEAS International Conference on Signal Processing, Computational Geometry & Artificial Vision, pp.83-88, August 21-23, 2006, Elounda, Greece.

[16] Shankar Bhausaheb Nikam , Suneeta Agarwal, Level 2 features and wavelet analysis based hybrid fingerprint matcher, Proceedings of the 1st Bangalore annual Compute conference, January 18-20, 2008, Bangalore, India.

[17] R. P. Wildes, Iris recognition: an emerging biometrics technology, Proc. IEEE, vol. 85, no. 9, pp. 1348–1363, Sep. 1997.

[18] R. W. Ives, A. J. Guidry, and D. M. Etter, "Iris recognition using histogram analysis," Thirty-Eighth Asilomar Conference on Signals, Systems, and Computers, pp. 562-566, 2005.

[19] M. K. Khan, J. Zhang, and S-J. Hong, "An effective iris recognition system for identification of humans," 8th International Multitopic Conference, pp. 114-117, 2004.

[20] J.-G. Ko, Y.-H. Gil, and J.-H. Yoo, "Iris Recognition using Cumulative SUM based Change Analysis," International Symposium on Intelligent Signal, 2006.

[21] N. Sudha, N. B. Puhan, X. Hua, and J. Xudong, "Iris recognition on edge maps," 6th International Information, Communications & Signal Processing, 2007.

[22] V. Conti, G. Milici, F. Sorbello, and S. Vitabile, "A Novel Iris Recognition System based on Micro-Features," IEEE Workshop on Automatic Identification Advanced Technologies, pp. 253-258, 2007.

[23] W. Anna, C. Yu, W. Jie, and Zhangxinhua, "Iris Recognition Based on Wavelet Transform and Neural Network," IEEE/ICME International Conference on Complex Medical Engineering, 2007.

[24] K. Miyazawa, K. Ito, T. Aoki, K. Kobayashi, and H. Nakajima, "An Effective Approach for Iris Recognition Using Phase-Based Image Matching," IEEE Transaction of Pattern Analysis and Machine Intelligence, vol. 30, no. 10, pp. 1741-1756, 2008.

[25] B. Duc, E. S. Bigün, J. Bigün, G. Maître, and S. Fischer, "Fusion of audio and video information for multi modal person authentication," Pattern Recognition Letters, vol. 18, no. 9, pp. 835-843, September 1997.

[26] L. Hong and A. K. Jain. Integrating Faces and Fingerprints for Personal Identification. IEEE Transactions on Pattern Analysis and Machine Intelligence, 20(12):1295-1307, December 1998.

[27] Chatzis, V., Borse, A.G., Pitas, I., Multimodal Decision-Level Fusion for Person Authentication, SMC-A(29), No. 6, November 1999, pp. 674.

[28] G. Shakhnarovich, L. Lee, T. Darrell, "Integrated Face and Gait Recognition From Multiple Views," cvpr, vol. 1, pp.439, 2001 IEEE Computer Society Conference on Computer Vision and Pattern Recognition (CVPR'01) – vol. 1, 2001.

[29] C. C. Chibelushi, J. S. D. Mason, and F. Deravi. Feature-level Data Fusion for Bimodal Person Recognition. In Proceedings of the Sixth International Conference on Image Processing and Its Applications, vol. 1, pp. 399-403, Dublin, Ireland, July 1997.

[30] Ross and R. Govindarajan. Feature Level Fusion Using Hand and Face Biometrics. In Proceedings of SPIE Conference on Biometric Technology for Human Identification II, vol. 5779, pp. 196-204, Orlando, USA, March 2005.

[31] Kale, A. K. RoyChowdhury, and R. Chellappa. Fusion of Gait and Face for Human Identification. In IEEE International Conference on Acoustics, Speech, and Signal Processing (ICASSP), vol. 5, pp. 901-904, Montreal, Canada, May 2004.

[32] S. Ben-Yacoub, Y. Abdeljaoued, and E. Mayoraz. Fusion of Face and Speech Data for Person Identity Verification. IEEE Transactions on Neural Networks,10(5):1065-1075, September 1999.

[33] C. Sanderson and K. K. Paliwal. Information Fusion and Person Verification Using Speech and Face Information. Technical Report IDIAP-RR 02-33, IDIAP, September 2002.

[34] K. Jain, K. Nandakumar, X. Lu, and U. Park. Integrating Faces, Fingerprints and Soft Biometric Traits for User Recognition. In Proceedings of ECCV International Workshop on Biometric Authentication (BioAW), vol. LNCS 3087, pp. 259-269, Prague, Czech Republic, May 2004. Springer.

[35] G. L. Marcialis and F. Roli. Fingerprint Verification by Fusion of Optical and Capacitive Sensors. Pattern Recognition Letters, 25(11):1315-1322, August 2004.

[36] K. I. Chang, K. W. Bowyer, and P. J. Flynn. An Evaluation of Multimodal 2D+3D Face Biometrics. IEEE Transactions on Pattern Analysis and Machine Intelligence, 27(4):619-624, April 2005.

[37] J. Fierrez-Aguilar, L. Nanni, J. Lopez-Penalba, J. Ortega-Garcia, and D. Maltoni. An On-line Signature Verification System based on Fusion of Local and Global Information. In Fifth International Conference on Audio- and Video-based Biometric Person Authentication (AVBPA), pp. 523-532, Rye Brook, USA, July 2005.

[38] J. Fierrez-Aguilar, D. Garcia-Romero, J. Ortega-Garcia, and J. Gonzalez Rodriguez. Bayesian Adaptation for User-Dependent Multimodal Biometric Authentication. Pattern Recognition, 38(8):1317-1319, August 2005.

[39] W. M. Campbell, D. A. Reynolds, and J. P. Campbell. Fusing Discriminative and Generative Methods for Speaker Recognition: Experiments on Switchboard and NFI/TNO Field Data. In Odyssey: The Speaker and Language Recognition Workshop, pp. 41-44, Toledo, Spain, May 2004.

[40] T. K. Ho, J. J. Hull, and S. N. Srihari. Decision Combination in Multiple Classifier Systems. IEEE Transactions on Pattern Analysis and Machine Intelligence, 16(1):66-75, January 1994.

[41] K. Woods, K. Bowyer, and W. P. Kegelmeyer. Combination of Multiple Classifiers Using Local Accuracy Estimates. IEEE Transactions on Pattern Analysis and Machine Intelligence, 19(4):405-410, April 1997.

[42] X. Lu, Y. Wang, and A. K. Jain. Combining Classifiers for Face Recognition. In IEEE International Conference on Multimedia and Expo (ICME), vol. 3, pp. 13-16, Baltimore, USA, July 2003.

[43] B. Yanikoglu and A. Kholmatov. Combining Multiple Biometrics to Protect Privacy. In Proceedings of ICPR Workshop on Biometrics: Challenges arising from Theory to Practice, Cambridge, UK, August 2004.

[44] S. Prabhakar and A. K. Jain. Decision-level Fusion in Fingerprint Verification. Pattern Recognition, 35(4):861-874, April 2002.

[45] J. Fierrez-Aguilar, J. Ortega-Garcia, J. Gonzalez-Rodriguez, and J. Bigun. Discriminative Multimodal Biometric Authentication based on Quality Measures. Pattern Recognition, 38(5):777-779, May 2005.

[46] P.Nicholl and A.Amira "DWT/PCA Face Recognition using Automatic Coefficient Selection" IEEE International Symposium on Design, Electronic, Test and Applications DELTA2008, 23-25 January 2008, Hong Kong.

[47] M. Tumer, "Texture discrimination by Gabor functions," Bioi. Cybern., vol. 55, pp. 71-82, 1986.

[48] J. Daugman, "High confidence visual recognition of persons by a test of statistical independence," IEEE Trans. on Pattern Anal. Machine Intell., vol. 15, pp. 1148-1161, 1993.

[49] J. Daugman, "Statistical richness of visual phase information: update on recognizing persons by iris patterns," Internat. J. on Comp. Vision, vol. 45, pp. 25-38, 2001.

[50] J. Daugman, "Demodulation by complex-valued wavelets for stochastic pattern recognition," Internat. J. on Wavelets, Multi-Res. and Info. Processing, vol. 1, no. 1, pp. 1-17, 2003.

[51] Jain, A.K., Prabhakar, S., Hong, L., A Multichannel Approach to Fingerprint Classification, PAMI(21), No. 4, April 1999, pp. 348-359.

[52] Paquet, A. H., Ward, R. K., and Pitas, I. 2003. Wavelet packets-based digital watermarking for image verification and authentication. Signal Process. 83, 10 (Oct. 2003), 2117-2132.

[53] Ingemar J. Cox, Matt L. Miller, Jeffrey A. Bloom, "Watermarking applications and their properties," itcc, pp.6, The International Conference on Information Technology: Coding and Computing (ITCC'00), 2000.

[54] Solachidis, V., Pitas, L., Optimal Detection for Multiplicative Watermarks Embedded in DFT Domain,ICIP03(II: 723-726). IEEE Abstract. 0312.

[55] Shu-Fen Tu, Ching-Sheng Hsu, "Digital Watermarking Method Based on Image Size Invariant Visual Cryptographic Scheme," uic-atc, pp.362-366, Symposia and Workshops on Ubiquitous, Autonomic and Trusted Computing, 2009.

[56] G. V. Wouwer, P. Scheunders, and D. V. Dyck, "Statistical texture characterization from discrete wavelet representations," IEEE Trans. Image Processing, vol. 8, pp. 592-598, Apr. 1999.

[57] N. Vasconcelos and A. Lippman, "Embedded mixture modeling for efficient probabilistic content-based indexing and retrieval," SPIE Multimedia Storage and Archiving Systems III, 1998.

[58] M. N. Do and M. Vetterli, "Wavelet-based texture retrieval using generalized Gaussian density and Kullback-Leibler distance," IEEE Trans. Image Process. vol. 11, no. 2, pp. 146-158, Feb. 2002.

[59] D. Maltoni, D. Maio, A. K. Jain, and S. Prabhakar, Handbook of Fingerprint Recognition. New York: Springer, 2003.

[60] Gray, A. "The Intuitive Idea of Distance on a Surface." §15.1 in Modern Differential Geometry of Curves and Surfaces with Mathematica, 2nd ed. Boca Raton, FL: CRC Press, pp. 341-345, 1997.

[61] L. Masek, "Recognition of Human Iris Patterns for Biometric Identification", MSc Thesis, The University of Western Australia, Australia, 2003.

[62] Biometric System Laboratory University of Bologna. FVC2004: The Fourth International Fingerprint Verification Competition. Available at http://bias.csr.unibo.it/fvc2004/default.asp.

[63] Smart Sensors Ltd. IRISBASE. Available at: http://www.irisbase.com.

[64] Erian Bezhani, Dequn Sun, Jean-Luc Nagel, and Sergio Carrato, "Optimized filterbank fingerprint recognition", Proc. SPIE Intern. Symp. Electronic Imaging 2003, 20-24 Jan. 2003, Santa Clara, California.

Appendix I: Parameter Estimation for GGD

Sample iris images quality measures results:

Img_Filename	Sharpness	Saturation	SNR	Average_Graylevel	Contrast	Occlusion_Percentage
g:\Shared\MIRLIN\Set1\DVD1\0001\L\0001.BMP	10	11	64	109	71	8
g:\Shared\MIRLIN\Set1\DVD1\0001\L\0001.BMP	10	11	64	109	71	8
g:\Shared\MIRLIN\Set1\DVD1\0001\L\0007.BMP	20	6	55	128	89	7
g:\Shared\MIRLIN\Set1\DVD1\0001\L\0007.BMP	20	6	55	128	89	7
g:\Shared\MIRLIN\Set1\DVD1\0001\R\0003.BMP	28	6	52	138	109	10
g:\Shared\MIRLIN\Set1\DVD1\0001\R\0001.BMP	12	12	58	107	93	14
g:\Shared\MIRLIN\Set1\DVD1\0017\L\0005.BMP	10	2	49	68	36	0
g:\Shared\MIRLIN\Set1\DVD1\0001\L\0013.bmp	9	13	64	109	75	9
g:\Shared\MIRLIN\Set1\DVD1\0001\L\0014.bmp	12	10	58	115	70	6
g:\Shared\MIRLIN\Set1\DVD1\0001\L\0015.bmp	18	8	58	118	76	7
g:\Shared\MIRLIN\Set1\DVD1\0001\L\0016.bmp	14	8	58	118	71	6
g:\Shared\MIRLIN\Set1\DVD1\0001\L\0017.bmp	9	13	65	111	72	8
g:\Shared\MIRLIN\Set1\DVD1\0001\L\0018.bmp	10	11	58	109	76	9
g:\Shared\MIRLIN\Set1\DVD1\0001\L\0019.bmp	10	10	58	110	72	8
g:\Shared\MIRLIN\Set1\DVD1\0001\L\0020.bmp	13	10	57	108	75	9
g:\Shared\MIRLIN\Set1\DVD1\0001\R\0001.bmp	12	12	58	107	93	14
g:\Shared\MIRLIN\Set1\DVD1\0001\R\0002.bmp	13	10	60	112	95	13
g:\Shared\MIRLIN\Set1\DVD1\0001\R\0003.bmp	28	6	52	138	109	10
g:\Shared\MIRLIN\Set1\DVD1\0001\R\0004.bmp	12	11	59	110	94	14
g:\Shared\MIRLIN\Set1\DVD1\0001\R\0005.bmp	13	11	59	111	89	12
g:\Shared\MIRLIN\Set1\DVD1\0001\R\0006.bmp	14	10	53	110	94	13
g:\Shared\MIRLIN\Set1\DVD1\0001\R\0007.bmp	14	12	59	112	94	13
g:\Shared\MIRLIN\Set1\DVD1\0001\R\0008.bmp	18	9	57	110	91	12
g:\Shared\MIRLIN\Set1\DVD1\0001\R\0009.bmp	34	5	46	122	117	13
g:\Shared\MIRLIN\Set1\DVD1\0001\R\0010.bmp	20	7	49	102	88	11
g:\Shared\MIRLIN\Set1\DVD1\0001\R\0011.bmp	39	5	46	130	105	6
g:\Shared\MIRLIN\Set1\DVD1\0001\R\0012.bmp	17	7	50	96	95	16
g:\Shared\MIRLIN\Set1\DVD1\0001\R\0013.bmp	14	10	58	106	91	13
g:\Shared\MIRLIN\Set1\DVD1\0001\R\0014.bmp	14	11	53	109	97	14
g:\Shared\MIRLIN\Set1\DVD1\0001\R\0015.bmp	13	11	59	109	95	13
g:\Shared\MIRLIN\Set1\DVD1\0001\R\0016.bmp	11	12	59	108	91	13
g:\Shared\MIRLIN\Set1\DVD1\0001\R\0017.bmp	15	9	58	105	90	13
g:\Shared\MIRLIN\Set1\DVD1\0001\R\0018.bmp	15	9	52	105	87	12
g:\Shared\MIRLIN\Set1\DVD1\0001\R\0019.bmp	13	11	57	106	80	10

g:\Shared\MIRLIN\Set1\DVD1\0001\R\0020.bmp	14	12 58	107	79	9
g:\Shared\MIRLIN\Set1\DVD1\0001\L\0001.bmp	10	11 64	109	71	8
g:\Shared\MIRLIN\Set1\DVD1\0001\L\0002.bmp	11	12 59	113	70	7
g:\Shared\MIRLIN\Set1\DVD1\0001\L\0003.bmp	11	11 63	111	62	5
g:\Shared\MIRLIN\Set1\DVD1\0001\L\0004.bmp	10	12 64	112	64	6
g:\Shared\MIRLIN\Set1\DVD1\0001\L\0005.bmp	8	14 65	111	68	7
g:\Shared\MIRLIN\Set1\DVD1\0001\L\0006.bmp	9	13 64	112	62	5
g:\Shared\MIRLIN\Set1\DVD1\0001\L\0007.bmp	20	6 55	128	89	7
g:\Shared\MIRLIN\Set1\DVD1\0001\L\0008.bmp	23	4 54	131	93	7
g:\Shared\MIRLIN\Set1\DVD1\0001\L\0009.bmp	10	11 63	108	69	7
g:\Shared\MIRLIN\Set1\DVD1\0001\L\0010.bmp	12	10 58	103	87	13
g:\Shared\MIRLIN\Set1\DVD1\0001\L\0011.bmp	20	7 55	127	85	7
g:\Shared\MIRLIN\Set1\DVD1\0001\L\0012.bmp	9	12 64	110	70	7
g:\Shared\MIRLIN\Set1\DVD1\0001\L\0013.bmp	9	13 64	109	75	9
g:\Shared\MIRLIN\Set1\DVD1\0001\L\0014.bmp	12	10 58	115	70	6
g:\Shared\MIRLIN\Set1\DVD1\0001\L\0015.bmp	18	8 58	118	76	7
g:\Shared\MIRLIN\Set1\DVD1\0001\L\0016.bmp	14	8 58	118	71	6
g:\Shared\MIRLIN\Set1\DVD1\0001\L\0017.bmp	9	13 65	111	72	8
g:\Shared\MIRLIN\Set1\DVD1\0001\L\0018.bmp	10	11 58	109	76	9
g:\Shared\MIRLIN\Set1\DVD1\0001\L\0019.bmp	10	10 58	110	72	8
g:\Shared\MIRLIN\Set1\DVD1\0001\L\0020.bmp	13	10 57	108	75	9
g:\Shared\MIRLIN\Set1\DVD1\0001\R\0001.bmp	12	12 58	107	93	14
g:\Shared\MIRLIN\Set1\DVD1\0001\R\0002.bmp	13	10 60	112	95	13
g:\Shared\MIRLIN\Set1\DVD1\0001\R\0003.bmp	28	6 52	138	109	10
g:\Shared\MIRLIN\Set1\DVD1\0001\R\0004.bmp	12	11 59	110	94	14
g:\Shared\MIRLIN\Set1\DVD1\0001\R\0005.bmp	13	11 59	111	89	12
g:\Shared\MIRLIN\Set1\DVD1\0001\R\0006.bmp	14	10 53	110	94	13
g:\Shared\MIRLIN\Set1\DVD1\0001\R\0007.bmp	14	12 59	112	94	13
g:\Shared\MIRLIN\Set1\DVD1\0001\R\0008.bmp	18	9 57	110	91	12
g:\Shared\MIRLIN\Set1\DVD1\0001\R\0009.bmp	34	5 46	122	117	13
g:\Shared\MIRLIN\Set1\DVD1\0001\R\0010.bmp	20	7 49	102	88	11
g:\Shared\MIRLIN\Set1\DVD1\0001\R\0011.bmp	39	5 46	130	105	6
g:\Shared\MIRLIN\Set1\DVD1\0001\R\0012.bmp	17	7 50	96	95	16
g:\Shared\MIRLIN\Set1\DVD1\0001\R\0013.bmp	14	10 58	106	91	13
g:\Shared\MIRLIN\Set1\DVD1\0001\R\0014.bmp	14	11 53	109	97	14
g:\Shared\MIRLIN\Set1\DVD1\0001\R\0015.bmp	13	11 59	109	95	13
g:\Shared\MIRLIN\Set1\DVD1\0001\R\0016.bmp	11	12 59	108	91	13
g:\Shared\MIRLIN\Set1\DVD1\0001\R\0017.bmp	15	9 58	105	90	13
g:\Shared\MIRLIN\Set1\DVD1\0001\R\0018.bmp	15	9 52	105	87	12
g:\Shared\MIRLIN\Set1\DVD1\0001\R\0019.bmp	13	11 57	106	80	10
g:\Shared\MIRLIN\Set1\DVD1\0001\R\0020.bmp	14	12 58	107	79	9
g:\Shared\MIRLIN\Set1\DVD1\0002\L\0001.bmp	24	9 58	132	50	0
g:\Shared\MIRLIN\Set1\DVD1\0002\L\0002.bmp	24	10 63	157	49	0
g:\Shared\MIRLIN\Set1\DVD1\0002\L\0003.bmp	24	10 69	157	49	0
g:\Shared\MIRLIN\Set1\DVD1\0002\L\0004.bmp	24	10 68	153	48	0

g:\Shared\MIRLIN\Set1\DVD1\0002\L\0005.bmp	26	9 62	154	52	0
g:\Shared\MIRLIN\Set1\DVD1\0002\L\0006.bmp	27	10 63	159	52	0
g:\Shared\MIRLIN\Set1\DVD1\0002\L\0007.bmp	28	9 63	162	53	0
g:\Shared\MIRLIN\Set1\DVD1\0002\L\0008.bmp	29	8 62	153	55	0
g:\Shared\MIRLIN\Set1\DVD1\0002\L\0009.bmp	29	9 62	154	56	0
g:\Shared\MIRLIN\Set1\DVD1\0002\L\0010.bmp	29	8 62	157	56	0
g:\Shared\MIRLIN\Set1\DVD1\0002\L\0011.bmp	27	8 63	159	55	0
g:\Shared\MIRLIN\Set1\DVD1\0002\L\0012.bmp	26	10 64	161	52	0
g:\Shared\MIRLIN\Set1\DVD1\0002\L\0013.bmp	21	12 69	151	43	0
g:\Shared\MIRLIN\Set1\DVD1\0002\L\0014.bmp	23	10 63	156	48	0
g:\Shared\MIRLIN\Set1\DVD1\0002\L\0015.bmp	21	10 68	153	46	0
g:\Shared\MIRLIN\Set1\DVD1\0002\L\0016.bmp	19	11 68	148	40	0
g:\Shared\MIRLIN\Set1\DVD1\0002\L\0017.bmp	18	12 68	145	40	0
g:\Shared\MIRLIN\Set1\DVD1\0002\L\0018.bmp	22	11 68	149	44	0
g:\Shared\MIRLIN\Set1\DVD1\0002\L\0019.bmp	16	12 67	139	37	0
g:\Shared\MIRLIN\Set1\DVD1\0002\L\0020.bmp	18	12 67	144	40	0
g:\Shared\MIRLIN\Set1\DVD1\0002\R\0001.bmp	18	12 61	131	72	5
g:\Shared\MIRLIN\Set1\DVD1\0002\R\0002.bmp	26	9 57	146	84	5
g:\Shared\MIRLIN\Set1\DVD1\0002\R\0003.bmp	20	10 56	136	79	5
g:\Shared\MIRLIN\Set1\DVD1\0002\R\0004.bmp	25	10 57	148	88	5
g:\Shared\MIRLIN\Set1\DVD1\0002\R\0005.bmp	31	6 43	119	132	19
g:\Shared\MIRLIN\Set1\DVD1\0002\R\0006.bmp	26	8 63	156	49	0
g:\Shared\MIRLIN\Set1\DVD1\0002\R\0007.bmp	17	8 48	109	125	22
g:\Shared\MIRLIN\Set1\DVD1\0002\R\0008.bmp	16	12 61	132	64	3
g:\Shared\MIRLIN\Set1\DVD1\0002\R\0009.bmp	20	12 65	134	39	0
g:\Shared\MIRLIN\Set1\DVD1\0002\R\0010.bmp	18	11 60	135	68	4
g:\Shared\MIRLIN\Set1\DVD1\0002\R\0011.bmp	17	9 44	103	126	25
g:\Shared\MIRLIN\Set1\DVD1\0002\R\0012.bmp	30	5 43	114	133	21
g:\Shared\MIRLIN\Set1\DVD1\0002\R\0013.bmp	21	9 66	141	43	0
g:\Shared\MIRLIN\Set1\DVD1\0002\R\0014.bmp	15	9 50	110	113	19
g:\Shared\MIRLIN\Set1\DVD1\0002\R\0015.bmp	18	10 68	149	40	0
g:\Shared\MIRLIN\Set1\DVD1\0002\R\0016.bmp	20	11 67	146	41	0
g:\Shared\MIRLIN\Set1\DVD1\0002\R\0017.bmp	21	11 66	141	44	0
g:\Shared\MIRLIN\Set1\DVD1\0002\R\0018.bmp	25	8 62	153	48	0
g:\Shared\MIRLIN\Set1\DVD1\0002\R\0019.bmp	23	11 67	145	43	0
g:\Shared\MIRLIN\Set1\DVD1\0002\R\0020.bmp	20	11 68	145	40	0
g:\Shared\MIRLIN\Set1\DVD1\0003\L\0001.bmp	27	10 55	145	114	11
g:\Shared\MIRLIN\Set1\DVD1\0003\L\0002.bmp	25	10 55	145	111	10
g:\Shared\MIRLIN\Set1\DVD1\0003\L\0003.bmp	27	9 55	146	111	10
g:\Shared\MIRLIN\Set1\DVD1\0003\L\0004.bmp	23	11 54	143	106	10
g:\Shared\MIRLIN\Set1\DVD1\0003\L\0005.bmp	27	10 55	144	111	10
g:\Shared\MIRLIN\Set1\DVD1\0003\L\0006.bmp	29	9 51	148	112	10
g:\Shared\MIRLIN\Set1\DVD1\0003\L\0007.bmp	38	6 49	142	102	7
g:\Shared\MIRLIN\Set1\DVD1\0003\L\0008.bmp	27	10 55	143	113	11
g:\Shared\MIRLIN\Set1\DVD1\0003\L\0009.bmp	26	10 54	145	111	10

g:\Shared\MIRLIN\Set1\DVD1\0003\L\0010.bmp	26	10 55	144	110	10
g:\Shared\MIRLIN\Set1\DVD1\0003\L\0011.bmp	32	7 53	147	93	6
g:\Shared\MIRLIN\Set1\DVD1\0003\L\0012.bmp	41	5 45	140	99	6
g:\Shared\MIRLIN\Set1\DVD1\0003\L\0013.bmp	34	7 50	149	98	6
g:\Shared\MIRLIN\Set1\DVD1\0003\L\0014.bmp	36	6 48	140	103	8
g:\Shared\MIRLIN\Set1\DVD1\0003\L\0015.bmp	23	10 55	144	111	11
g:\Shared\MIRLIN\Set1\DVD1\0003\L\0016.bmp	27	10 55	149	107	9
g:\Shared\MIRLIN\Set1\DVD1\0003\L\0017.bmp	39	6 48	141	102	7
g:\Shared\MIRLIN\Set1\DVD1\0003\L\0018.bmp	25	11 55	148	105	9
g:\Shared\MIRLIN\Set1\DVD1\0003\L\0019.bmp	36	6 49	145	100	7
g:\Shared\MIRLIN\Set1\DVD1\0003\L\0020.bmp	34	8 51	152	92	5
g:\Shared\MIRLIN\Set1\DVD1\0003\R\0001.bmp	29	8 49	125	84	6
g:\Shared\MIRLIN\Set1\DVD1\0003\R\0002.bmp	29	9 50	128	81	5
g:\Shared\MIRLIN\Set1\DVD1\0003\R\0003.bmp	30	8 50	131	84	5
g:\Shared\MIRLIN\Set1\DVD1\0003\R\0004.bmp	38	7 47	137	89	5
g:\Shared\MIRLIN\Set1\DVD1\0003\R\0005.bmp	31	8 50	130	81	5
g:\Shared\MIRLIN\Set1\DVD1\0003\R\0006.bmp	25	9 54	125	73	4
g:\Shared\MIRLIN\Set1\DVD1\0003\R\0007.bmp	29	8 49	127	80	5
g:\Shared\MIRLIN\Set1\DVD1\0003\R\0008.bmp	37	7 46	131	88	5
g:\Shared\MIRLIN\Set1\DVD1\0003\R\0009.bmp	22	11 56	133	76	5
g:\Shared\MIRLIN\Set1\DVD1\0003\R\0010.bmp	38	8 48	141	90	5
g:\Shared\MIRLIN\Set1\DVD1\0003\R\0011.bmp	32	8 51	134	89	6
g:\Shared\MIRLIN\Set1\DVD1\0003\R\0012.bmp	29	9 51	134	79	4
g:\Shared\MIRLIN\Set1\DVD1\0003\R\0013.bmp	32	7 49	128	84	5
g:\Shared\MIRLIN\Set1\DVD1\0003\R\0014.bmp	38	7 48	145	90	4
g:\Shared\MIRLIN\Set1\DVD1\0003\R\0015.bmp	37	8 51	142	65	0
g:\Shared\MIRLIN\Set1\DVD1\0003\R\0016.bmp	32	8 53	144	99	7
g:\Shared\MIRLIN\Set1\DVD1\0003\R\0017.bmp	36	7 48	138	90	5
g:\Shared\MIRLIN\Set1\DVD1\0003\R\0018.bmp	23	10 55	127	75	5
g:\Shared\MIRLIN\Set1\DVD1\0003\R\0019.bmp	30	8 50	129	81	5
g:\Shared\MIRLIN\Set1\DVD1\0003\R\0020.bmp	37	6 45	123	94	7
g:\Shared\MIRLIN\Set1\DVD1\0004\L\0001.bmp	40	5 48	148	72	0
g:\Shared\MIRLIN\Set1\DVD1\0004\L\0002.bmp	38	6 48	150	71	0
g:\Shared\MIRLIN\Set1\DVD1\0004\L\0003.bmp	28	8 53	141	102	8
g:\Shared\MIRLIN\Set1\DVD1\0004\L\0004.bmp	38	5 51	147	71	0
g:\Shared\MIRLIN\Set1\DVD1\0004\L\0005.bmp	30	7 52	137	105	9
g:\Shared\MIRLIN\Set1\DVD1\0004\L\0006.bmp	30	7 53	149	85	4
g:\Shared\MIRLIN\Set1\DVD1\0004\L\0007.bmp	24	7 50	126	94	9
g:\Shared\MIRLIN\Set1\DVD1\0004\L\0008.bmp	36	6 51	147	69	0
g:\Shared\MIRLIN\Set1\DVD1\0004\L\0009.bmp	36	6 51	146	69	0
g:\Shared\MIRLIN\Set1\DVD1\0004\L\0010.bmp	40	6 48	148	70	0
g:\Shared\MIRLIN\Set1\DVD1\0004\L\0011.bmp	37	6 51	148	70	0
g:\Shared\MIRLIN\Set1\DVD1\0004\L\0012.bmp	38	6 52	149	71	0
g:\Shared\MIRLIN\Set1\DVD1\0004\L\0013.bmp	30	7 52	137	103	9
g:\Shared\MIRLIN\Set1\DVD1\0004\L\0014.bmp	30	8 54	153	94	6

g:\Shared\MIRLIN\Set1\DVD1\0004\L\0015.bmp	41	6 52	150	68	0
g:\Shared\MIRLIN\Set1\DVD1\0004\L\0016.bmp	39	5 51	147	70	0
g:\Shared\MIRLIN\Set1\DVD1\0004\L\0017.bmp	34	6 53	150	93	5
g:\Shared\MIRLIN\Set1\DVD1\0004\L\0018.bmp	28	8 52	142	95	7
g:\Shared\MIRLIN\Set1\DVD1\0004\L\0019.bmp	31	6 52	138	102	8
g:\Shared\MIRLIN\Set1\DVD1\0004\L\0020.bmp	27	8 52	135	101	9
g:\Shared\MIRLIN\Set1\DVD1\0004\R\0001.bmp	16	12 53	111	96	14
g:\Shared\MIRLIN\Set1\DVD1\0004\R\0002.bmp	17	11 54	112	95	13
g:\Shared\MIRLIN\Set1\DVD1\0004\R\0003.bmp	21	9 52	109	88	11
g:\Shared\MIRLIN\Set1\DVD1\0004\R\0004.bmp	22	10 52	128	110	13
g:\Shared\MIRLIN\Set1\DVD1\0004\R\0005.bmp	21	10 53	120	86	9
g:\Shared\MIRLIN\Set1\DVD1\0004\R\0006.bmp	26	6 51	126	124	16
g:\Shared\MIRLIN\Set1\DVD1\0004\R\0007.bmp	27	7 51	132	106	11
g:\Shared\MIRLIN\Set1\DVD1\0004\R\0008.bmp	27	1 31	86	151	40
g:\Shared\MIRLIN\Set1\DVD1\0004\R\0009.bmp	18	9 53	113	100	14
g:\Shared\MIRLIN\Set1\DVD1\0004\R\0010.bmp	20	9 51	126	110	14
g:\Shared\MIRLIN\Set1\DVD1\0004\R\0011.bmp	15	11 54	110	99	15
g:\Shared\MIRLIN\Set1\DVD1\0004\R\0012.bmp	25	7 52	129	116	14
g:\Shared\MIRLIN\Set1\DVD1\0004\R\0013.bmp	20	9 51	126	110	14
g:\Shared\MIRLIN\Set1\DVD1\0004\R\0014.bmp	23	8 50	126	101	11
g:\Shared\MIRLIN\Set1\DVD1\0004\R\0015.bmp	22	8 51	125	112	14
g:\Shared\MIRLIN\Set1\DVD1\0004\R\0016.bmp	18	9 53	113	100	14
g:\Shared\MIRLIN\Set1\DVD1\0004\R\0017.bmp	49	0 25	112	107	8
g:\Shared\MIRLIN\Set1\DVD1\0004\R\0018.bmp	20	9 51	111	83	9
g:\Shared\MIRLIN\Set1\DVD1\0004\R\0019.bmp	23	8 51	129	102	11
g:\Shared\MIRLIN\Set1\DVD1\0004\R\0020.bmp	27	1 30	89	153	40
g:\Shared\MIRLIN\Set1\DVD1\0005\L\0001.bmp	26	4 56	147	58	0
g:\Shared\MIRLIN\Set1\DVD1\0005\L\0002.bmp	27	5 57	149	59	0
g:\Shared\MIRLIN\Set1\DVD1\0005\L\0003.bmp	26	4 56	147	59	0
g:\Shared\MIRLIN\Set1\DVD1\0005\L\0004.bmp	27	4 57	151	59	0

Sample iris images properties:

Img_Filename	Pupil_X	Pupil_Y	Pupil_R	Iris_X	Iris_Y	Iris_R
g:\Shared\MIRLIN\Set1\DVD1\0001\L\0001.bmp	299	171	39	303	170	104
g:\Shared\MIRLIN\Set1\DVD1\0001\L\0002.bmp	298	172	40	298	172	100
g:\Shared\MIRLIN\Set1\DVD1\0001\L\0003.bmp	302	175	38	300	173	100
g:\Shared\MIRLIN\Set1\DVD1\0001\L\0004.bmp	301	175	38	300	173	100
g:\Shared\MIRLIN\Set1\DVD1\0001\L\0005.bmp	301	174	38	305	173	106
g:\Shared\MIRLIN\Set1\DVD1\0001\L\0006.bmp	304	175	38	304	173	104
g:\Shared\MIRLIN\Set1\DVD1\0001\L\0007.bmp	303	177	42	306	175	104
g:\Shared\MIRLIN\Set1\DVD1\0001\L\0008.bmp	302	175	41	311	175	109
g:\Shared\MIRLIN\Set1\DVD1\0001\L\0009.bmp	303	177	41	308	175	105
g:\Shared\MIRLIN\Set1\DVD1\0001\L\0010.bmp	302	175	41	308	175	105
g:\Shared\MIRLIN\Set1\DVD1\0001\L\0011.bmp	301	175	41	310	175	108
g:\Shared\MIRLIN\Set1\DVD1\0001\L\0012.bmp	303	176	41	309	174	108
g:\Shared\MIRLIN\Set1\DVD1\0001\L\0013.bmp	303	178	40	306	176	105
g:\Shared\MIRLIN\Set1\DVD1\0001\L\0014.bmp	304	176	38	304	176	103
g:\Shared\MIRLIN\Set1\DVD1\0001\L\0015.bmp	301	176	39	300	175	100
g:\Shared\MIRLIN\Set1\DVD1\0001\L\0016.bmp	301	176	39	305	175	105
g:\Shared\MIRLIN\Set1\DVD1\0001\L\0017.bmp	301	176	39	306	175	105
g:\Shared\MIRLIN\Set1\DVD1\0001\L\0018.bmp	303	178	37	302	177	100
g:\Shared\MIRLIN\Set1\DVD1\0001\L\0019.bmp	302	174	41	307	174	104
g:\Shared\MIRLIN\Set1\DVD1\0001\L\0020.bmp	303	173	39	305	172	103
g:\Shared\MIRLIN\Set1\DVD1\0001\R\0001.bmp	328	210	42	327	209	100
g:\Shared\MIRLIN\Set1\DVD1\0001\R\0002.bmp	329	211	41	327	209	99
g:\Shared\MIRLIN\Set1\DVD1\0001\R\0003.bmp	329	212	40	322	210	106
g:\Shared\MIRLIN\Set1\DVD1\0001\R\0004.bmp	329	211	39	325	210	102
g:\Shared\MIRLIN\Set1\DVD1\0001\R\0005.bmp	330	211	40	328	210	100
g:\Shared\MIRLIN\Set1\DVD1\0001\R\0006.bmp	334	210	38	327	209	104
g:\Shared\MIRLIN\Set1\DVD1\0001\R\0007.bmp	333	210	38	329	209	102
g:\Shared\MIRLIN\Set1\DVD1\0001\R\0008.bmp	334	210	38	332	209	99
g:\Shared\MIRLIN\Set1\DVD1\0001\R\0009.bmp	339	208	39	337	207	100
g:\Shared\MIRLIN\Set1\DVD1\0001\R\0010.bmp	339	208	38	337	206	100
g:\Shared\MIRLIN\Set1\DVD1\0001\R\0011.bmp	338	206	42	336	204	96
g:\Shared\MIRLIN\Set1\DVD1\0001\R\0012.bmp	335	205	43	335	205	101
g:\Shared\MIRLIN\Set1\DVD1\0001\R\0013.bmp	335	210	40	335	210	100
g:\Shared\MIRLIN\Set1\DVD1\0001\R\0014.bmp	336	211	42	331	210	104
g:\Shared\MIRLIN\Set1\DVD1\0001\R\0015.bmp	335	210	41	331	210	104
g:\Shared\MIRLIN\Set1\DVD1\0001\R\0016.bmp	331	208	41	328	208	105
g:\Shared\MIRLIN\Set1\DVD1\0001\R\0017.bmp	334	209	41	331	209	105
g:\Shared\MIRLIN\Set1\DVD1\0001\R\0018.bmp	334	209	42	329	208	105
g:\Shared\MIRLIN\Set1\DVD1\0001\R\0019.bmp	335	209	41	333	208	100
g:\Shared\MIRLIN\Set1\DVD1\0001\R\0020.bmp	335	209	41	333	208	100
g:\Shared\MIRLIN\Set1\DVD1\0002\L\0001.bmp	350	224	37	350	222	99
g:\Shared\MIRLIN\Set1\DVD1\0002\L\0002.bmp	351	226	37	352	224	98
g:\Shared\MIRLIN\Set1\DVD1\0002\L\0003.bmp	351	226	37	351	225	99

g:\Shared\MIRLIN\Set1\DVD1\0002\L\0004.bmp	351	226	37	352	225	99
g:\Shared\MIRLIN\Set1\DVD1\0002\L\0005.bmp	353	225	37	352	224	99
g:\Shared\MIRLIN\Set1\DVD1\0002\L\0006.bmp	353	225	36	352	222	99
g:\Shared\MIRLIN\Set1\DVD1\0002\L\0007.bmp	354	225	37	356	223	99
g:\Shared\MIRLIN\Set1\DVD1\0002\L\0008.bmp	353	222	37	354	222	99
g:\Shared\MIRLIN\Set1\DVD1\0002\L\0009.bmp	355	216	37	354	215	98
g:\Shared\MIRLIN\Set1\DVD1\0002\L\0010.bmp	355	216	37	355	215	99
g:\Shared\MIRLIN\Set1\DVD1\0002\L\0011.bmp	357	217	38	356	215	99
g:\Shared\MIRLIN\Set1\DVD1\0002\L\0012.bmp	359	237	37	358	235	98
g:\Shared\MIRLIN\Set1\DVD1\0002\L\0013.bmp	358	235	37	359	234	98
g:\Shared\MIRLIN\Set1\DVD1\0002\L\0014.bmp	357	234	38	357	234	100
g:\Shared\MIRLIN\Set1\DVD1\0002\L\0015.bmp	359	236	38	359	234	98
g:\Shared\MIRLIN\Set1\DVD1\0002\L\0016.bmp	360	235	38	360	233	98
g:\Shared\MIRLIN\Set1\DVD1\0002\L\0017.bmp	360	235	38	359	232	98
g:\Shared\MIRLIN\Set1\DVD1\0002\L\0018.bmp	361	235	38	361	233	98
g:\Shared\MIRLIN\Set1\DVD1\0002\L\0019.bmp	358	233	37	360	233	98
g:\Shared\MIRLIN\Set1\DVD1\0002\L\0020.bmp	361	235	38	360	232	98
g:\Shared\MIRLIN\Set1\DVD1\0002\R\0001.bmp	349	165	40	342	164	104
g:\Shared\MIRLIN\Set1\DVD1\0002\R\0002.bmp	348	163	40	342	163	104
g:\Shared\MIRLIN\Set1\DVD1\0002\R\0003.bmp	349	164	40	341	163	104
g:\Shared\MIRLIN\Set1\DVD1\0002\R\0004.bmp	348	164	40	341	163	104
g:\Shared\MIRLIN\Set1\DVD1\0002\R\0005.bmp	350	163	39	348	162	96
g:\Shared\MIRLIN\Set1\DVD1\0002\R\0006.bmp	339	169	40	333	169	104
g:\Shared\MIRLIN\Set1\DVD1\0002\R\0007.bmp	340	167	40	332	166	104
g:\Shared\MIRLIN\Set1\DVD1\0002\R\0008.bmp	339	154	39	331	152	104
g:\Shared\MIRLIN\Set1\DVD1\0002\R\0009.bmp	338	154	40	336	154	96
g:\Shared\MIRLIN\Set1\DVD1\0002\R\0010.bmp	342	158	39	337	158	103
g:\Shared\MIRLIN\Set1\DVD1\0002\R\0011.bmp	346	156	39	337	157	104
g:\Shared\MIRLIN\Set1\DVD1\0002\R\0012.bmp	345	157	40	338	156	104
g:\Shared\MIRLIN\Set1\DVD1\0002\R\0013.bmp	345	158	39	339	158	104
g:\Shared\MIRLIN\Set1\DVD1\0002\R\0014.bmp	346	154	37	340	154	104
g:\Shared\MIRLIN\Set1\DVD1\0002\R\0015.bmp	346	154	37	341	154	103
g:\Shared\MIRLIN\Set1\DVD1\0002\R\0016.bmp	347	152	38	345	152	98
g:\Shared\MIRLIN\Set1\DVD1\0002\R\0017.bmp	349	150	38	346	151	96
g:\Shared\MIRLIN\Set1\DVD1\0002\R\0018.bmp	349	150	39	341	150	104
g:\Shared\MIRLIN\Set1\DVD1\0002\R\0019.bmp	349	148	40	347	148	98
g:\Shared\MIRLIN\Set1\DVD1\0002\R\0020.bmp	347	148	40	340	148	104
g:\Shared\MIRLIN\Set1\DVD1\0003\L\0001.bmp	271	226	50	279	226	126
g:\Shared\MIRLIN\Set1\DVD1\0003\L\0002.bmp	271	223	49	279	223	127
g:\Shared\MIRLIN\Set1\DVD1\0003\L\0003.bmp	274	223	49	279	222	127
g:\Shared\MIRLIN\Set1\DVD1\0003\L\0004.bmp	272	222	49	280	222	126
g:\Shared\MIRLIN\Set1\DVD1\0003\L\0005.bmp	271	226	51	278	226	127
g:\Shared\MIRLIN\Set1\DVD1\0003\L\0006.bmp	272	223	49	280	223	126
g:\Shared\MIRLIN\Set1\DVD1\0003\L\0007.bmp	290	219	46	295	219	126
g:\Shared\MIRLIN\Set1\DVD1\0003\L\0008.bmp	271	223	49	278	223	127

g:\Shared\MIRLIN\Set1\DVD1\0003\L\0009.bmp	273	226	52	278	225	127
g:\Shared\MIRLIN\Set1\DVD1\0003\L\0010.bmp	272	226	51	278	226	127
g:\Shared\MIRLIN\Set1\DVD1\0003\L\0011.bmp	272	221	47	278	221	127
g:\Shared\MIRLIN\Set1\DVD1\0003\L\0012.bmp	292	219	43	298	219	125
g:\Shared\MIRLIN\Set1\DVD1\0003\L\0013.bmp	291	220	44	298	220	125
g:\Shared\MIRLIN\Set1\DVD1\0003\L\0014.bmp	289	220	46	295	220	126
g:\Shared\MIRLIN\Set1\DVD1\0003\L\0015.bmp	272	222	49	279	222	127
g:\Shared\MIRLIN\Set1\DVD1\0003\L\0016.bmp	270	226	49	277	226	126
g:\Shared\MIRLIN\Set1\DVD1\0003\L\0017.bmp	288	220	46	295	220	125
g:\Shared\MIRLIN\Set1\DVD1\0003\L\0018.bmp	272	225	49	277	225	126
g:\Shared\MIRLIN\Set1\DVD1\0003\L\0019.bmp	290	218	46	295	219	125
g:\Shared\MIRLIN\Set1\DVD1\0003\L\0020.bmp	274	219	46	280	219	127
g:\Shared\MIRLIN\Set1\DVD1\0003\R\0001.bmp	281	264	41	276	264	125
g:\Shared\MIRLIN\Set1\DVD1\0003\R\0002.bmp	293	265	42	289	265	125
g:\Shared\MIRLIN\Set1\DVD1\0003\R\0003.bmp	297	259	39	291	258	126
g:\Shared\MIRLIN\Set1\DVD1\0003\R\0004.bmp	294	264	42	287	263	125
g:\Shared\MIRLIN\Set1\DVD1\0003\R\0005.bmp	294	265	41	288	264	125
g:\Shared\MIRLIN\Set1\DVD1\0003\R\0006.bmp	295	259	38	290	259	125
g:\Shared\MIRLIN\Set1\DVD1\0003\R\0007.bmp	295	258	39	291	258	125
g:\Shared\MIRLIN\Set1\DVD1\0003\R\0008.bmp	294	264	42	288	263	125
g:\Shared\MIRLIN\Set1\DVD1\0003\R\0009.bmp	295	265	40	289	264	125
g:\Shared\MIRLIN\Set1\DVD1\0003\R\0010.bmp	295	265	40	288	265	125
g:\Shared\MIRLIN\Set1\DVD1\0003\R\0011.bmp	274	261	43	269	261	124
g:\Shared\MIRLIN\Set1\DVD1\0003\R\0012.bmp	293	264	40	288	264	125
g:\Shared\MIRLIN\Set1\DVD1\0003\R\0013.bmp	294	266	42	287	264	125
g:\Shared\MIRLIN\Set1\DVD1\0003\R\0014.bmp	287	262	39	283	262	124
g:\Shared\MIRLIN\Set1\DVD1\0003\R\0015.bmp	282	264	40	276	264	125
g:\Shared\MIRLIN\Set1\DVD1\0003\R\0016.bmp	256	263	41	250	262	122
g:\Shared\MIRLIN\Set1\DVD1\0003\R\0017.bmp	294	266	42	288	264	125
g:\Shared\MIRLIN\Set1\DVD1\0003\R\0018.bmp	288	266	38	281	265	125
g:\Shared\MIRLIN\Set1\DVD1\0003\R\0019.bmp	292	264	41	288	264	125
g:\Shared\MIRLIN\Set1\DVD1\0003\R\0020.bmp	270	266	41	263	264	123
g:\Shared\MIRLIN\Set1\DVD1\0004\L\0001.bmp	315	187	45	320	187	119
g:\Shared\MIRLIN\Set1\DVD1\0004\L\0002.bmp	317	190	45	322	189	119
g:\Shared\MIRLIN\Set1\DVD1\0004\L\0003.bmp	313	187	44	320	187	120
g:\Shared\MIRLIN\Set1\DVD1\0004\L\0004.bmp	315	187	46	320	187	119
g:\Shared\MIRLIN\Set1\DVD1\0004\L\0005.bmp	315	186	43	321	186	118
g:\Shared\MIRLIN\Set1\DVD1\0004\L\0006.bmp	317	191	45	324	191	119
g:\Shared\MIRLIN\Set1\DVD1\0004\L\0007.bmp	320	190	46	326	189	118
g:\Shared\MIRLIN\Set1\DVD1\0004\L\0008.bmp	317	186	45	322	186	119
g:\Shared\MIRLIN\Set1\DVD1\0004\L\0009.bmp	317	188	45	322	188	119
g:\Shared\MIRLIN\Set1\DVD1\0004\L\0010.bmp	316	188	45	312	188	110
g:\Shared\MIRLIN\Set1\DVD1\0004\L\0011.bmp	315	188	46	322	188	119
g:\Shared\MIRLIN\Set1\DVD1\0004\L\0012.bmp	317	188	45	322	188	119
g:\Shared\MIRLIN\Set1\DVD1\0004\L\0013.bmp	317	187	41	322	186	118

g:\Shared\MIRLIN\Set1\DVD1\0004\L\0014.bmp	314	186	44	321	186	119
g:\Shared\MIRLIN\Set1\DVD1\0004\L\0015.bmp	316	191	45	311	190	110
g:\Shared\MIRLIN\Set1\DVD1\0004\L\0016.bmp	316	186	44	320	186	118
g:\Shared\MIRLIN\Set1\DVD1\0004\L\0017.bmp	314	186	44	321	186	119
g:\Shared\MIRLIN\Set1\DVD1\0004\L\0018.bmp	315	187	45	320	187	118
g:\Shared\MIRLIN\Set1\DVD1\0004\L\0019.bmp	313	192	44	320	192	118
g:\Shared\MIRLIN\Set1\DVD1\0004\L\0020.bmp	314	188	45	320	188	119
g:\Shared\MIRLIN\Set1\DVD1\0004\R\0001.bmp	320	185	45	319	185	110
g:\Shared\MIRLIN\Set1\DVD1\0004\R\0002.bmp	318	187	44	316	186	110
g:\Shared\MIRLIN\Set1\DVD1\0004\R\0003.bmp	317	187	45	317	187	109
g:\Shared\MIRLIN\Set1\DVD1\0004\R\0004.bmp	305	182	45	295	182	118
g:\Shared\MIRLIN\Set1\DVD1\0004\R\0005.bmp	306	182	45	296	181	118
g:\Shared\MIRLIN\Set1\DVD1\0004\R\0006.bmp	304	173	46	293	173	122
g:\Shared\MIRLIN\Set1\DVD1\0004\R\0007.bmp	305	173	45	293	173	120
g:\Shared\MIRLIN\Set1\DVD1\0004\R\0008.bmp	306	182	45	296	182	223
g:\Shared\MIRLIN\Set1\DVD1\0004\R\0009.bmp	307	173	44	297	174	118
g:\Shared\MIRLIN\Set1\DVD1\0004\R\0010.bmp	304	181	45	293	182	120
g:\Shared\MIRLIN\Set1\DVD1\0004\R\0011.bmp	306	174	46	298	174	118
g:\Shared\MIRLIN\Set1\DVD1\0004\R\0012.bmp	307	183	46	297	182	118
g:\Shared\MIRLIN\Set1\DVD1\0004\R\0013.bmp	304	181	45	293	182	120
g:\Shared\MIRLIN\Set1\DVD1\0004\R\0014.bmp	306	184	47	295	184	118
g:\Shared\MIRLIN\Set1\DVD1\0004\R\0015.bmp	304	181	47	296	181	118
g:\Shared\MIRLIN\Set1\DVD1\0004\R\0016.bmp	307	173	44	297	174	118
g:\Shared\MIRLIN\Set1\DVD1\0004\R\0017.bmp	308	173	44	298	173	223
g:\Shared\MIRLIN\Set1\DVD1\0004\R\0018.bmp	304	173	45	302	173	110
g:\Shared\MIRLIN\Set1\DVD1\0004\R\0019.bmp	305	172	46	293	173	120
g:\Shared\MIRLIN\Set1\DVD1\0004\R\0020.bmp	308	171	47	298	171	225
g:\Shared\MIRLIN\Set1\DVD1\0005\L\0001.bmp	308	257	45	316	256	117
g:\Shared\MIRLIN\Set1\DVD1\0005\L\0002.bmp	308	257	45	316	256	116
g:\Shared\MIRLIN\Set1\DVD1\0005\L\0003.bmp	306	259	46	314	257	117
g:\Shared\MIRLIN\Set1\DVD1\0005\L\0004.bmp	303	256	46	311	256	117
g:\Shared\MIRLIN\Set1\DVD1\0005\L\0005.bmp	303	258	47	311	256	117
g:\Shared\MIRLIN\Set1\DVD1\0005\L\0006.bmp	306	258	43	314	257	116
g:\Shared\MIRLIN\Set1\DVD1\0005\L\0007.bmp	303	258	44	311	257	117
g:\Shared\MIRLIN\Set1\DVD1\0005\L\0008.bmp	302	256	44	311	256	116
g:\Shared\MIRLIN\Set1\DVD1\0005\L\0009.bmp	305	263	46	311	260	117
g:\Shared\MIRLIN\Set1\DVD1\0005\L\0010.bmp	304	260	49	312	259	117
g:\Shared\MIRLIN\Set1\DVD1\0005\L\0011.bmp	303	258	49	312	258	116
g:\Shared\MIRLIN\Set1\DVD1\0005\L\0012.bmp	302	256	50	310	256	117
g:\Shared\MIRLIN\Set1\DVD1\0005\L\0013.bmp	301	258	50	310	258	117
g:\Shared\MIRLIN\Set1\DVD1\0005\L\0014.bmp	302	261	51	310	259	117
g:\Shared\MIRLIN\Set1\DVD1\0005\L\0015.bmp	303	261	52	311	258	116
g:\Shared\MIRLIN\Set1\DVD1\0005\L\0016.bmp	303	262	52	311	259	116
g:\Shared\MIRLIN\Set1\DVD1\0005\L\0017.bmp	303	260	53	312	260	117
g:\Shared\MIRLIN\Set1\DVD1\0005\L\0018.bmp	301	259	47	310	259	117

g:\Shared\MIRLIN\Set1\DVD1\0005\L\0019.bmp	304	264	47	311	263	117
g:\Shared\MIRLIN\Set1\DVD1\0005\L\0020.bmp	304	262	44	311	260	117
g:\Shared\MIRLIN\Set1\DVD1\0005\R\0001.bmp	252	247	47	246	246	117
g:\Shared\MIRLIN\Set1\DVD1\0005\R\0002.bmp	256	250	45	250	249	117
g:\Shared\MIRLIN\Set1\DVD1\0005\R\0003.bmp	245	251	54	238	250	116
g:\Shared\MIRLIN\Set1\DVD1\0005\R\0004.bmp	240	239	56	235	239	117
g:\Shared\MIRLIN\Set1\DVD1\0005\R\0005.bmp	235	233	49	230	233	117
g:\Shared\MIRLIN\Set1\DVD1\0005\R\0006.bmp	236	236	48	229	235	117
g:\Shared\MIRLIN\Set1\DVD1\0005\R\0007.bmp	235	239	47	228	238	116
g:\Shared\MIRLIN\Set1\DVD1\0005\R\0008.bmp	235	241	49	227	239	117
g:\Shared\MIRLIN\Set1\DVD1\0005\R\0009.bmp	230	239	50	225	239	116
g:\Shared\MIRLIN\Set1\DVD1\0005\R\0010.bmp	232	242	51	225	240	117
g:\Shared\MIRLIN\Set1\DVD1\0005\R\0011.bmp	231	246	51	225	243	116
g:\Shared\MIRLIN\Set1\DVD1\0005\R\0012.bmp	232	245	52	225	242	117
g:\Shared\MIRLIN\Set1\DVD1\0005\R\0013.bmp	230	245	53	223	242	116
g:\Shared\MIRLIN\Set1\DVD1\0005\R\0014.bmp	231	241	48	224	238	117
g:\Shared\MIRLIN\Set1\DVD1\0005\R\0015.bmp	230	240	50	223	238	116
g:\Shared\MIRLIN\Set1\DVD1\0005\R\0016.bmp	232	241	51	224	238	116
g:\Shared\MIRLIN\Set1\DVD1\0005\R\0017.bmp	230	240	51	223	238	116
g:\Shared\MIRLIN\Set1\DVD1\0005\R\0018.bmp	230	242	52	223	239	117
g:\Shared\MIRLIN\Set1\DVD1\0005\R\0019.bmp	232	243	49	224	240	117

Vitae

Ahmed Abdullah Bahjat
P.O.Box 1357
Saudi Arabia,Dhahran 31261
E-mail: bahjat@kfupm.edu.sa , abahjat@gmail.com
Nationality: Saudi

Education

2006- 2009: Master's degree in computer science, King Fahd University of Petroleum & Minerals, Dhahran, Saudi Arabia.
2001 – 2006: Bachelors degree in software engineering with Honor Distinction, King Fahd University of Petroleum & Minerals, Dhahran, Saudi Arabia.

Publications

K. Salah, F. Haidari, A. Bahjat and A. Manaa; Implementation and experimental evaluation of a simple packet rate Estimator. AEU - International Journal of Electronics and Communications, August, 2008.

A. Bahjat, H. Aljamaan, M. Alshayeb; SQL-GUARD DESIGN PATTERN. SEDE-2009 - 18th International Conference on Software Engineering and Data Engineering, USA, June 2009.

Professional Experience

- July, 2006 – present: Teaching assistant, King Fahad University of Petroleum & Minerals, Dhahran, Saudi Arabia

- June 2005 - Sep 2005 : ERP solution using Oracle Application 11i in HR and Finance and integration API, International Medical Center in Jeddah, Saudi Arabia

- Sep 2005 – June 2006: Develop WAMY Training System using ASP.NET 2, World Assembly of Muslim Youth.

- Sep 2006 – June 2006: Experimental Investigation of the Performance of Popular Interrupt Handling Schemes for Gigabit-Network Hosts.

- June 2008 – Oct 2008: Requirement and Design for School management System and teacher information system, Ministry of Education (MOE), Saudi Arabia.

Awards

- Distinctive teaching award for year 2006/2007. King Fahd University of Petroleum & Minerals.
- Second Place winner (Saudi regional contest) in Microsoft Imagine Cup Microsoft regional contest, Jeddah, Saudi Arabia, 2006
- Third Place Winner for the Saudi National Contest in 2007. Arranged by College of Telecom and Information (NCCC), Saudi Arabia

Memberships

- Institute of Electrical and Electronics Engineers, Inc. (IEEE) the Computer Society.
- Saudi Council Of Engineers.
- Center Of Excellence in Information Assurance (COEIA).
- Member of International Society for Computers and Their Applications.
- Computer Club of King Fahd University of Petroleum & Minerals (2002 – 2005) & Chairman Executive Committee for year 2005.
- Scout Club in King Fahd University of Petroleum & Minerals (2002 -2005).